

# **A CP GPS ANTENNA FROM 1.1 TO 1.6 GHZ**

A Major Qualifying Project Report  
Submitted to the Faculty of the

WORCESTER POLYTECHNIC INSTITUTE

In partial fulfillment of the requirements for the  
Degree of Bachelor of Science

By:

---

Jessica Nieves

---

Garabed Hagopian

April, 2008

APPROVED:

---

Prof. Sergey Makarov, Advisor  
Electrical and Computer Engineering Department

# Table of Contents

<b>ABSTRACT .....</b>	<b>1</b>
<b>ACKNOWLEDGMENTS.....</b>	<b>2</b>
<b>EXECUTIVE SUMMARY .....</b>	<b>3</b>
<b>INTRODUCTION .....</b>	<b>5</b>
APPLICATIONS.....	6
REQUIREMENTS.....	7
<b>PARTS.....</b>	<b>8</b>
HYBRIDS .....	8
90° Hybrid (Quadrature).....	9
180° Hybrids.....	9
BALUN .....	12
PRINTED CIRCUIT BOARD.....	13
CHOKER RING .....	14
<b>ANSOFT.....</b>	<b>16</b>
WHAT IS ANSOFT?.....	17
ANTENNA SIMULATION .....	17
OPTIMIZATION.....	19
<b>ANTENNA ASSEMBLY .....</b>	<b>21</b>
PROCESS.....	21
Problems.....	22
<b>TESTING .....</b>	<b>22</b>
PROCESS.....	22
$S_{11/22}$ Calibration Tests.....	22
$S_{21}$ Calibration Tests.....	23
RESULTS.....	23
<b>FIRST DESIGN CONCLUSIONS.....</b>	<b>27</b>
<b>NEW ANTENNA DESIGN .....</b>	<b>29</b>
PARTS.....	29
Printed Circuit Board Design.....	29
Balun.....	31
ANTENNA FABRICATION .....	32
Testing Results .....	35
<b>SECOND ANTENNA CONCLUSIONS .....</b>	<b>42</b>
<b>APPENDIX A: DESIGN PARAMETERS .....</b>	<b>45</b>
<b>APPENDIX B: MATLAB CODE .....</b>	<b>47</b>
$S_{11}$ CALIBRATION.....	47
$S_{21}$ CALIBRATION .....	49
<b>APPENDIX C: TESTING RESULTS OF THE FIRST DESIGN.....</b>	<b>51</b>
PRIMARY TESTING RESULTS .....	51
Antenna 1.....	51
Antenna 2.....	54
Antenna 3.....	57
RESULTS OF TESTING WITHOUT GROUND PLANE.....	59

<i>Antenna 1</i> .....	59
<i>Antenna 2</i> .....	62
<i>Antenna 3</i> .....	65
IMPEDANCE TESTING.....	68
<i>Antenna 1</i> .....	68
<i>Antenna 2</i> .....	70
<i>Antenna 3</i> .....	72
HYBRIDS TAPED TO GROUND PLANE .....	74
<i>Antenna 1</i> .....	74
<i>Antenna 2</i> .....	76
<i>Antenna 3</i> .....	78
<b>APPENDIX D: TESTING RESULTS OF THE SECOND DESIGN.....</b>	<b>81</b>
1.2 MM CENTER CONDUCTOR ANTENNAS.....	81
<i>Antenna 1</i> .....	81
<i>Antenna 2</i> .....	85
2 MM CENTER CONDUCTOR ANTENNA .....	89
3 MM CENTER CONDUCTOR ANTENNA .....	92
<b>REFERENCES .....</b>	<b>95</b>

## Table of Figures

Figure 1: An example of triangulation [1] .....	5
Figure 2: Four satellites are better than three [1] .....	5
Figure 3: Base station in Summit Camp, Greenland [4] .....	7
Figure 4: Circular polarization [5] .....	8
Figure 5: Circuit Representation of a Branch Line Hybrid.....	9
Figure 6: Ring Hybrid in Microstrip Form .....	10
Figure 7: Tapered Coupled Line Hybrid.....	10
Figure 8: Waveguide Hybrid Junction (magic-T).....	11
Figure 9: Classic Dyson balun for a) dipole antenna; b) – loop antenna. ....	12
Figure 10: Dyson Balun Top view.....	13
Figure 11: PCB design done in PCB Artist .....	14
Figure 12: 3D Simulation of PCB in Ansoft.....	14
Figure 13: Choke ring and received waves.....	15
Figure 14: Choke ring .....	16
Figure 15: Top View .....	17
Figure 16: Side view .....	18
Figure 17: Angle view .....	18
Figure 18: Simulated voltages using wave ports .....	19
Figure 19: Results for $SD_{11}$ from parameter sweep of both beta (degrees) and wing length (mm) .....	20
.....	20
Figure 20: Results for $SD_{21}$ from parameter sweep of both beta (degrees) and wing length (mm) .....	20
.....	20
Figure 21: Results of differential equations using optimized values of beta and wing length .....	21
Figure 22: Antenna 3 Return Loss .....	24
Figure 23: Antenna 3 $S_{11}$ Impedance .....	24
Figure 24: Antenna 3 Isolation .....	25
Figure 25: Antenna 3 Return Loss without Ground plane.....	25
Figure 26: Antenna 3 Isolation without Ground plane .....	26
Figure 27: Antenna 3 Return Loss with Hybrids taped to Ground plane .....	26
Figure 28: Cross Sectional Balun Dimensions .....	32
Figure 29: Teflon Block.....	32
Figure 30: Completed Teflon Pyramid .....	33
Figure 31: Balun Jig.....	34
Figure 32: Completed Balun.....	34
Figure 33: 1.2mm Center Conductor Antenna 1 $S_{11}$ .....	35
Figure 34: 1.2mm Center Conductor Antenna 1 $S_{11}$ Impedance .....	36
Figure 35: Antenna 1 $S_{21}$ Measured without Teflon or Wings .....	36
Figure 36: Antenna 1 $S_{21}$ Measured with Teflon, without Wings .....	37
Figure 37: 2 mm Antenna Balun Cross Section.....	38
Figure 38: 2 mm Antenna $S_{11}$ .....	38
Figure 39: 2 mm Antenna $S_{22}$ .....	39
Figure 40: 2 mm Antenna $S_{21}$ .....	39
Figure 41: 3 mm Antenna $S_{11}$ .....	40
Figure 42: 3 mm Antenna $S_{22}$ .....	41
Figure 43: 3 mm Antenna $S_{21}$ .....	41

Figure 44: 3 mm Antenna $S_{11}$ with 90° hybrid .....	42
Figure 45: Final Design Top View .....	43
Figure 46: Final Design Bottom View.....	43
Figure 47: Final Design Side View.....	44
Figure 48: Design parameters for first design.....	45
Figure 49: Design parameters for second design.....	46
Figure 50: First Antenna 1 $S_{11}$ .....	51
Figure 51: First Antenna 1 $S_{11}$ Impedance.....	51
Figure 52: Second Antenna 1 $S_{11}$ .....	52
Figure 53: Second Antenna 1 $S_{11}$ Impedance .....	52
Figure 54: Antenna 1 $S_{21}$ .....	53
Figure 55: Antenna 1 $S_{21}$ Calibration Impedance Results .....	53
Figure 56: Antenna 1 $S_{11}$ Measured by Network Analyzer .....	54
Figure 57: Antenna 1 $S_{21}$ Measured by Network Analyzer .....	54
Figure 58: Antenna 2 $S_{11}$ .....	55
Figure 59: Antenna 2 $S_{11}$ Impedance .....	55
Figure 60: Antenna 2 $S_{21}$ .....	56
Figure 61: Antenna 2 $S_{21}$ Impedance .....	56
Figure 62: Antenna $S_{21}$ Measured by Network Analyzer .....	57
Figure 63: Antenna 3 $S_{11}$ .....	57
Figure 64: Antenna 3 $S_{11}$ Impedance .....	58
Figure 65: Antenna 3 $S_{21}$ .....	58
Figure 66: Antenna 3 $S_{21}$ Impedance .....	59
Figure 67: Antenna 1 $S_{11}$ without Ground plane .....	59
Figure 68: Antenna 1 $S_{11}$ Impedance without Ground plane.....	60
Figure 69: Antenna 1 $S_{22}$ without Ground plane .....	60
Figure 70: Antenna 1 $S_{22}$ Impedance without Ground plane.....	61
Figure 71: Antenna 1 $S_{21}$ without Ground plane .....	61
Figure 72: Antenna 1 $S_{21}$ Impedance without Ground plane.....	62
Figure 73: Antenna 2 $S_{11}$ without Ground plane .....	62
Figure 74: Antenna 2 $S_{11}$ Impedance .....	63
Figure 75: Antenna 2 $S_{22}$ without Ground plane .....	63
Figure 76: Antenna 2 $S_{22}$ Impedance without Ground plane.....	64
Figure 77: Antenna 2 $S_{21}$ without Ground plane .....	64
Figure 78: Antenna 2 $S_{21}$ Impedance without Ground plane.....	65
Figure 79: Antenna 3 $S_{11}$ without Ground plane .....	65
Figure 80: Antenna 3 $S_{11}$ Impedance without Ground plane.....	66
Figure 81: Antenna 3 $S_{22}$ without Ground plane .....	66
Figure 82: Antenna 3 $S_{22}$ Impedance without Ground plane.....	67
Figure 83: Antenna 3 $S_{21}$ without Ground plane .....	67
Figure 84: Antenna 3 $S_{21}$ Impedance without Ground plane.....	68
Figure 85: Antenna 1 Port 1 Impedance .....	68
Figure 86: Antenna 1 Port 2 Impedance .....	69
Figure 87: Antenna 1 Port 3 Impedance .....	69
Figure 88: Antenna 1 Port 4 Impedance .....	70
Figure 89: Antenna 2 Port 1 Impedance .....	70
Figure 90: Antenna 2 Port 2 Impedance .....	71
Figure 91: Antenna 2 Port 3 Impedance .....	71
Figure 92: Antenna 2 Port 4 Impedance .....	72

Figure 93: Antenna 3 Port 1 Impedance .....	72
Figure 94: Antenna 3 Port 2 Impedance .....	73
Figure 95: Antenna 3 Port 3 Impedance .....	73
Figure 96: Antenna 3 Port 4 Impedance .....	74
Figure 97: Antenna 1 $S_{11}$ with Hybrids Taped to Ground plane.....	74
Figure 98: Antenna 1 $S_{11}$ Impedance with Hybrids Taped to Ground plane.....	75
Figure 99: Antenna 1 $S_{22}$ with Hybrids Taped to Ground plane.....	75
Figure 100: Antenna 1 $S_{22}$ Impedance with Hybrids Taped to Ground plane.....	76
Figure 101: Antenna 2 $S_{11}$ with Hybrids Taped to Ground plane.....	76
Figure 102: Antenna 2 $S_{11}$ Impedance with Hybrids Taped to Ground plane.....	77
Figure 103: Antenna 2 $S_{22}$ Impedance with Hybrids Taped to Ground plane.....	77
Figure 104: Antenna 2 $S_{22}$ Impedance with Hybrids Taped to Ground plane.....	78
Figure 105: Antenna 3 $S_{11}$ with Hybrids Taped to Ground plane.....	78
Figure 106: Antenna 3 $S_{11}$ Impedance with Hybrids Taped to Ground plane.....	79
Figure 107: Antenna 3 $S_{22}$ with Hybrids Taped to Ground plane.....	79
Figure 108: Antenna 3 $S_{22}$ Impedance with Hybrids Taped to Ground plane.....	80
Figure 109: 1.2mm Center Conductor Antenna 1 $S_{11}$ .....	81
Figure 110: 1.2mm Center Conductor Antenna 1 $S_{11}$ Impedance .....	81
Figure 111: 1.2mm Center Conductor Antenna 1 $S_{22}$ .....	82
Figure 112: 1.2mm Center Conductor Antenna 1 $S_{22}$ Impedance .....	82
Figure 113: 1.2mm Center Conductor Antenna 1 $S_{21}$ .....	83
Figure 114: 1.2mm Center Conductor Antenna 1 $S_{21}$ Impedance .....	83
Figure 115: Antenna 1 $S_{21}$ Measured without Teflon or Wings .....	84
Figure 116: Antenna 1 $S_{21}$ Impedance Measured without Teflon or Wings.....	84
Figure 117: Antenna 1 $S_{21}$ Measured with Teflon, without Wings .....	85
Figure 118: Antenna 1 $S_{21}$ Impedance Measured with Teflon, without Wings.....	85
Figure 119: Antenna 2 $S_{21}$ Measured without Teflon or Wings .....	86
Figure 120: Antenna 2 $S_{21}$ Impedance Measured without Teflon or Wings.....	86
Figure 121: First Trial Antenna 2 $S_{21}$ Measured with Teflon, without Wings .....	87
Figure 122: First Trial Antenna 2 $S_{21}$ Impedance Measured with Teflon, without Wings.....	87
Figure 123: Second Trial Antenna 2 $S_{21}$ Measured with Teflon, without Wings.....	88
Figure 124: Second Trial Antenna 2 $S_{21}$ Impedance Measured with Teflon, without Wings .....	88
Figure 125: 2 mm Center Conductor Antenna $S_{21}$ Measured with no Teflon or Wings .....	89
Figure 126: 2 mm Center Conductor Antenna $S_{21}$ Impedance Measured with no Teflon or Wings .....	89
Figure 127: 2 mm Center Conductor Antenna $S_{11}$ .....	90
Figure 128: 2 mm Center Conductor Antenna $S_{11}$ Impedance .....	90
Figure 129: 2 mm Center Conductor Antenna $S_{22}$ .....	91
Figure 130: 2 mm Center Conductor Antenna $S_{22}$ Impedance .....	91
Figure 131: 2 mm Center Conductor Antenna $S_{21}$ .....	92
Figure 132: 2 mm Center Conductor Antenna $S_{21}$ Impedance .....	92
Figure 133: 3 mm Center Conductor Antenna $S_{11}$ .....	93
Figure 134: 3 mm Center Conductor Antenna $S_{22}$ .....	93
Figure 135: 3 mm Center Conductor Antenna $S_{21}$ .....	94
Figure 136: 3 mm Center Conductor Antenna $S_{11}$ with 90° Hybrid .....	94

## Table of Tables

Table 1: Hybrid 1 Test Results .....	11
Table 2: Hybrid 2 Test Results .....	11
Table 3: Differential Variables .....	19
Table 4: Optimization Results .....	20

## **Abstract**

The aim of the project is to design a circularly polarized antenna for permanent GPS base station applications with low return loss, high isolation, and a bandwidth of 1.1 to 1.6 GHz. The antenna was designed, built, and tested.

## **Acknowledgments**

We would like to acknowledge Professor Sergey Makarov for all the help, insight, and direction he gave to this project.

We would also like to recognize Mr. Eduardo Oliveira for the use of his MATLAB calibration testing code as well as the multitude of answers he provided to any question we had.

We would like to especially thank Mr. Patrick Morrison for the tireless effort he gave to this project. His patience in showing us the many uses of each machine in the ECE shop is much appreciated.

Lastly, we would like to thank Dr. Francesca Scappuzzo and Physical Sciences Inc. for sponsoring our project.

Every one of these people was crucial to the completion of this project.

## Executive Summary

Global Positioning System (GPS) was developed by the U.S. Department of Defense because of the need of a precise positioning system. This worldwide radio navigation system consists of 24 satellites and ground stations. GPS utilizes the L-band which is roughly 1-2 GHz and can be further broken down into smaller bands L1-L5. The most common and well known form of GPS is the navigation systems found in vehicles (TOM TOM, Garmin etc.), boats and planes which are becoming more and more common; however there are many other uses for GPS. For instance, GPS is being used in science for the observation of volcanic activity and observation of weather affects on building structures.

Our antenna should work in the L band so the frequency range will be 1.1-1.6 GHz. Within this frequency range there should be good isolation which means it should have minimal crosstalk between ports and low return loss or low power ratio ( $P_R / P_T$ ). The antenna should also have circular polarization. Before anything could be built, the concept of the antenna had to be designed and simulated. Piece by piece the antenna was created in a 3D software called Ansoft HFSS 10. This section describes the software used, the simulation process and how Ansoft was used to optimize the measurements for our antenna.

After ordering parts, the first step was to construct the wings out of brass. Initially, we created wings 28 mm in length because our simulations early on in the project had shown that was the best wing length. After further optimization simulations, it was decided that the best combination of wing length and droop angle was 20.5 mm and 50 degrees (respectively). We used the band saw to cut the brass and the belt sander to adjust the dimensions on a finer scale. Afterwards, we use a file to smooth out the cuts and give the wings a better appearance.

Next, we created the foundation for the antenna. After receiving 63 mm sections of a 0.5 inch (diameter) Teflon rod, we used the lathe to drill out the inside. We slowly worked

up to a diameter that could house the four coaxial cables inside the tube. Since the printed circuit board (PCB) vias were still outside of that diameter, we expanded the circle for about 1 cm into the end of the tube where the PCB would be in contact. Once the antenna was built, we could proceed to test it.

The result did not turn out as we had expected. The most disconcerting characteristic about the poor performance of the antennas is the fact that the results differed so greatly from the Ansoft simulation results. This could have been caused by one a few different variations from the simulated design. For instance, the simulated design contained an electrically conductive sheet that connected the center conductors of the coaxial cables to the wings.

The previous design did not meet requirements. For our new design we will continue to use the Dyson balun but instead of coaxial cables we will use a quad line. Some modifications will need to be made to accommodate this change. The following section describes the modified parts and design for the new antenna.

The 1.2 mm antenna's results were similar to the results of our first design. Increasing the size of the center conductor seemed to drastically improve the performance of the antenna. The quad line antenna with the 3 mm by 3 mm center conductor is a very good design. In addition to the good results, the design is very sturdy, and is easily fixed to a choke ring ground plane. Also, the antennas can easily be replicated, since the Teflon pyramid, brass wings, printed circuit board, and coaxial cable connectors can be accurately recreated in large numbers. The balun would be the only part requiring creativity, since the jig that we used for the 1.2 mm center conductor balun was too small for the 3 mm center conductor balun. For these reasons, we needed to use clamps to hold the microstrip lines to the center conductor as well as a great deal of patience.

## Introduction

Global Positioning System (GPS) was developed by the U.S. Department of Defense because of the need of a precise positioning system. This worldwide radio navigation system consists of 24 satellites and ground stations. GPS works off of trilateration which is “a method of determining the relative positions of objects using the geometry of triangles” however a word often used in its place for simplicity is triangulation. This is done by measuring the travel time of the radio signals which provides the distance of the satellite. This is done using three satellites as can be seen in Figure 1 below hence the name triangulation.

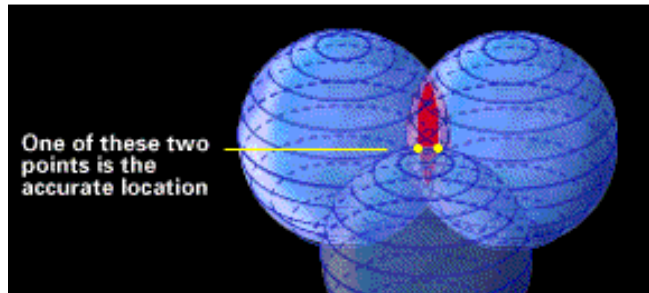


Figure 1: An example of triangulation [1]

If travel time is used to find the distance from the satellite to the receiver then the timing needs to be precise. The satellites use atomic clocks which are extremely precise however the cost of implementing an atomic clock on both the receiver and the satellite would be extremely expensive. Instead the timing faults at the receiver are compensated for with the use of an extra satellite as shown in Figure 2.

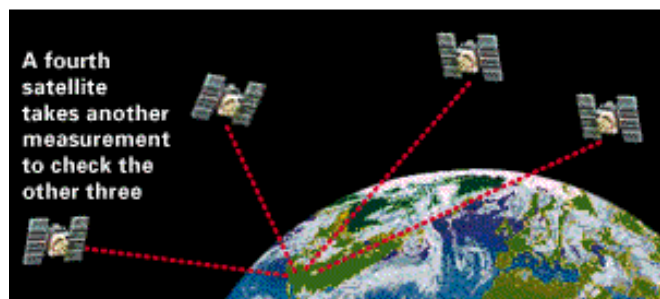


Figure 2: Four satellites are better than three [1]

All GPS receivers have an almanac programmed into their computers that informs them where each satellite is at all times. The charged particles located in the ionosphere and the water vapor of the troposphere also create timing errors as the signals move through them. Once the signal is closer buildings, tunnels, trees etc. can also cause an error that is referred to as multipath.

GPS utilizes the L-band which is roughly 1-2 GHz and can be further broken down into smaller bands L1-L5. The L1 band is centered at 1575.42 MHz and is used for coarse-acquisition (C/A) code and encrypted precision P(Y) code. The L2 band is centered at 1227.60 MHz and is used for P(Y) code. The L3 band is centered at 1381.05 MHz and is used to enforce nuclear test ban treaties. The L4 band is centered at 1379.913 MHz and is currently being studied for additional correction in the ionosphere. The L5 band is centered at 1176.45 MHz and is used as an internationally protected range for aeronautical navigation, which has little to no interference under any circumstances.

### ***Applications***

The most common and well known form of GPS is the navigation systems found in vehicles (TOM TOM, Garmin etc.), boats and planes which are becoming more and more common; however there are many other uses for GPS. Tracking has become easier with the use of GPS. This can be seen in the Precision Personnel Locator project which is a project developed “to help protect the lives of emergency personnel through a system for indoor personnel location and tracking” [2]. An Inertially augmented GPS landing system is being developed by Leonard R. Anderson and Melville D. McIntyr which also utilizes tracking.

“The guidance software may be executed by a conventional airplane processor, such as the GPS landing system processor, the internal reference system processor or the airplane's autopilot processor, or by a separate stand-alone processor. The runway centerline information is stored at the ground station or in local memory. The ground station can also provide differential GPS information.” [3]

This means that there is a stationary receiver that has the runway information stored and the plane is able to communicate with the ground station to make landing easier and safer. The military utilizes GPS in the form of missile guidance and search and rescue missions. GPS is also being used in science for the observation of volcanic activity and observation of weather effects on building structures. For these scientific observations permanent base stations are used. Like the name implies, these antennas are permanently placed in a location to provide high precision accuracy. UNAVCO is a company that specializes in such antennas and base stations. More specifically their “survey systems provide real-time kinematic (RTK) broadcasts for centimeter level differential corrections to properly equipped users, simplifying many GPS survey tasks that would otherwise require time consuming collection and post-processing of data. The equipment may also be used for post-processed static and kinematic surveys.” [4] Below in Figure 3 is a base station UNAVCO and VECO Polar Resources operate at Summit Camp, Greenland.



**Figure 3: Base station in Summit Camp, Greenland [4]**

### ***Requirements***

Our antenna should work in the L band so the frequency range will be 1.1-1.6 GHz. Within this frequency range there should be good isolation which means it should have minimal crosstalk between ports and low return loss or low power ratio ( $P_R / P_T$ ). The antenna should also have circular polarization. Right handed circular polarization is occurs when a wave propagates through the air in a circular motion, giving the

appearance of a spiral. It is created when two dipoles are exactly 90 degrees out of phase. Right handed circular polarization is crucial to GPS antennas, since it allows for received signals from any direction. A linearly polarized signal will not be received by a dipole antenna if the antenna does not exactly line up with the signal. A circularly polarized will always line up with a turnstile antenna.

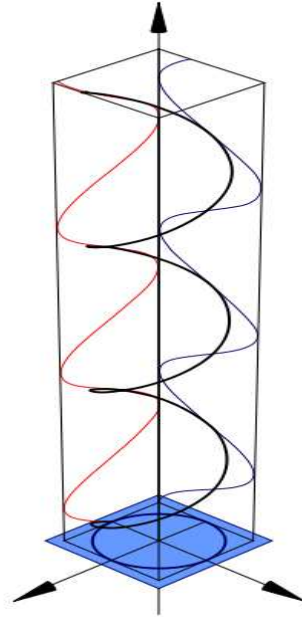


Figure 4: Circular polarization [5]

## Parts

In the following section the parts needed for the assembly of our antenna will be described in detail along with why they were chosen.

## Hybrids

90° and 180° hybrids are passive circuits used for higher frequency applications. They are classified as power dividers and directional couplers, and are used for power division and combination (respectively). These hybrids are often connected to an antenna in order to create circle polarization. Circle polarization is necessary for all antennas that are not fixed in one spot.

## 90° Hybrid (Quadrature)

The 90° hybrid is a four port network with one input port, two output ports, and one isolated port. When a voltage signal is sent through the input port, there a 90° phase difference will appear on the output ports. A circuit representation a branch line hybrid is show in Figure 5:

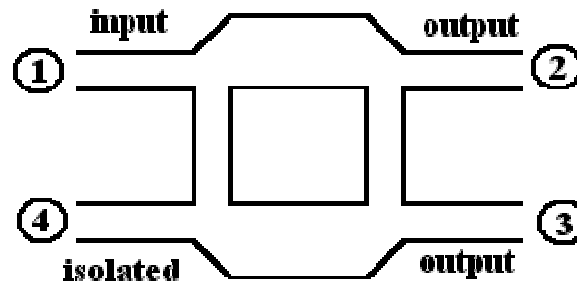


Figure 5: Circuit Representation of a Branch Line Hybrid

As can be seen from Figure 5, the branch line hybrid is symmetrical. This causes the S-parameters to also be symmetrical. The scattering matrix for a branch line hybrid is shown in Equation 1:

$$[S] = \frac{-1}{\sqrt{2}} \begin{bmatrix} 0 & j & 1 & 0 \\ j & 0 & 0 & 1 \\ 1 & 0 & 0 & j \\ 0 & 1 & j & 0 \end{bmatrix} \quad (1)$$

## 180° Hybrids

180° hybrids are also four port networks with one input port (port 1), two output ports (ports 2 and 3), and one isolated port (port 4). When a voltage signal is sent into the port 1 input, a phase difference of 0° will appear across ports 2 and 3, while port 4 will be isolated. However, when a voltage signal is sent into port 4, an 180° phase difference will appear across ports 2 and 3, while port 1 will be isolated. In both cases, the components of voltage signal that appear at ports 2 and 3 will be equal in magnitude.

When an 180° hybrid is used as a coupler, voltage signals are sent into the output ports (ports 2 and 3). When this happens, the sum of the signals will appear at port 1, while the difference of the two signals will appear at port 4. The scattering matrix for an 180° hybrid is shown in Equation 2:

$$[S] = \frac{-j}{\sqrt{2}} \begin{bmatrix} 0 & 1 & 1 & 0 \\ 1 & 0 & 0 & -1 \\ 1 & 0 & 0 & 1 \\ 0 & -1 & 1 & 0 \end{bmatrix} \quad (2)$$

It should be noted that the scattering matrix for the 180° hybrid is both unitary and symmetric. Three common 180° hybrids are shown below:

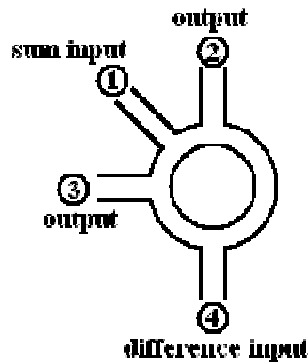


Figure 6: Ring Hybrid in Microstrip Form

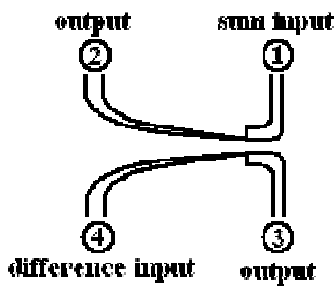


Figure 7: Tapered Coupled Line Hybrid

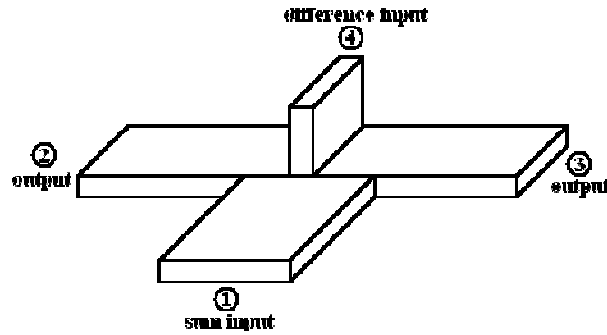


Figure 8: Waveguide Hybrid Junction (magic-T)

Since these antennas were created for GPS applications, we needed to create circular polarization. For this reason, we decided to use two 180° hybrids. After careful research, we decided to order the two hybrids from Mini-Circuits. We selected hybrids that had a specified bandwidth of 1000 to 2000 MHz, since our antennas need to operate in the L Band. Table 1 and Table 2 show the results for the preliminary testing on the two hybrids.

	S12, dB		S21, dB		Ss1, dB		Ss2, dB	
	power (dB)	frequency (GHz)						
max	-31.3	1.10	-31.4	1.10	-4.4	1.16	-4.67	1.10
min	-42.8	1.43	-42.8	1.43	-48	1.44	-4.95	1.44

Table 1: Hybrid 1 Test Results

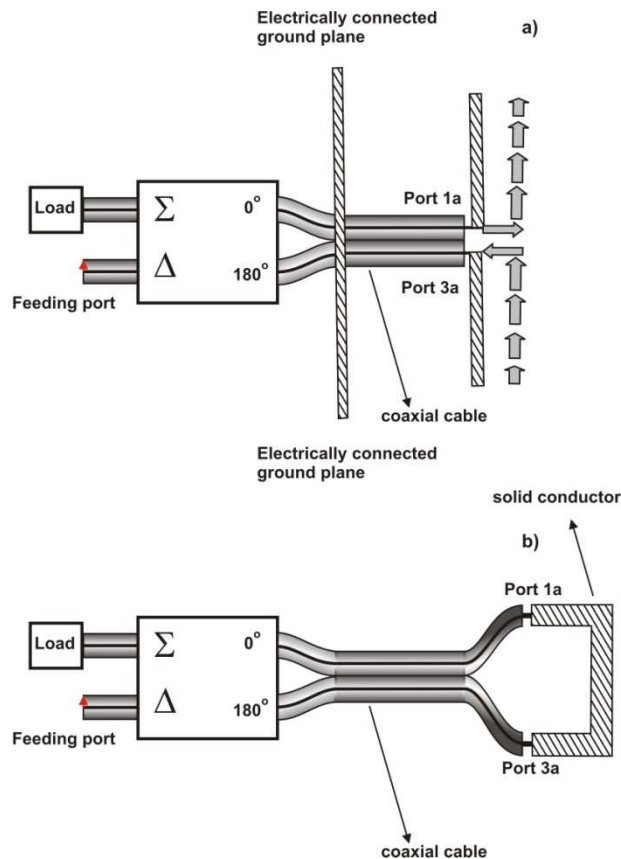
	S12, dB		S21, dB		Ss1, dB		Ss2, dB	
	power (dB)	frequency (GHz)						
max	-30.9	1.10	-30.9	1.10	-4.9	1.60	-4.9	1.60
min	-43.6	1.44	-43.5	1.44	-4.6	1.10	-4.6	1.10

Table 2: Hybrid 2 Test Results

Both of these hybrids are very broadband, with a very flat linear response. The hybrids also showed good isolation, with cross talk values below 40 dB.

## Balun

The term balun is an abbreviation of the words balance and unbalance. It is a device that connects a balanced two-conductor line to an unbalanced coaxial line. We selected the Dyson balun for our antenna. Its concept is shown in Figure 5 that follows.



**Figure 9: Classic Dyson balun for a) dipole antenna; b) – loop antenna.**

Either wing of the dipole in Fig. 5a is fed with a separate coaxial line, sharing the same outer ground; both lines are 180 deg out of phase. This ensures the proper balanced current distribution along the dipole. A similar setup can also be applied to a loop antenna – see Figure 5b. The proper power division and the proper phase shift can be obtained by the use of a 180 deg standard hybrid shown in Figure 5. The hybrid is thus playing the role of a balun; the ground is the case of the hybrid. Electric current on both lines feeding the dipole can be considered having  $\pm 90$  deg phase shift versus ground reference with no current.

The Dyson balun has widely used for standard dipoles and other symmetric antennas. For a symmetric antenna load, Dyson balun provides equal current, voltage, and power division between two dipole wings. For a non-symmetric antenna load, the Dyson balun functions as an ideal current, voltage, or power divider, depending on the termination of the sum port of the hybrid.

The Dyson balun allows to achieve a considerably wider bandwidth (over octave and wider) compared to the spilt-coaxial balun, whose bandwidth may be tuned to typically 20-25%. Another advantage of the Dyson balun is its direct applicability to a turnstile dipole element with two crossed dipoles or dipole-like antennas fed with two separate hybrids. The balun inherently provides a higher isolation between two turnstile antenna elements since two pairs of feeding transmission lines are shielded. Plus, the phase center of two crossed dipoles remains the same.

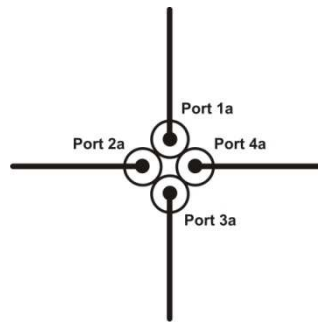


**Figure 10: Dyson Balun Top view**

Our design is similar to the Dyson balun shown in Figure 7, with four coaxial cables connecting to the wings of the antenna.

### ***Printed Circuit Board***

The material chosen for enclosing the four coaxial cables of the balun was Teflon; therefore it would not be possible to attach the wings of the antenna directly to the coaxial cables while remaining sturdy. For this reason, a printed circuit board was designed to be placed securely on top of the Teflon portion of the balun. This would allow for the connection between the coax cables and the wings of the antenna to be

made and remain sturdy. After designing several layouts for the PCB in a program called PCB Artist, we decided on the preliminary design shown in Figure 11 below:

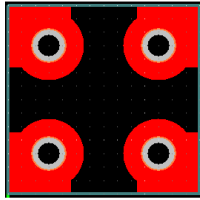


**Figure 11: PCB design done in PCB Artist**

The diagonal length of the board was designed to be  $\frac{1}{2}$  inches so that the PCB is able to sit properly on the balun with no protruding edges. The vias were designed to be the 40 mils so that the inner conductors of the coaxial cables were able to fit through with ease. The copper pads were laid out in such a way so that the area of each pad could be increased to the desired size while keeping the sides of the board symmetrical. The board design was then sent to Advanced Circuits to be printed.

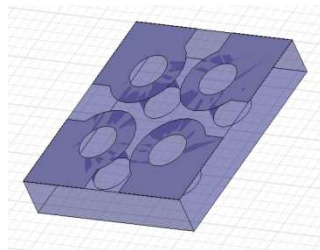


**Figure 12: 3D Simulation of PCB in Ansoft**

### ***Choke Ring***

A choke ring ground plane consists of several concentric thin rings around the center where the antenna is located. The areas between the rings are referred to as "grooves". The signal that is received by the antenna is composed of two components. There is a "direct" signal, which is the signal we want, and a "reflected" signal, which is the unwanted, signal that could be waves reflected off of buildings, trees, etc.

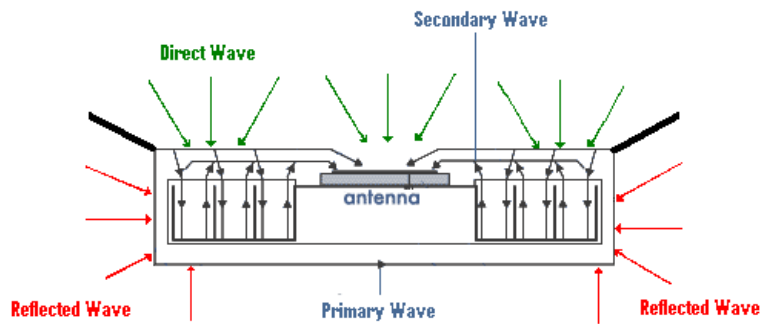


**Figure 13: Choke ring and received waves**

The electromagnetic field of the reflected signal in the vicinity of the choke ring ground plane can be viewed as sum of two field waves. The first of the two, primary waves, move around the perimeter of the ground plane never entering the grooves, as shown in Figure 10. This behavior is similar to how a reflected wave would act on a flat ground plane. The second of the two, secondary waves, are reflected waves created by the electromagnetic field of the grooves.

Primary and secondary reflected signals propagate to the antenna element and contribute to the total signal that also includes direct signal from the satellite to the antenna. The objective of the choke ring ground plane is for the primary and secondary reflected signals to cancel each other out and have the direct signal remain the dominant signal.

The phase relationship between the primary and the secondary reflected signals at the antenna output depends on the difference in path lengths that each signal travels. This path difference is twice the depth of the grooves. The amplitude ratio of the two signals depends on the characteristics of the antenna element, its location on the ground plane, the width and the number of the grooves. If the amplitude of the primary and the secondary waves are equal in magnitude and the phase between them is 180 degrees, then the two waves cancel each other out and multi-path is suppressed, allowing for the objective of the choke ring to be obtained, making the direct signal the dominant signal.

“For a given choke ring ground plane the complete suppression of multi-path only occurs for certain elevation angles and for others the multi-path is partially suppressed. The maximum suppression usually occurs for the

angles close to zenith and minimal suppression at angles close to horizon.”

[6]

Therefore it acts as a kind of band pass filter only allowing waves to reach that are within a given angle.

Studies have concluded that the depth of the grooves should be close to the quarter of the wavelength but slightly more to avoid creation of another surface wave component which destroys the required phase and amplitude ratios between the primary and the secondary waves. [6]

For our antenna a choke ring ground plane, provided by Physical Science Inc. (PSI), will be used to suppress any multi-path. The choke ring can be seen below in Figure 11.



**Figure 14: Choke ring**

## **Ansoft**

Before anything could be built, the concept of the antenna had to be designed and simulated. Piece by piece the antenna was created in a 3D software called Ansoft HFSS 10. This section describes the software used, the simulation process and how Ansoft was used to optimize the measurements for our antenna.

## ***What is Ansoft?***

“Ansoft HFSS is an interactive software package for calculating the electromagnetic behavior of a structure. The software includes post-processing commands for analyzing this behavior in detail. In using HFSS, you can compute:

- Basic electromagnetic field quantities and, for open boundary problems, radiated near and far fields.
- Characteristic port impedances and propagation constants.
- Generalized S-parameters and S-parameters renormalized to specific port impedances.
- The eigen modes, or resonances, of a structure.” [7]

## ***Antenna Simulation***

The wings, balun and printed circuit board were created in Ansoft. All of the values entered for all parts were parameterized so that values could be easily changed when needed. The wings and coaxial cables were assigned a boundary of Perfect E (electric field) which implies that the conductivity for each is high. While the PCB itself was assigned a FR4 boundary which implies the conductivity is low but the traces on the board and ground plane were assigned Perfect E boundary. Figure 15 provides a top view of the simulated antenna, Figure 16 a side view and Figure 17 an angular view.

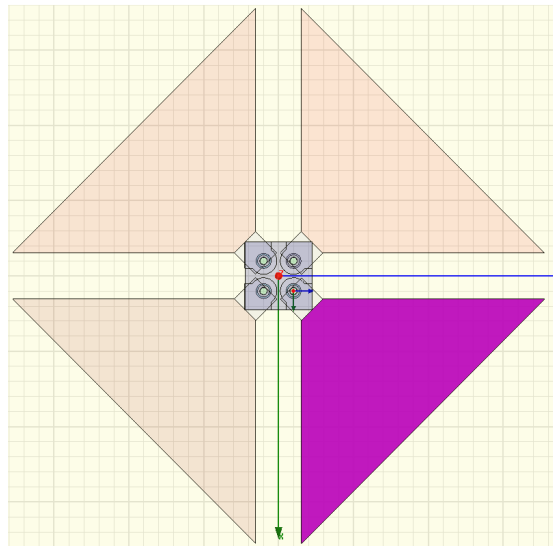


**Figure 15: Top View**

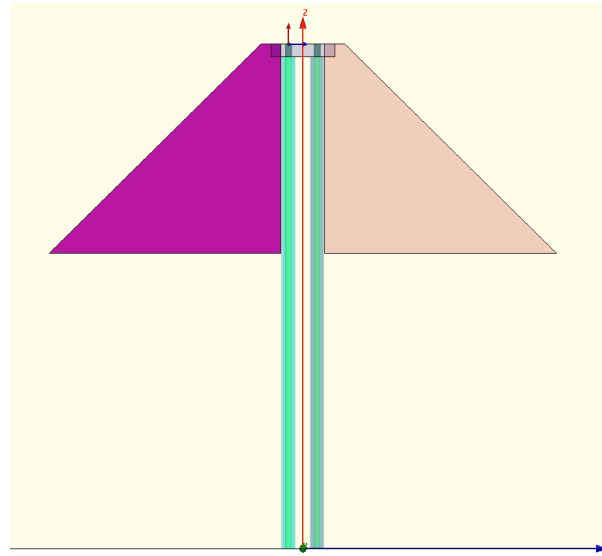


**Figure 16: Side view**

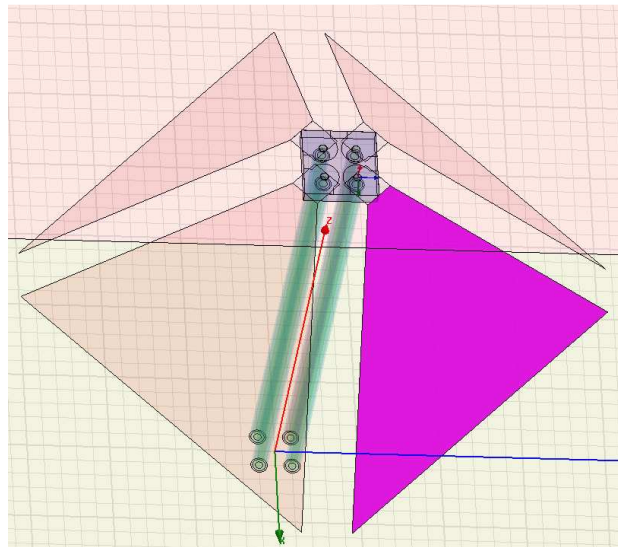


**Figure 17: Angle view**

Lumped ports are used for modeling internal ports within a structure. Wave ports are assigned to a structure to indicate the area where energy enters and exits the conductive shield. Wave ports are also used to calculate characteristic impedance, complex propagation constant and generalized S-parameters. For our simulation we assigned wave ports to the base of each coaxial cable. The wave ports were assigned from the inner conductor to the outer conductor on each of the four coaxial cables. The wave port can be seen highlighted in pink in Figure 18 below.

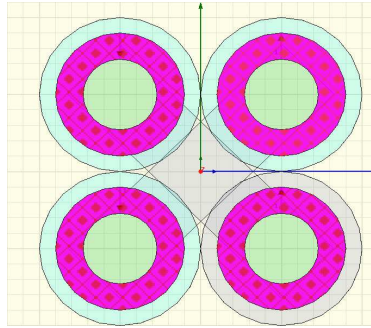


**Figure 18: Simulated voltages using wave ports**

### ***Optimization***

The two most important variables to our design were the droop angle (beta) and the wing length. In order to determine the most favorable combination of values, we set the beta and wing length variables to run parametric sweeps at the same time. The beta sweep was run from 35 degrees to 70 degrees at 5 degree increments, while the wing length sweep was run from 20 to 28 mm at 0.5 mm increments. The differential variables used to examine the sweeps are shown in Table 3. The right column illustrates the optimal results for each.

<b>Variable</b>	<b>Equation</b>	<b>Optimal Result</b>
<i>SD11</i>	$\frac{1}{2}(S_{11} + S_{33} - S_{13} - S_{31})$	-10 dB
<i>SD22</i>	$\frac{1}{2}(S_{22} + S_{44} - S_{24} - S_{42})$	-10 dB
<i>SD21</i>	$\frac{1}{2}(S_{21} + S_{43} - S_{41} - S_{23})$	-40 dB

**Table 3: Differential Variables**

The following figures depict the results of the frequency sweeps.

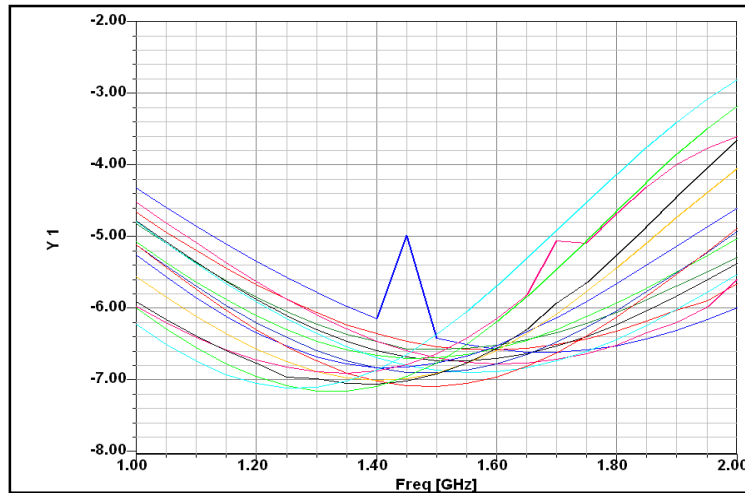


Figure 19: Results for  $SD_{11}$  from parameter sweep of both beta (degrees) and wing length (mm)

Note: The data for  $SD_{22}$  is not shown because  $SD_{22} \approx SD_{11}$ .

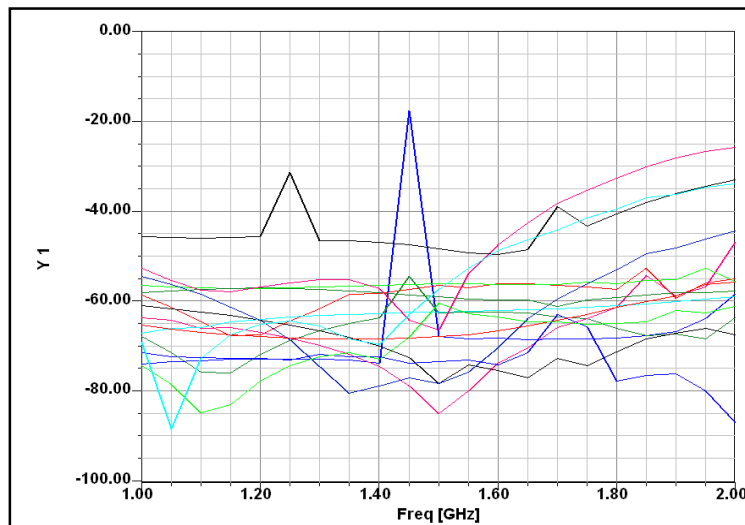


Figure 20: Results for  $SD_{21}$  from parameter sweep of both beta (degrees) and wing length (mm)

Using the above results of  $SD_{11}$  and  $SD_{21}$ , the variables wing length and beta were optimized to the following.

Variable	Description	Result
Wing Length	Length from middle of the base to the tip of wing 	20.5 mm
Beta	Droop angle	50 degrees

Table 4: Optimization Results

The following figure depicts the results of the optimized results.

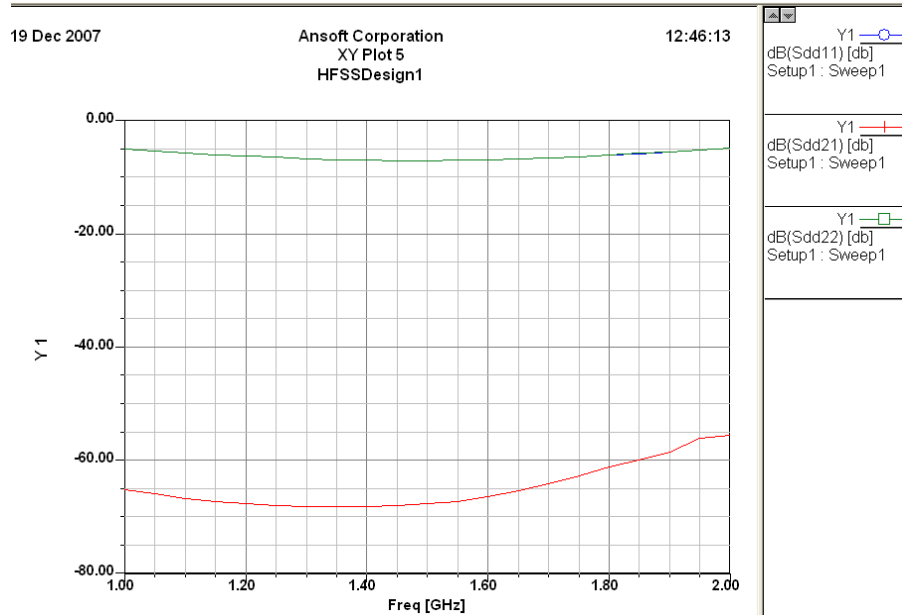


Figure 21: Results of differential equations using optimized values of beta and wing length

## Antenna Assembly

After the optimization process, we knew the critical measurements, such as the wing length and beta, and could begin the building process. This section walks through the building process of the antenna and discusses problems that occurred along the way and any concerns we have about the results.

### Process

After ordering parts, the first step was to construct the wings out of brass. Initially, we created wings 28 mm in length because our simulations early on in the project had shown that was the best wing length. After further optimization simulations, it was decided that the best combination of wing length and droop angle was 20.5 mm and 50 degrees (respectively). We used the band saw to cut the brass and the belt sander to adjust the dimensions on a finer scale. Afterwards, we use a file to smooth out the cuts and give the wings a better appearance.

Next, we created the foundation for the antenna. After receiving 63 mm sections of a 0.5 inch (diameter) Teflon rod, we used the lathe to drill out the inside. We slowly worked

up to a diameter that could house the four coaxial cables inside the tube. Since the PCB vias were still outside of that diameter, we expanded the circle for about 1 cm into the end of the tube where the PCB would be in contact.

Unfortunately, the PCBs came with a solder mask on the copper portions to which we attached the wings. Therefore, we needed to use a razor blade in order to scratch off the solder mask. We stripped the coaxial cables and threaded them through the tube, with the inner conductor for each of the cables going through one of the PCB vias. Then, we soldered the inner conductor of the coaxial cables directly to the PCB. Next, we soldered the wings to the PCB and glued the PCB to the Teflon tube.

## **Problems**

There existed a great difficulty in creating wings that matched the exact dimensions that we needed. The difficulty lied in matching said dimensions to within mere millimeters. Shortening the wings turned out to be very time consuming. However, the problem with shortening the wings we had was that it made any inequality in the lengths of the sides of the wings much more pronounced.

## **Testing**

### ***Process***

In order to test the antennas, we must consider the turnstile antenna as two separate dipole antennas that share a common balun. We must test both of these individual dipole antennas in order to determine the return loss. We then must test the two dipole antennas at the same time, in order to measure the interference (crosstalk) between the two antennas. Ed Oliveira provided us with MATLAB m-files that performed calibrated tests using the network analyzer.

### **$S_{11/22}$ Calibration Tests**

When we were measuring the individual dipoles, we connected two 50 ohm terminations to the two ports of the dipole that was not being measured. Next, we connected the network analyzer to port  $S$  of the 180 degree hybrid and two short standard terminations

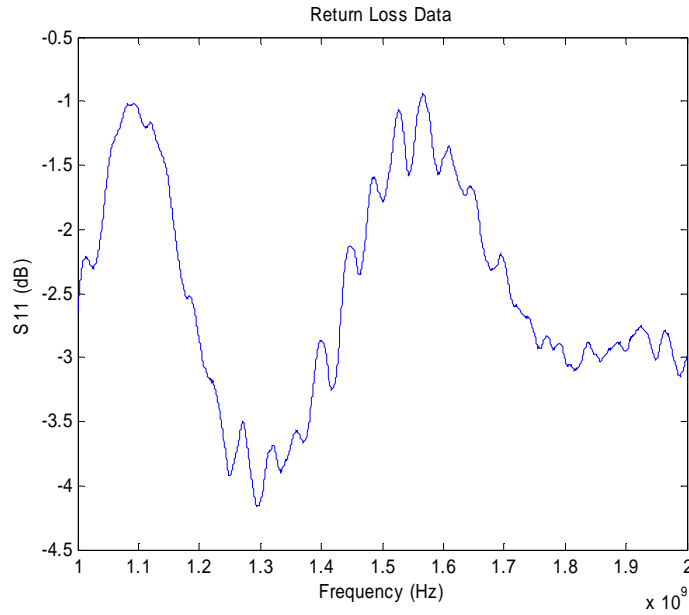
to ports  $1$  and  $2$ , as necessitated by the m-file. The m-file then used the network analyzer to perform a frequency sweep from 1 to 2 GHz (as determined by the user inputs). After the sweep, we connected the two 50 ohm standard terminations to ports  $1$  and  $2$  of the 180 degree hybrid. After the network analyzer ran another sweep, we connected the two ports of the hybrid to the dipole antenna. After the third and final sweep was run, the m-file produced a graph of the  $S_{11}$  (or  $S_{22}$ ) return loss and impedance data (both real and complex).

### **$S_{21}$ Calibration Tests**

When we needed to measure the crosstalk, we connected both network analyzer ports to port  $S$  of two different 180 degree hybrids. We then connected both of the port  $1$ 's and  $2$ 's to each other using two SMA to SMA coaxial connections. After the m-file ran a sweep of the data, we connected one dipole to ports  $1$  and  $2$  of one of the hybrids and the other dipole to ports  $1$  and  $2$  of the other hybrid. The m-file ran one more sweep, producing a graph of the  $S_{21}$  return loss and impedance data.

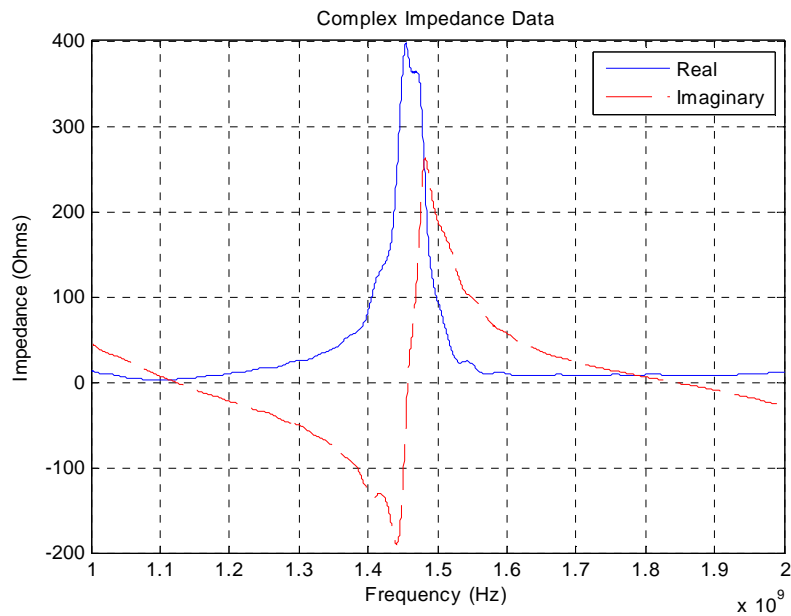
### **Results**

The testing of this antenna yielded poor results. Ideally, we would have a frequency range in which the return loss stays below 10 dB. This was certainly not the case. There were times that the return loss did not even drop below 5 dB, as shown in Figure 22:



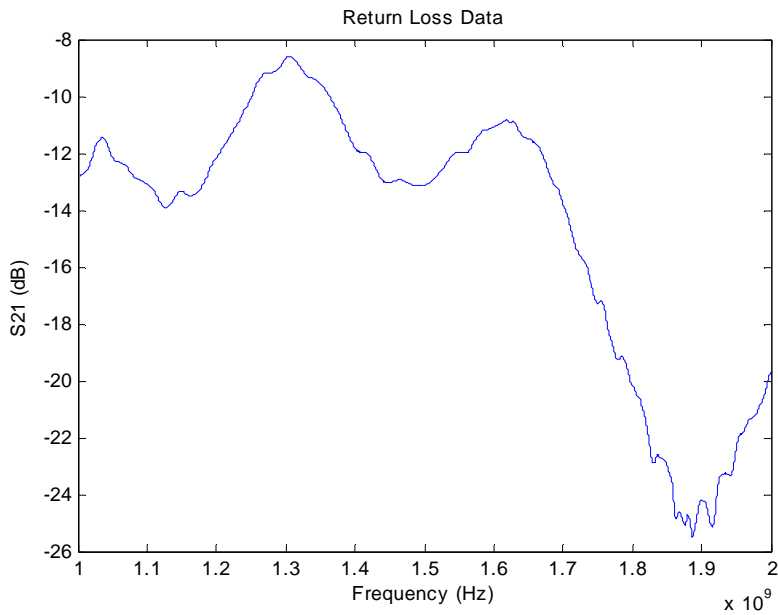
**Figure 22: Antenna 3 Return Loss**

We also saw that there was a substantial impedance mismatch, shown in Figure 23:



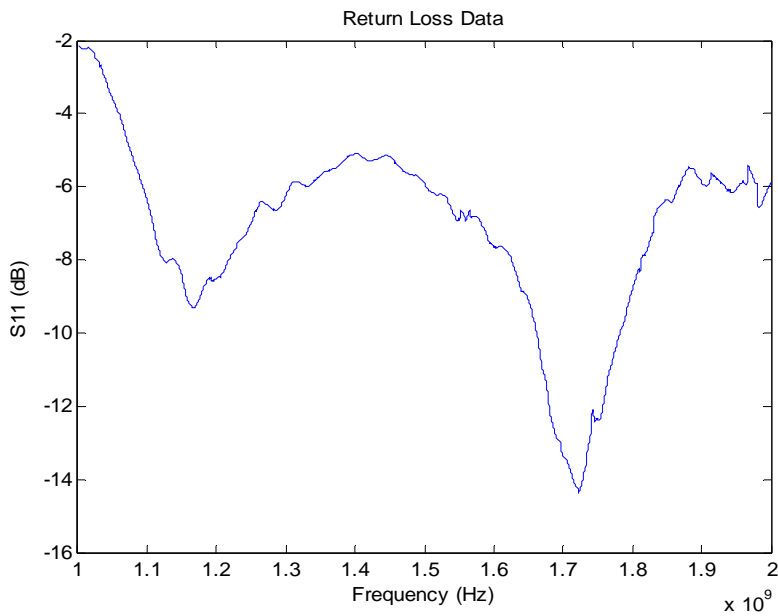
**Figure 23: Antenna 3  $S_{11}$  Impedance**

The calibration testing also yielded poor isolation results. We would like to see 30 dB across the whole band, but would expect, at the very least, 20 dB. The isolation was measured to be as poor as 12 dB in some instances, shown in Figure 24:



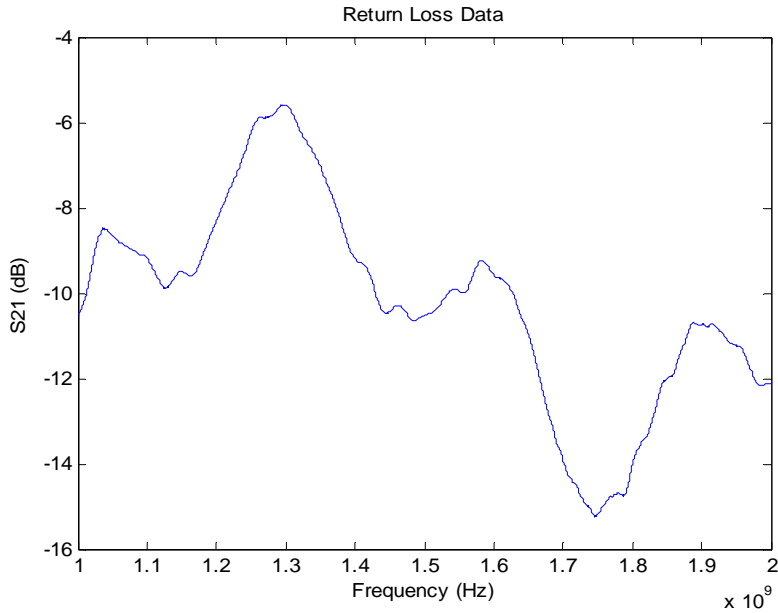
**Figure 24: Antenna 3 Isolation**

The next step was to determine whether or not the ground plane was at fault for the poor performance of the antennas. Therefore, we ran the calibration tests without the ground plane. Figure 25 shows the return loss of antenna 3 without a ground plane:



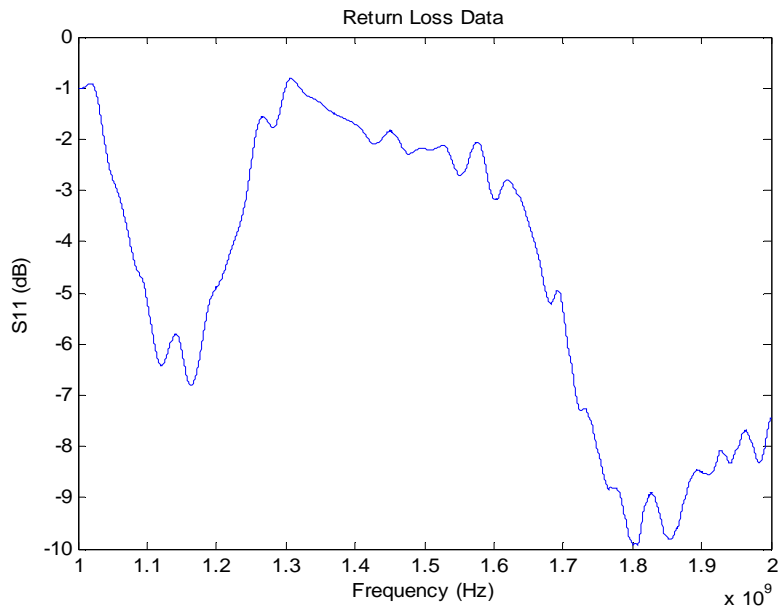
**Figure 25: Antenna 3 Return Loss without Ground plane**

Figure 26 shows the isolation of antenna 3 without a ground plane:



**Figure 26: Antenna 3 Isolation without Ground plane**

While taking the ground plane appeared to have helped the return loss slightly, it seems to have hurt the isolation slightly. Nevertheless, we would expect better results. The ground plane does not seem to be an issue. We then proceeded to tape the hybrids to the ground plane in order to determine if having the hybrids close to each other were causing any problems. Antenna 3's return loss is shown in Figure 27:



**Figure 27: Antenna 3 Return Loss with Hybrids taped to Ground plane**

This did not seem to help the return loss. The overall performance of this antenna design was poor, and nothing that we attempted to do seemed to improve this performance. All of the results from the calibration testing are shown in Appendix C: Testing Results of the First Design.

## **First Design Conclusions**

The most disconcerting characteristic about the poor performance of the antennas is the fact that the results differed so greatly from the Ansoft simulation results. This could have been caused by one a few different variations from the simulated design. For instance, the simulated design contained an electrically conductive sheet that connected the center conductors of the coaxial cables to the wings.

When we built the antennas we used liquid rosin flux and solder. There existed a great difficulty in soldering the wings to the PCB. At first, the copper wings would not form a strong enough bond, causing antenna instability. The continual soldering eventually lead to a couple of the copper traces on the PCB separating from the PCB, leaving only the via to which the wing could be soldered. We overcame the antenna instability issues by using a larger amount of liquid rosin flux before we soldered, which increased the strength of the connected that was capable of being formed by the solder. The fact that we had the copper pads in the corners of the PCB might have impaired the ease of creating a good solder connection. We originally designed the PCB in such way because we wanted to minimize crosstalk.

The center conductor of the coaxial cables did not lay completely flat on the PCB. Our Ansoft model had center conductors that were terminated at the top of the PCB. Since ours had a finite thickness on the PCB's copper pad, the wings could not stay perfectly flat, which in turn led to another notable problem. The wings were hard to solder at the correct droop angle. Our simulations had shown that the droop angle affects the return loss, resonance, and isolation.

Another solution to the stability problem involved using epoxy to help solidify the overall structure. The epoxy was used to help keep the wings stable as well as to form a bond between the Teflon balun and PCB. While the epoxy performed in excellent job in increasing the antenna's durability, it was not included Ansoft simulations. For this reason, we cannot overlook the fact that it may very well have had a certain degree of influence on the results. However, we could not have realistically created an antenna using our design without the epoxy.

When we built the antennas, we stripped back the outer shielding of the coaxial cables about 1 cm, and taped the outer conductors together, creating a ground between all of the coaxial cable grounds. In our Ansoft model, we did not have an outer shielding for the coaxial cables. Instead, we had a 2 mm gap between the conductors. This could have been one of the factors that caused the experimental results to differ from the simulation results.

The most distinctive negative trait of our antennas can easily be seen after a quick visual test: the wings lack symmetry. When creating designs that need to be accurate to within one or two millimeters, a small difference in one or more wings becomes a noticeable problem. The size of the wings affected the droop angle we used in fabrication. We could not let the wing tabs sit flat on the PCB since some of the wings would have made contact at the corners. Such an electrical connection would have severely damaged the antenna's ability to operate to any degree of success.

The antenna wings may have contained flaws for a couple of different reasons. First, the antenna wings were created by inexperienced machine operators. We were not extremely familiar with the use of the band saw in cutting copper, and this may have contributed in a negative manner. While every intention was made to be accurate to within a millimeter, the difficulty may have been too great for inexperienced operators on older equipment. It might have been better to use the shears in order to cut the wings. We had originally avoided using the shears because we wanted to avoid any bending of the

copper, especially given the thickness of the wings we were using. The copper that we used for the wings needed to be relatively thick because the wings had to be durable.

While the four coaxial cable Dyson balun design was good idealistically, it proved to be rather difficult to fabricate accurately to the simulation. Combined with the stability problems, it proved to be impractical. Since we did not have any antenna fabrication experience, we were not aware of the difficulties that might have been associated with our design.

## **New Antenna Design**

The previous design did not meet requirements. For our new design we will continue to use the Dyson balun but instead of coaxial cables we will use a quad line. Some modifications will need to be made to accommodate this change. The following section describes the modified parts and design for the new antenna.

### ***Parts***

#### **Printed Circuit Board Design**

Since we were merely modifying a design that had already been built, the main priority was to redesign everything that needed changing, which was primarily the PCB. We needed to perform a small amount of microstrip transmission line analysis in order to determine the proper dimensions for the PCB.

From the charts on p. 66 of Ludwig/Bretchko, we estimate the w/h (width to height) ratio for a 50 ohm microstrip transmission line on FR-4 to be approximately 1.8 to 2. We can assume that the w/h ratio is between one and two. For  $w/h \leq 2$ , the following equation gives the exact value of w/h:

$$\frac{w}{h} = \frac{8e^A}{e^{2A} - 2} \quad (3)$$

The quantity  $A$  is a constant defined by the following equation:

$$A = 2\pi \cdot \frac{Z_o}{\eta_o} \cdot \sqrt{\frac{\epsilon_r + 1}{2}} + \frac{\epsilon_r - 1}{\epsilon_r + 1} \left( 0.23 + \frac{0.11}{\epsilon_r} \right) \quad (4)$$

$Z_o$  is defined as the characteristic impedance of the transmission line. We want the characteristic impedance to be 50 ohms. FR-4 has a relative dielectric constant that ranges from 4.2 to 4.6. For this reason, we used the middle value in the range, 4.4.  $\eta_o$  is defined as the impedance of space in a vacuum, which is given by the following equation:

$$\eta_o = \sqrt{\frac{\mu_o}{\epsilon_o}} = \sqrt{\frac{4\pi \cdot 10^{-7} \text{ H/m}}{8.85418 \cdot 10^{-12} \text{ F/m}}} \approx 376.7 \quad (5)$$

If we substitute the appropriate values into equation 4 we arrive at the following value for  $A$ :

$$A = 2\pi \cdot \frac{50\Omega}{376.7\Omega} \cdot \sqrt{\frac{4.4+1}{2}} + \frac{4.4-1}{4.4+1} \left( 0.23 + \frac{0.11}{4.4} \right) = 1.531 \quad (6)$$

We can then substitute the value we found for  $A$  into equation 3:

$$\frac{w}{h} = \frac{8e^{1.531}}{e^{2 \cdot 1.531} - 2} = 1.91 \quad (7)$$

Before we use this ratio, we need to verify that a microstrip transmission line with a width to height ratio of 1.91 will have a characteristic impedance of 50 ohms. First, we need to find the effective dielectric constant. Since our width is greater than the height, we need to use the formula for wide transmission lines:

$$\epsilon_{eff} = \frac{\epsilon_r + 1}{2} + \frac{\epsilon_r - 1}{2} \left( 1 + 12 \frac{h}{w} \right)^{-1/2} = \frac{4.4+1}{2} + \frac{4.4-1}{2} \left( 1 + 12 \cdot \frac{1}{1.91} \right)^{-1/2} = 3.3 \quad (8)$$

Using this value, we can now find the characteristic impedance:

$$Z_o = \frac{\eta_o}{\sqrt{\epsilon_{eff}} \left(1.393 + \frac{w}{h} + \frac{2}{3} \ln\left(\frac{w}{h} + 1.444\right)\right)} \quad (9)$$

If we insert the appropriate values:

$$Z_o = \frac{376.7\Omega}{\sqrt{3.3} \left(1.393 + 1.91 + \frac{2}{3} \ln(1.91 + 1.444)\right)} = 50.46\Omega \quad (10)$$

This value differs from the expected value due to rounding error. Since we are using a PCB with a height of 62 mils, we can calculate the width of the microstrip line to be 118.42 mils, or 3.0 millimeters.

Next, we need to determine the appropriate length for the 4 traces. We need to calculate the length of the wave propagating down the microstrip line at the center frequency of the frequency range:

$$\lambda = \frac{c}{f \sqrt{\epsilon_{eff}}} = \frac{299792458 m/s}{1.3 \cdot 10^9 s^{-1} \sqrt{3.3}} = 126.95 mm \quad (11)$$

Since we want the length of the traces to be a quarter of the wavelength, we can determine that the length of our microstrip lines should be 31.7 mm.

## Balun

The new design contains a four microstrip transmission balun. Each transmission line contains two copper microstrips with Rogers duroid in the middle. Each transmission line measures 50 mils in thickness, and is has one microstrip line face soldered to a rectangular copper center conductor containing a 1.2 mm by 1.2 mm cross section. The dimensions of the balun are given in Figure 28:

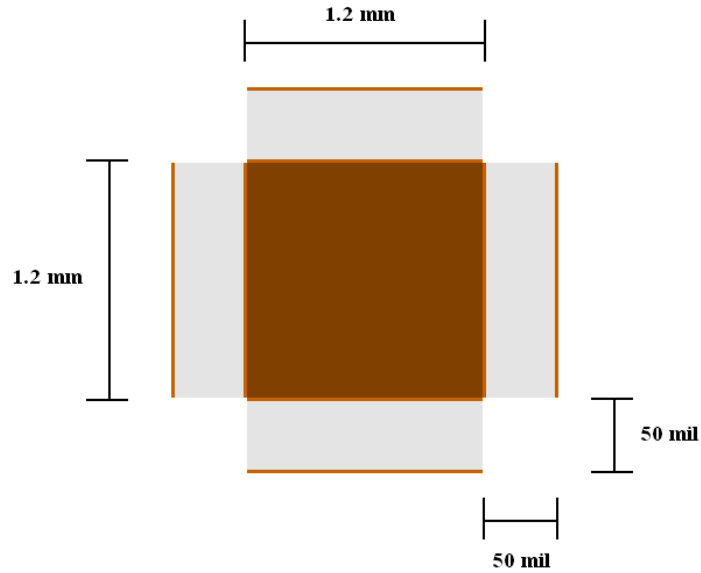


**Figure 28: Cross Sectional Balun Dimensions**

The height of the balun was designed to be 1.77 inches.

### ***Antenna Fabrication***

The most laborious part of the building the newly designed antennas was creating the Teflon block. We had to start with Teflon cylinder that measured 4 inches in diameter and 4 inches high. We then used the lathe to square off both sides. Next we used the Bridgeport machine in order to mill down the cylinder into a block that measured 2.75 inches by 2.75 inches and 1.77 inches tall, shown in Figure 29:

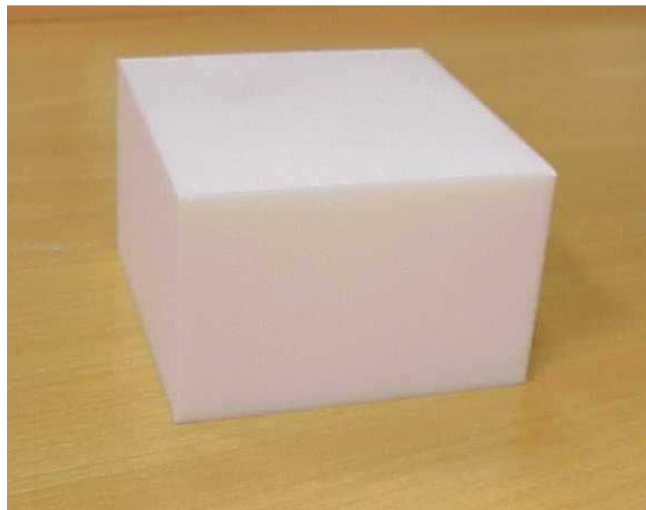


**Figure 29: Teflon Block**

Next, we used calipers to create tick marks on the Teflon block for the angles. Using the Bridgeport, we were able to create each of the four angled faces. Since the Bridgeport could keep the Teflon pyramid square, we used it to drill the hole through the center of the Teflon block. Using an end mill attachment to the Bridgeport machine, we created two troughs in line with the center hole of the pyramid, in order to allow for the solder needed for connecting the balun to the PCB and the four coaxial cable connectors to the PCB. This led to the creating of the pyramid shown in Figure 30:

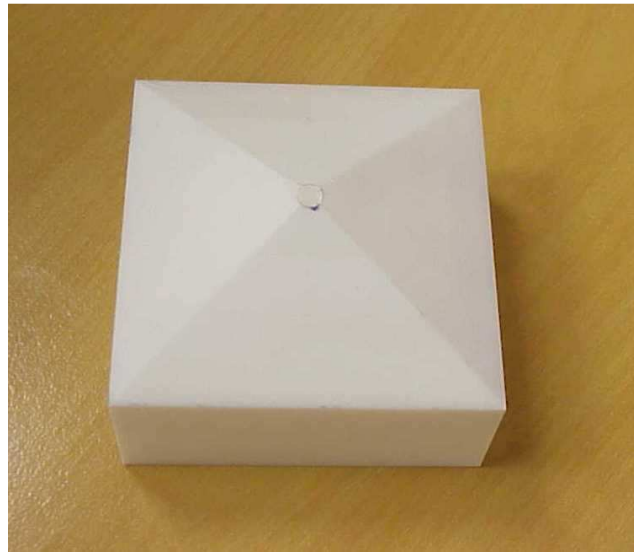


**Figure 30: Completed Teflon Pyramid**

The next step in the manufacturing process was creating the balun. We needed to cut out a center conductor out of a piece of stock copper using the Bridgeport machine. Next, we needed to use the shears to cut the four microstip transmission lines out of the larger board. For the antenna with the center conductor measuring 1.2 mm by 1.2 mm, we were able to use a jig created by Patrick Morrison of the ECE shop in order to solder the four transmission lines to the center conductor. The jig is shown in Figure 31:

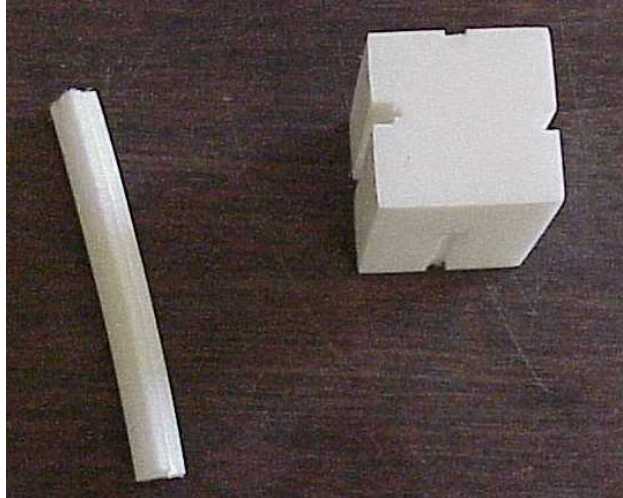


**Figure 31: Balun Jig**

Each of the transmission lines were coated with liquid rosin flux, and solder paste. Once each side of the center conductor was covered with liquid rosin flux, the four transmission lines were inserted into the jig so that each one of them had a microstrip line face connected to the center conductor. Next, a soldering iron was used to heat up the center conductor, subsequently melting the solder paste, which in turn formed a solid connection. We then ensured the four transmission lines were flush with the center conductor on end of the balun, and were trimmed back on the other, so that we could file the center conductor into a circle capable of fitting into the PCB's center conductor via. A picture of a completed balun, minus the trimming and filing, is shown in Figure 32:

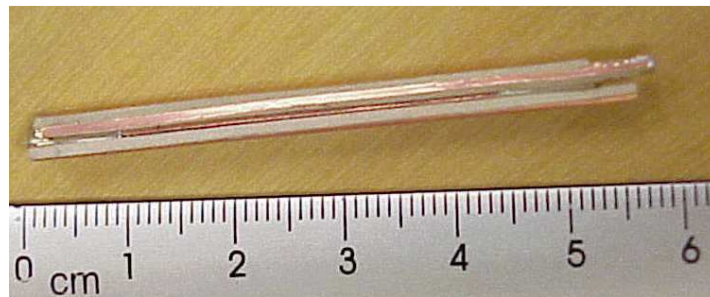


**Figure 32: Completed Balun**

Next, we needed to focus on the PCB. We found four 90 degree coaxial cable connectors, and filed them down so that they would lay flat against the grounded side of the PCB, while their center conductors went through the PCB's via. We attached the

cables to the connectors, soldered the connectors to the PCB, and then soldered the balun to the PCB.

We determined, after our experience with our first design, that the best way to create the wings would be to use the shears. Since the wings were going to lie flat on a Teflon pyramid, we did not need to focus on creating extremely durable wings, consequently allowing us to create the wings thinner. This was very important, since thinner brass is easier to shear accurately. Once the wings were created, we put the Teflon pyramid on top of the PCB, with balun going through the pyramid's central hole. After soldering the wings to the balun, we proceeded with the calibration testing.

### Testing Results

The initial calibration testing results did not produce positive results. The return loss was lower than an acceptable level, as shown in Figure 33:

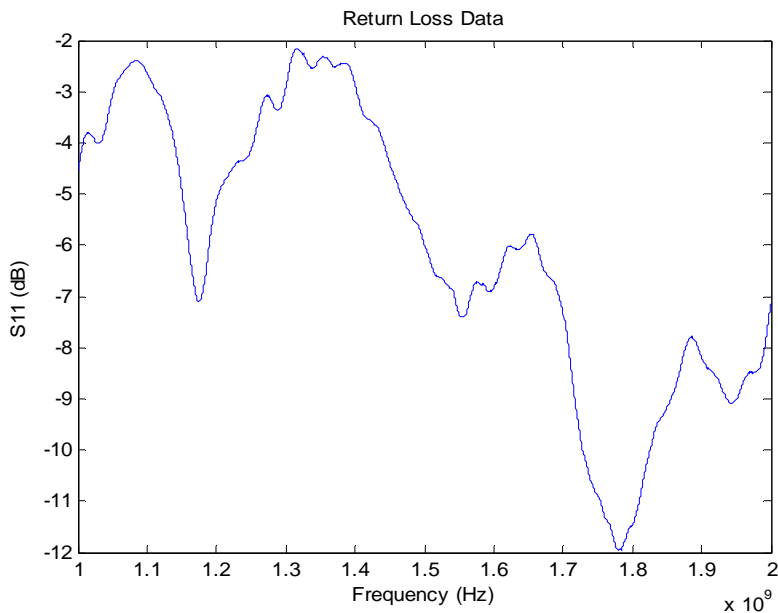
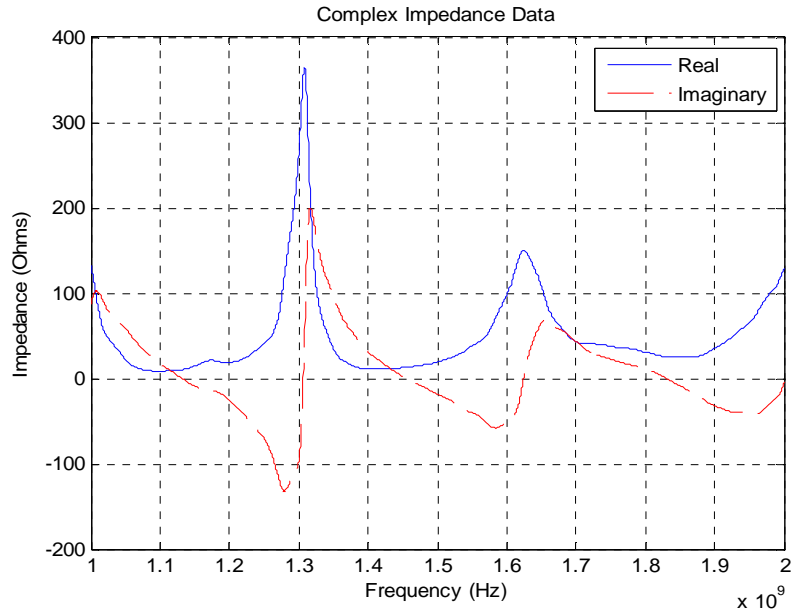


Figure 33: 1.2mm Center Conductor Antenna 1 S<sub>11</sub>

The isolation was measured to be unsatisfactory:



**Figure 34: 1.2mm Center Conductor Antenna 1  $S_{11}$  Impedance**

In order to trouble shoot the problem, we took removed the wings and Teflon pyramid, and retested the isolation, ascertaining the results shown in Figure 35:

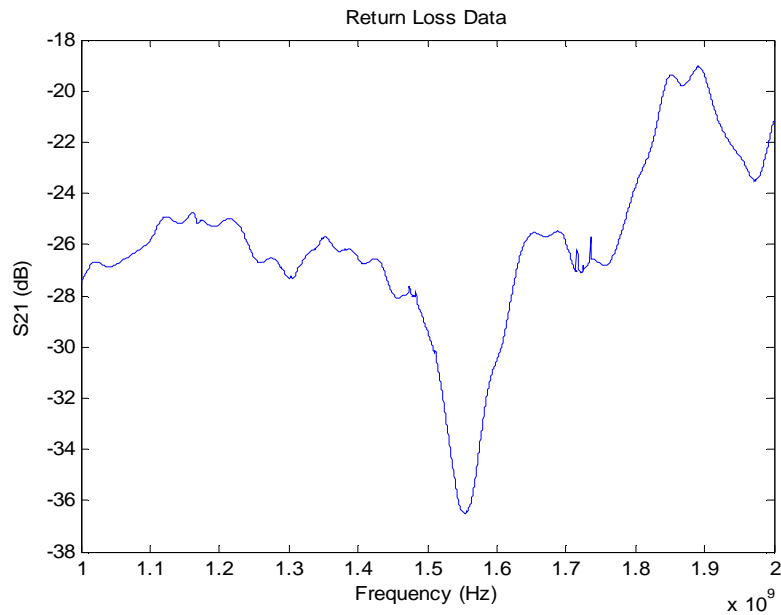


**Figure 35: Antenna 1  $S_{21}$  Measured without Teflon or Wings**

Since this seemed to improve the performance of the antenna, we put the Teflon pyramid on top of the PCB again and retested the antenna's isolation in order to determine

whether or not the wings were the root cause of the poor performance. The result is shown in Figure 36:

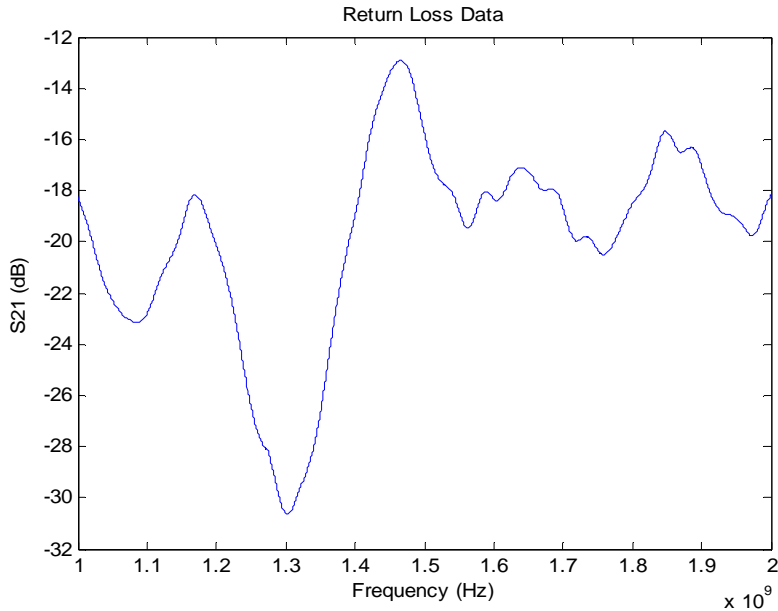


**Figure 36: Antenna 1 S<sub>21</sub> Measured with Teflon, without Wings**

It appeared the Teflon pyramid seemed to be causing the poor performance of the antenna. In order to side step this issue, we decided (per the instruction of Professor Makarov) to increase the balun size and redesign the PCB accordingly.

We redesigned the balun so that the center conductor's cross section measured 2 mm by 2 mm, as shown in Figure 37:

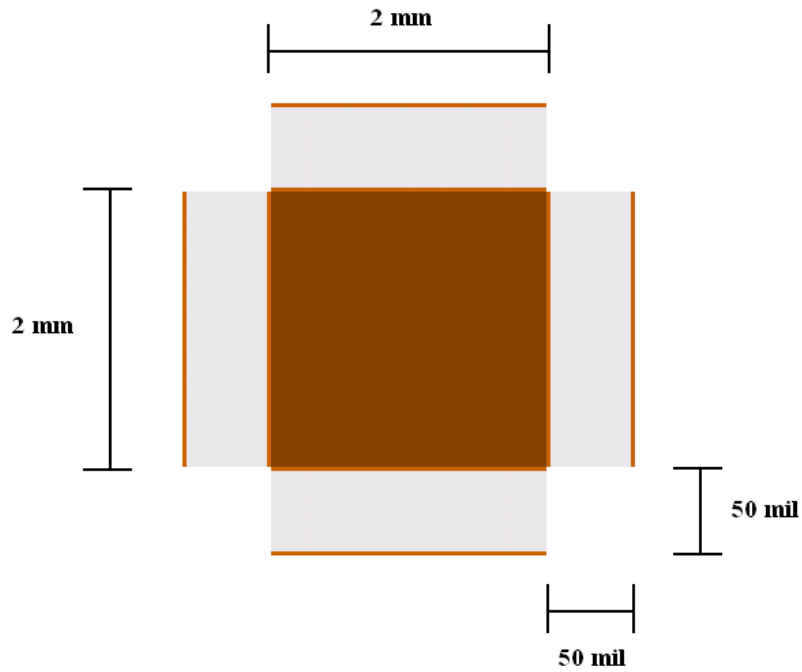


**Figure 37: 2 mm Antenna Balun Cross Section**

Calibration testing produced the following return loss for  $S_{11}$ :

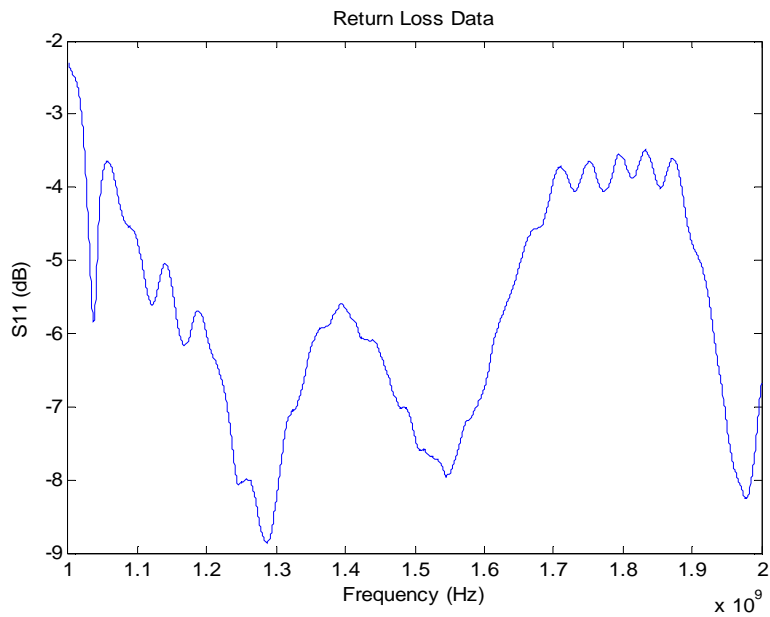


**Figure 38: 2 mm Antenna  $S_{11}$**

Calibration testing produced the following return loss for  $S_{22}$ :

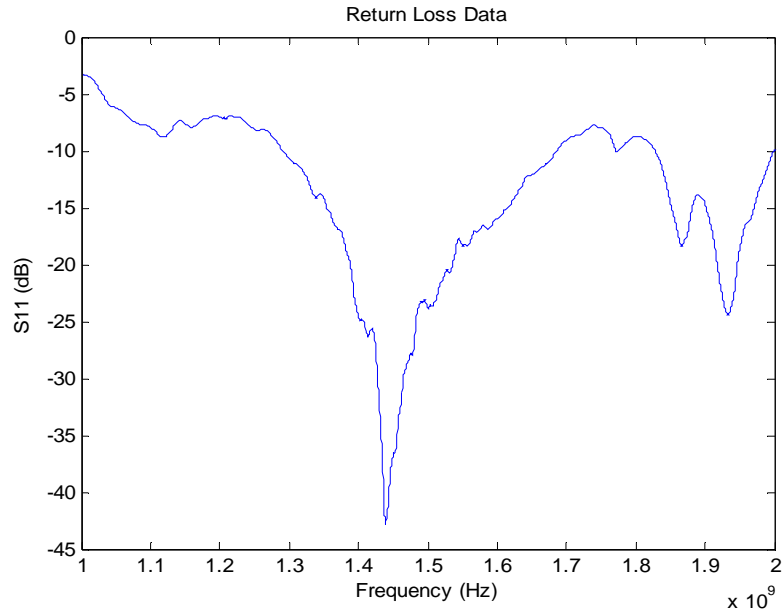


**Figure 39: 2 mm Antenna  $S_{22}$**

Calibration testing produced the isolation:

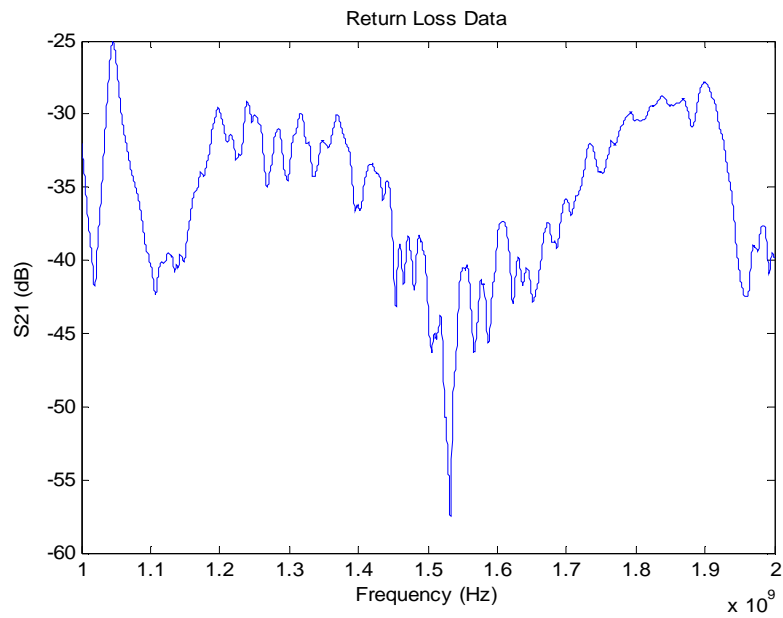


**Figure 40: 2 mm Antenna  $S_{21}$**

The most important thing to note is that the isolation is around -30 dB in the band for which we are designing the antenna (1.1 GHz to 1.6 GHz). We would like to see better

return loss results for both  $S_{11}$  and  $S_{22}$ . Ideally, we would like to see around -10 dB across the band.

These results were better than the 1.2 mm center conductor design, but there was still room for improvement. Therefore, we proceed to scale the balun up in size; we created a balun whose center conductor was 3 mm by 3 mm. Unfortunately, we were unable to perform calibration testing on the 3 mm antenna. The initial look at the network analyzer showed positive results, so we fixed the hybrids and the antenna to the choke ring ground plane so that it could later be shipped to UNAVCO for testing. We then reconnected the antenna to the network analyzer to measure the return loss and isolation with everything fixed to the ground plane. Figure 41 shows the  $S_{11}$  return loss:

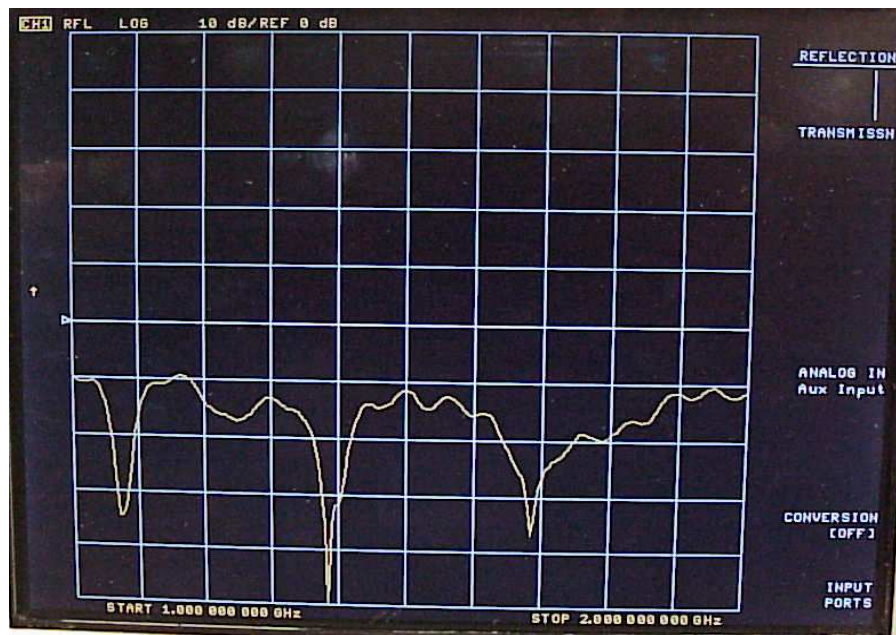


Figure 41: 3 mm Antenna  $S_{11}$

Figure 42 shows the  $S_{22}$  return loss:

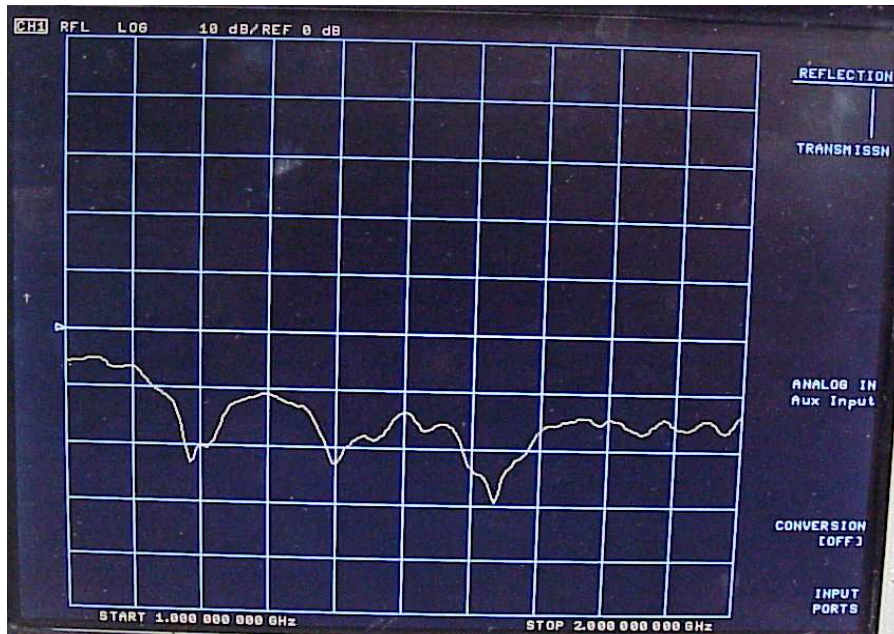


Figure 42: 3 mm Antenna  $S_{22}$

Figure 43 shows the isolation:

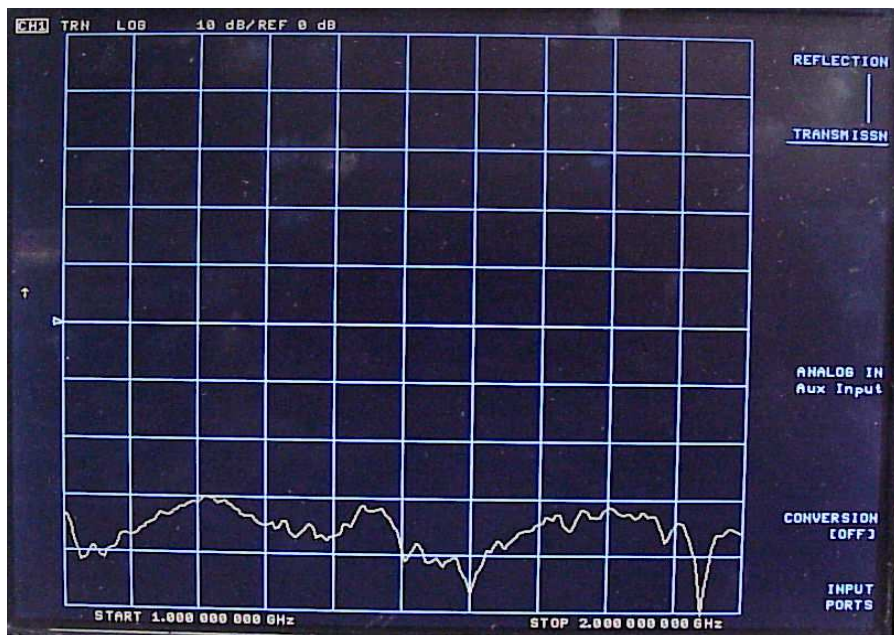


Figure 43: 3 mm Antenna  $S_{21}$

Next, we connected both of the  $180^\circ$  hybrids to a  $90^\circ$  in order to produce RHCP. We then drove the  $90^\circ$  hybrid with port 1 of the network analyzer and took a picture of the results:

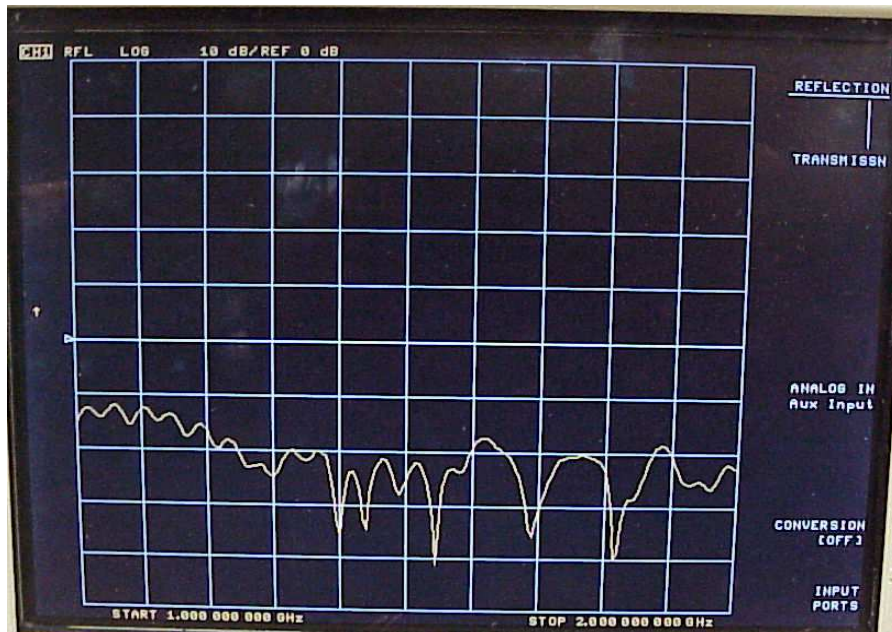


Figure 44: 3 mm Antenna  $S_{11}$  with  $90^\circ$  hybrid

The results from this antenna are very good. All of the return loss measurements indicate a -10 dB bandwidth from around 1 to 2 GHz as well as -30 dB isolation.

## Second Antenna Conclusions

The 1.2 mm antenna's results were similar to the results of our first design. Increasing the size of the center conductor seemed to drastically improve the performance of the antenna. The quad line antenna with the 3 mm by 3 mm center conductor is a very good design. In addition to the good results, the design is very sturdy, and is easily fixed to a choke ring ground plane. Also, the antennas can easily be replicated, since the Teflon pyramid, brass wings, printed circuit board, and coaxial cable connectors can be accurately recreated in large numbers. The balun would be the only part requiring creativity, since the jig that we used for the 1.2 mm center conductor balun was too small for the 3 mm center conductor balun. For these reasons, we needed to use clamps to hold the microstrip lines to the center conductor as well as a great deal of patience.

The following figures depict the final antenna attached to the ground plane:



**Figure 45: Final Design Top View**

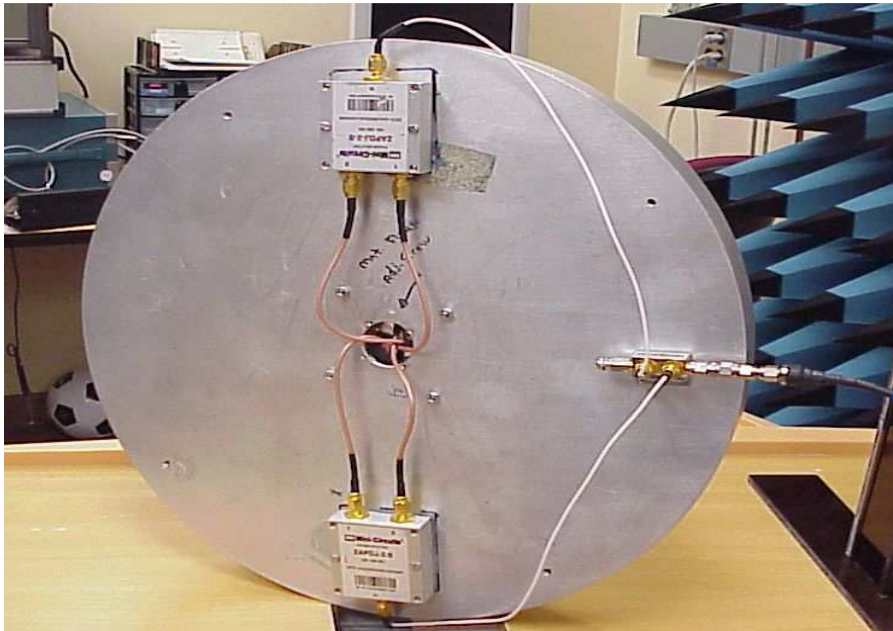


**Figure 46: Final Design Bottom View**



**Figure 47: Final Design Side View**

## Appendix A: Design Parameters

Properties: Project2\_actual\_with\_pcb - HFSSDesign1

Local Variables

Value
  Optimization
  Tuning
  Sensitivity
  Statistics

Name	Value	Unit	Evaluated Value	Description
dipole_radius	2	mm	2mm	the radius of the dipole
dipole_wing_length	75	mm	75mm	Length of each dipole
x_box	500	mm	500mm	radiation box
y_box	500	mm	500mm	radiation box
z_box	500	mm	500mm	radiation box
radius_coax_outer	1	mm	1mm	radius of each cable
thickness	0.2	mm	0.2mm	thickness of the outer cylinder
radius_coax_inner	radius_coax_o...		0.8mm	radius of the inner layer of the...
coax_height	63	mm	63mm	the height of the cable
center_cond_radius	0.4572	mm	0.4572mm	radius of the center conductor
center_cond_height	coax_height+....		64.5748mm	Height of the inner conductor
space_gap	2	mm	2mm	gap between the outer cylind...
alpha	90	deg	90deg	the angle the wing spreads out
wing_length	20.5	mm	20.5mm	length of the wing
wing_depth	tan(-beta)*win...		-17.2015424391342mm	sets the points for the wings u...
mystery_angle	45 deg - alpha/2		0deg	used in trig to alter wing para...
dist	(center_cond_...		29.6379564693654mm	used in trig to alter wing para...
beta	40	deg	40deg	droop angle
plate_position	1	mm	1mm	
offset_inner	offset_inner0-1...		3mm	
gamma	1	mm	1mm	choke ring - bottom corrugatio..
H	10	mm	10mm	choke ring - ring period (varia...
w_x	9	mm	9mm	choke ring
ground1	180	mm	180mm	choke ring - total diameter (v...
G	6	mm	6mm	choke ring - ring thickness { [...
offset	-3.5	mm	-3.5mm	choke ring
height	height_var+off...		23mm	choke ring - tooth height (vari...
radius_outer_base	65	mm	65mm	choke ring - radius of the cent..
delta	-1	mm	-1mm	choke ring - top corrugation t...
offset_inner0	15	mm	15mm	choke ring - bottom height at t..
s	0.94		0.94	choke ring scale for all
height_var	8	mm	8mm	
xtra_height	0	mm	0mm	
start	0	mm	0mm	

Figure 48: Design parameters for first design

Properties: raytheon\_antenna - HFSSDesign1

Local Variables

Value
  Optimization
  Tuning
  Sensitivity
  Statistics

Name	Value	Unit	Evaluated Value	Description
phi_scan	0	deg	0deg	dummy
theta_scan	0	deg	0deg	dummy
x_box	2.5*d		100mm	big box
y_box	2.5*d		100mm	big box
z_box	150	mm	150mm	big box
delta	0	mm	0mm	antenna wing convexity
offset	0.6	mm	0.6mm	dummy here
trace_width	1		1	dummy here
c	20	mm	20mm	dummy here
pcb_thickness	62*25.4mm/10...		1.5748mm	PCB
feed_width	2*a1		1.27mm	feed trace width
a	150*25.4mm/1...		1.905mm	feed column 3x width
a1	50*25.4mm/10...		0.635mm	feed column width
b	30	mm	30mm	antenna half width
h	15	mm	15mm	flower height only
width	2*b		60mm	antenna full width
center_height	45	mm	45mm	antenna height above ground
d	40	mm	40mm	unit cell half size
d1	d		40mm	ground plane size
k	0.2		0.2	relative size of bottom pad
m	1.8		1.8	relative width of one wing
h_bottom	2	mm	2mm	offset from bottom
microstrip_length	20	mm	20mm	BALUN
microstrip_width	microstrip_mil*...		2.54mm	BALUN
microstrip_mil	100		100	BALUN
microstrip_width0	50*25.4mm/10...		1.27mm	BALUN
center_strip	3	mm	3mm	BALUN
feed_radius	1.5	mm	1.5mm	BALUN
feed_center	0.5	mm	0.5mm	BALUN
border_offset	1	mm	1mm	BALUN
filter_center_x	d/2		20mm	FILTER
filter_center_y	0	mm	0mm	FILTER
filter_length	25	mm	25mm	FILTER
filter_width	0.5	mm	0.5mm	FILTER
filter_gap	0.4	mm	0.4mm	FILTER
filter_cut_length	2.5	mm	2.5mm	FILTER
filter_via_radius	0.3	mm	0.3mm	FILTER

Add... Remove

Figure 49: Design parameters for second design

## Appendix B: MATLAB Code

All MATLAB calibration testing code was provided by Eduardo Oliveira.

### ***S<sub>11</sub> Calibration***

```
%S11 calibration
%fun with freq resp emo
%Ed Oliveira
%Oct 15 2007
% based on MVL code
% fixed transmission line impedance rotation

%clear
%startf=0.550e9;
startf=1e9;
%stopf=0.7e9;
stopf=2e9;
fstep=.4e6;
%fstep=5e4;
startf=input('Input start frequency in Hz:')
stopf=input('\nInput stop frequency in Hz:')

%freqs =
linspace(freq_resp_lib.start,freq_resp_lib.stop,numel(freq_resp_lib.freq_data));
freqs= (startf:fstep:stopf);

fprintf('\nConnect GPIB cable between computer and network analyzer')
input(' and press return\n')

fprintf('Connect the short standard to the end of the input cable')
input(' and press return\n')
freq_resp_lib = get_freq_resp(startf, stopf, fstep, 'S11');
freq_resp_lib.freq_data = conj(freq_resp_lib.freq_data);
s11short=freq_resp_lib.freq_data;
```

```

fprintf('Connect the 50 ohm standard to the end of the input cable')
input(' and press return\n')
freq_resp_lib = get_freq_resp(startf, stopf, fstep, 'S11');
freq_resp_lib.freq_data = conj(freq_resp_lib.freq_data);
s11matched=freq_resp_lib.freq_data;

fprintf('Connect the antenna to the end of the input cable')
input(' and press return\n')
freq_resp_lib = get_freq_resp(startf, stopf, fstep, 'S11');
freq_resp_lib.freq_data = conj(freq_resp_lib.freq_data);
s11rot=freq_resp_lib.freq_data;

freq_resp_lib.freq_data=(s11rot-s11matched)./(s11matched-s11short);

Zt = 50*(freq_resp_lib.freq_data + 1)./(1- freq_resp_lib.freq_data);

figure(1);
plot(freqs,20*log10(abs(freq_resp_lib.freq_data))), title ('Return Loss
Data'), xlabel ('Frequency (Hz)'), ylabel('S11 (dB)');
figure(2)
plot(freqs,real(Zt)), title ('Complex Impedance Data'), xlabel
('Frequency (Hz)'), ylabel ('Impedance (Ohms)');
hold on; grid on;
plot(freqs,imag(Zt),'r--');
legend ('Real', 'Imaginary');
hold off
%figure(2)
%plot(freqs,(real(freq_resp_lib.freq_data)));
%subplot(3,1,3);
%figure(3)
%plot(freqs,(imag(freq_resp_lib.freq_data)));
%line(freqs,unwrap(angle(freq_resp_lib.freq_data)));
% figure(2);
% subplot(3,1,1);
% plot(freqs,abs(Impedance));
% subplot(3,1,2);
% plot(freqs,real(Impedance));
% subplot(3,1,3);

```

```
% plot(freqs,imag(Impedance));
```

## **$S_{21}$ Calibration**

```
%S11 calibration
%fun with freq resp emo
%Ed Oliveira
%Oct 15 2007
% based on MVL code
% fixed transmission line impedance rotation

clear;
%startf=0.550e9;
startf=1e9;
%stopf=0.7e9;
stopf=2e9;
fstep=.4e6;
%fstep=5e4;

%freqs =
linspace(freq_resp_lib.start,freq_resp_lib.stop,numel(freq_resp_lib.freq_data));
freqs= (startf:fstep:stopf);

fprintf('Connect GPIB cable between computer and network analyzer')
input(' and press return\n')

fprintf('Connect the Through standard to the end of the input cable')
input(' and press return\n')
freq_resp_lib = get_freq_resp(startf, stopf, fstep, 'S21');
freq_resp_lib.freq_data = conj(freq_resp_lib.freq_data);
s11through=freq_resp_lib.freq_data;

% fprintf('Connect the 50 ohm standard to the end of the input cable')
% input(' and press return\n')
% freq_resp_lib = get_freq_resp(startf, stopf, fstep, 'S11');
% freq_resp_lib.freq_data = conj(freq_resp_lib.freq_data);
% s11matched=freq_resp_lib.freq_data;
```

```

fprintf('Connect the antenna to the end of the input cable')
input(' and press return\n')
freq_resp_lib = get_freq_resp(startf, stopf, fstep, 'S21');
freq_resp_lib.freq_data = conj(freq_resp_lib.freq_data);
s11rot=freq_resp_lib.freq_data;

freq_resp_lib.freq_data=(s11rot)./(s11through);
Zt = 50*(freq_resp_lib.freq_data + 1)./(1- freq_resp_lib.freq_data);

figure(1);
plot(freqs,20*log10(abs(freq_resp_lib.freq_data))), title ('Return Loss
Data'), xlabel ('Frequency (Hz)'), ylabel('S21 (dB)');
figure(2)
plot(freqs,real(Zt)), title ('Complex Impedance Data'), xlabel
('Frequency (Hz)'), ylabel ('Impedance (Ohms)');
hold on; grid on;
plot(freqs,imag(Zt),'r--');
legend ('Real', 'Imaginary');
hold off
%figure(2)
%plot(freqs,(real(freq_resp_lib.freq_data)));
%subplot(3,1,3);
%figure(3)
%plot(freqs,(imag(freq_resp_lib.freq_data)));
%line(freqs,unwrap(angle(freq_resp_lib.freq_data)));
% figure(2);
% subplot(3,1,1);
% plot(freqs,abs(Impedance));
% subplot(3,1,2);
% plot(freqs,real(Impedance));
% subplot(3,1,3);
% plot(freqs,imag(Impedance));

```

# Appendix C: Testing Results of the First Design

## Primary Testing Results

### Antenna 1

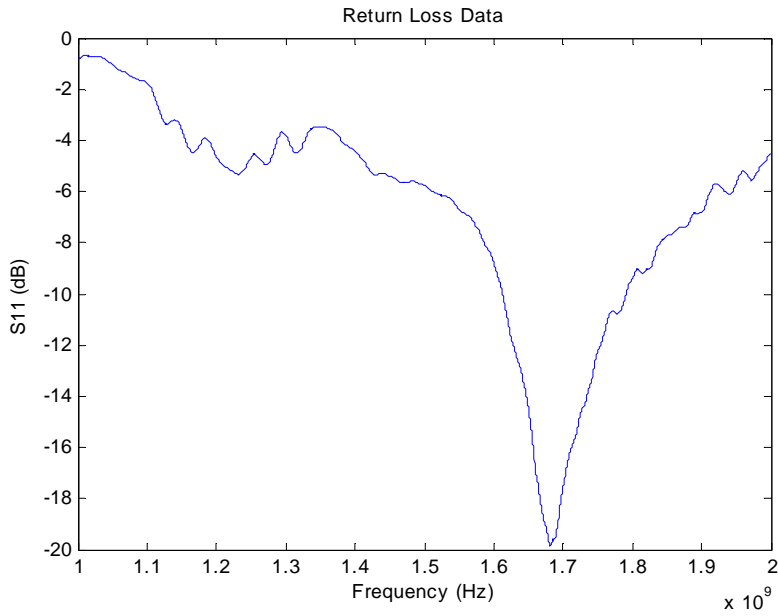


Figure 50: First Antenna 1  $S_{11}$

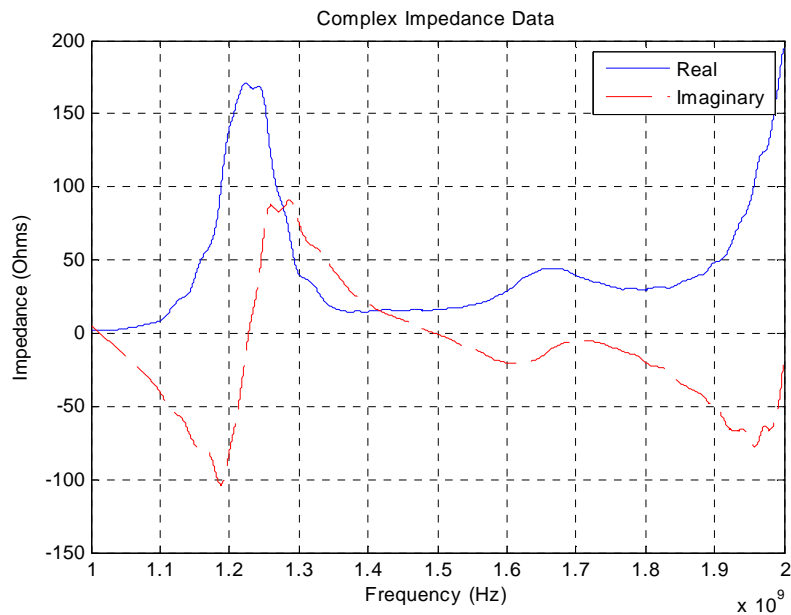
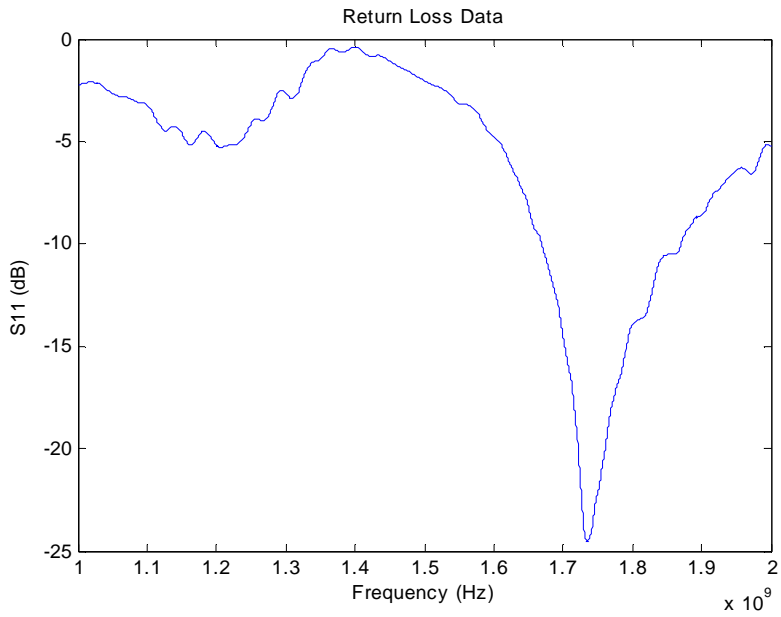
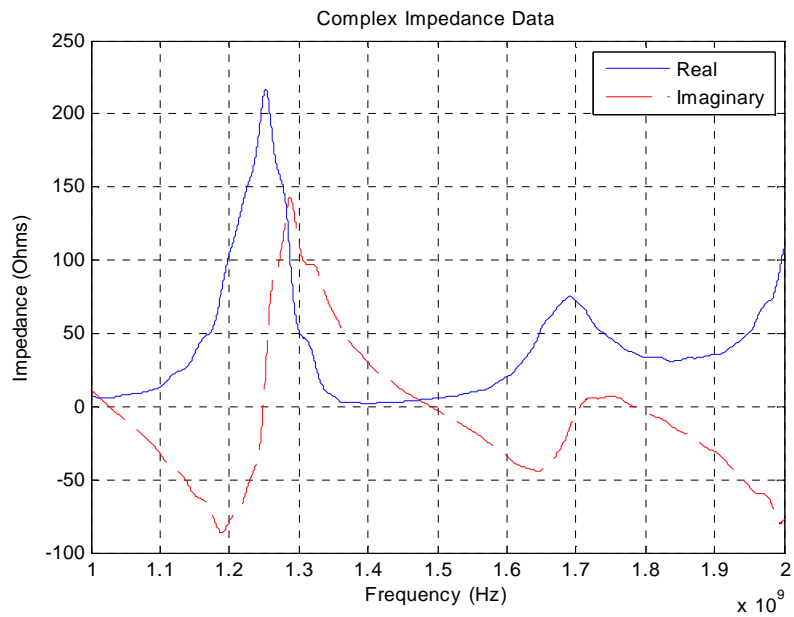


Figure 51: First Antenna 1  $S_{11}$  Impedance



**Figure 52: Second Antenna 1  $S_{11}$**



**Figure 53: Second Antenna 1  $S_{11}$  Impedance**

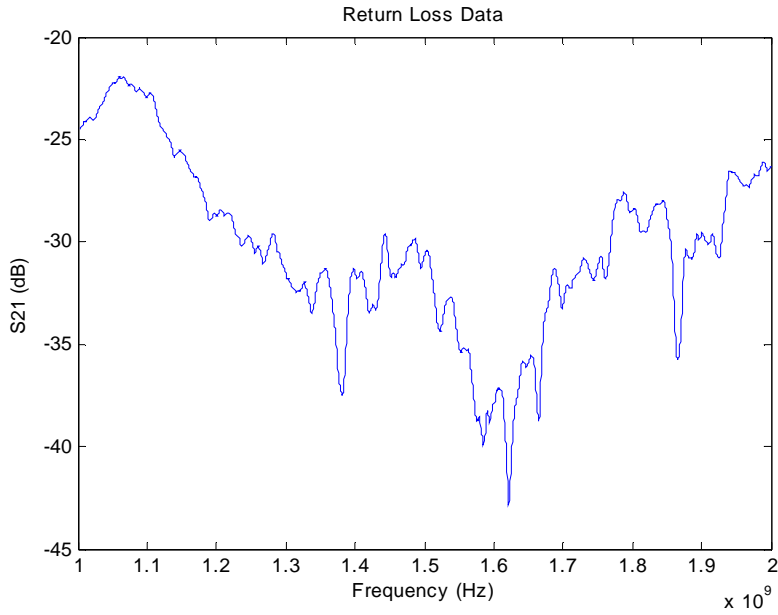


**Figure 54: Antenna 1 S<sub>21</sub>**

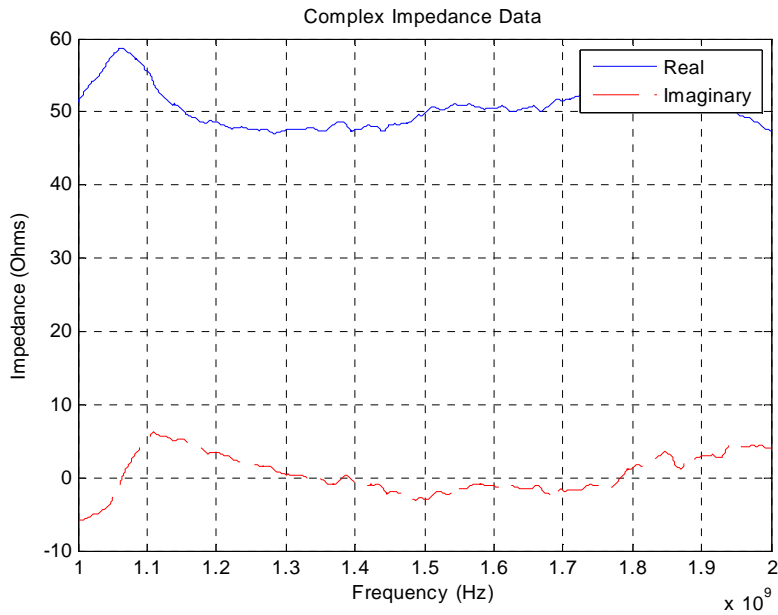


**Figure 55: Antenna 1 S<sub>21</sub> Calibration Impedance Results**

Since the graphs obtained by the computer generated calibrations were notably different than the network analyzer, we took a few pictures of the network analyzer. These pictures were taken while both hybrids were connected to the antenna.

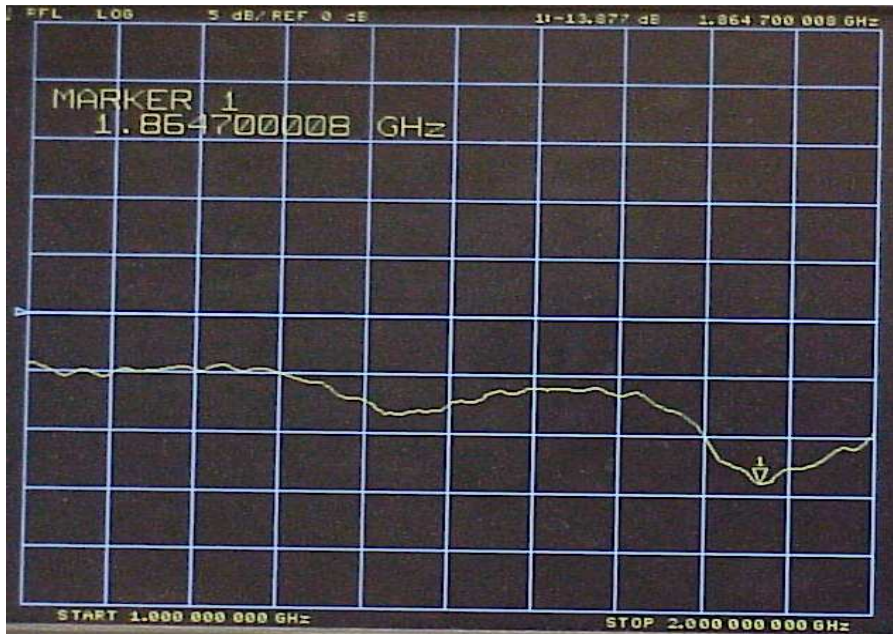


Figure 56: Antenna 1  $S_{11}$  Measured by Network Analyzer

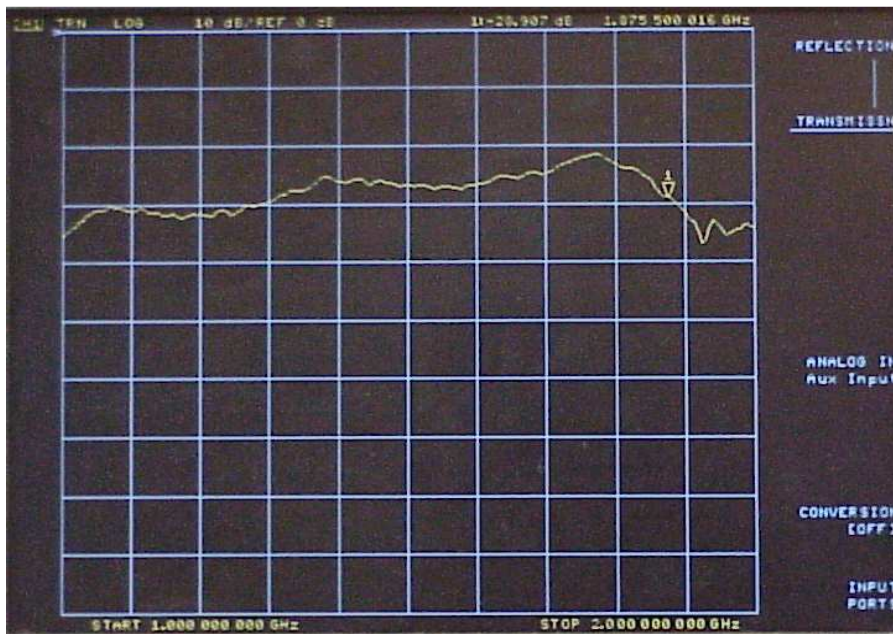
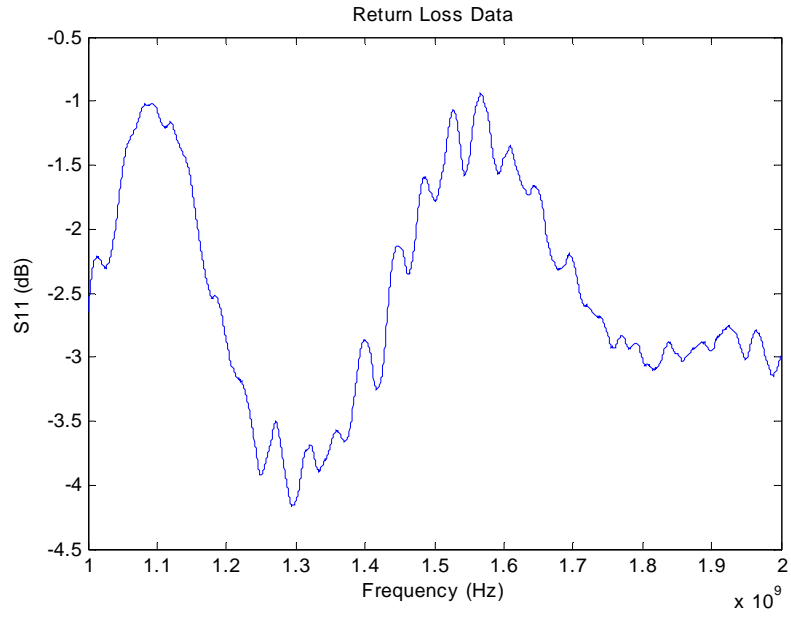
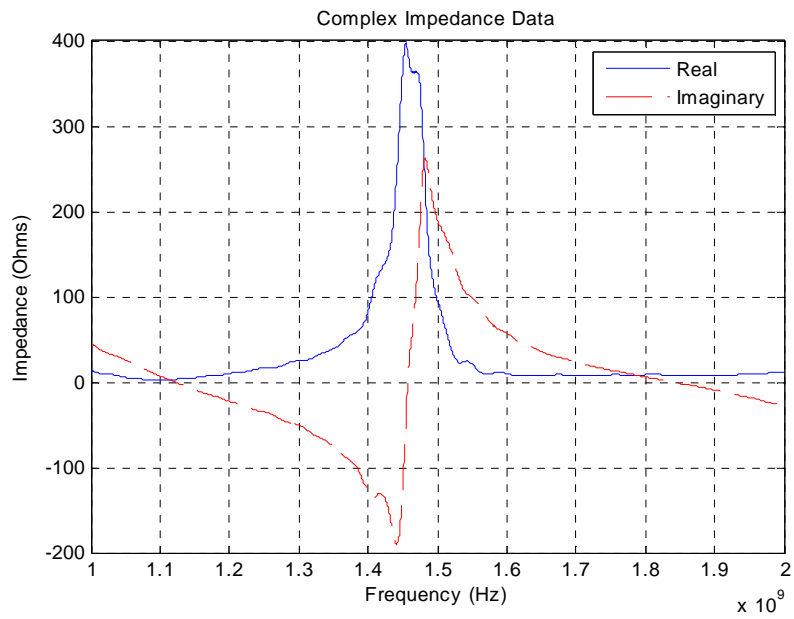


Figure 57: Antenna 1  $S_{21}$  Measured by Network Analyzer

## Antenna 2



**Figure 58: Antenna 2  $S_{11}$**



**Figure 59: Antenna 2  $S_{11}$  Impedance**

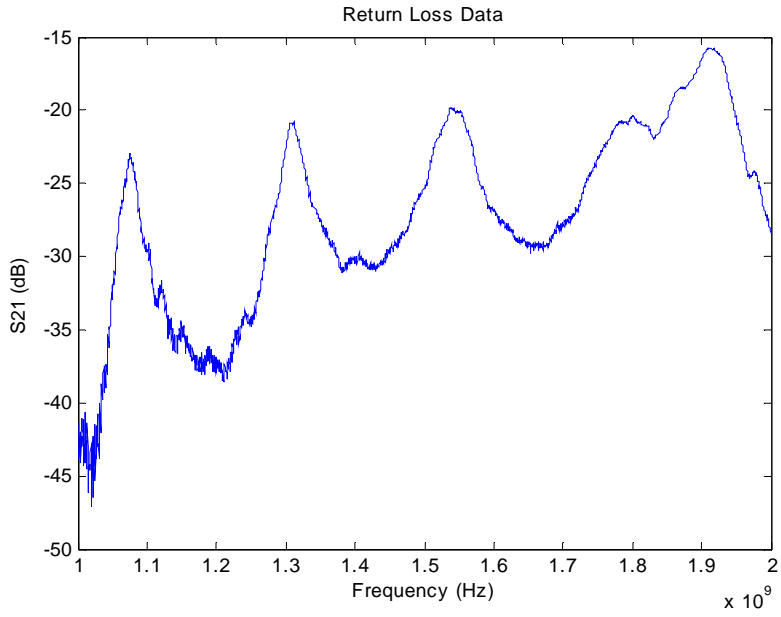


**Figure 60: Antenna 2  $S_{21}$**

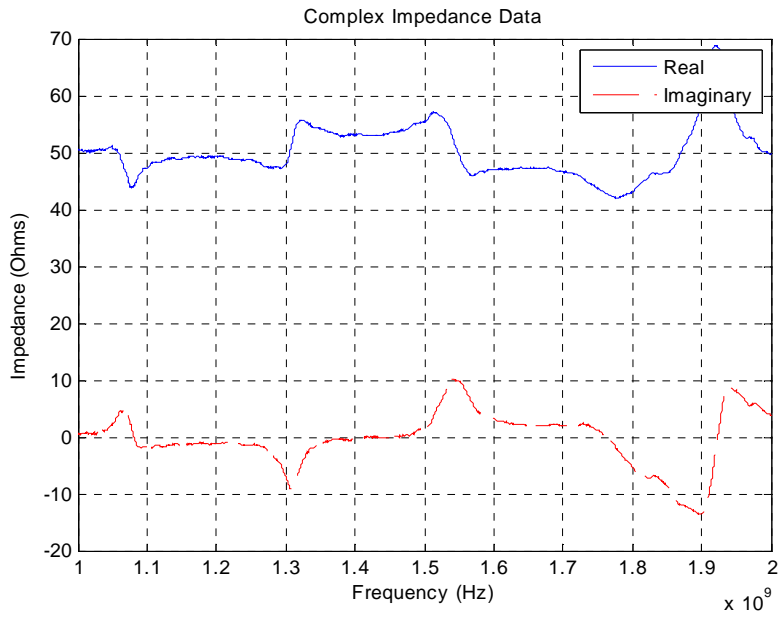


**Figure 61: Antenna 2  $S_{21}$  Impedance**

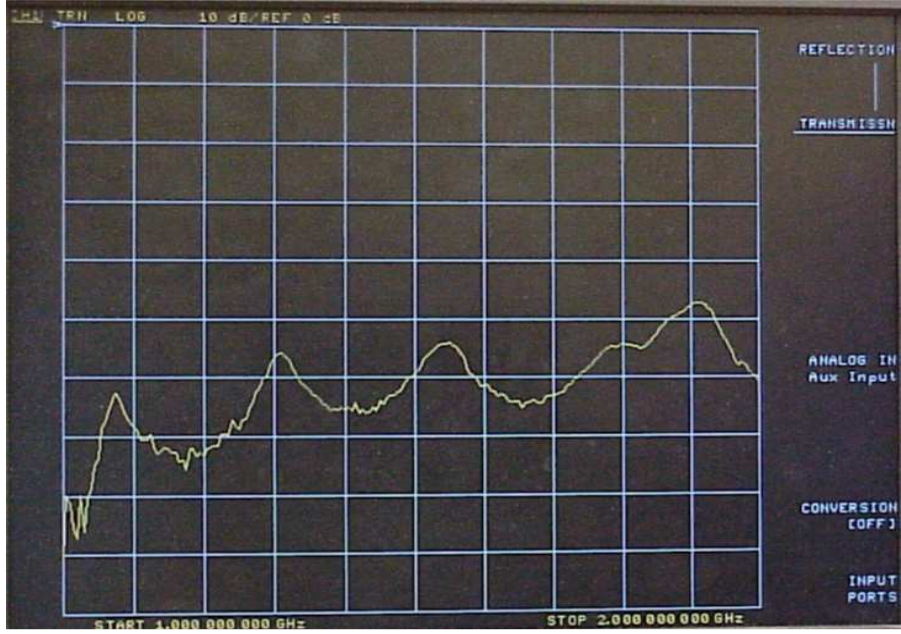


Figure 62: Antenna  $S_{21}$  Measured by Network Analyzer

### Antenna 3

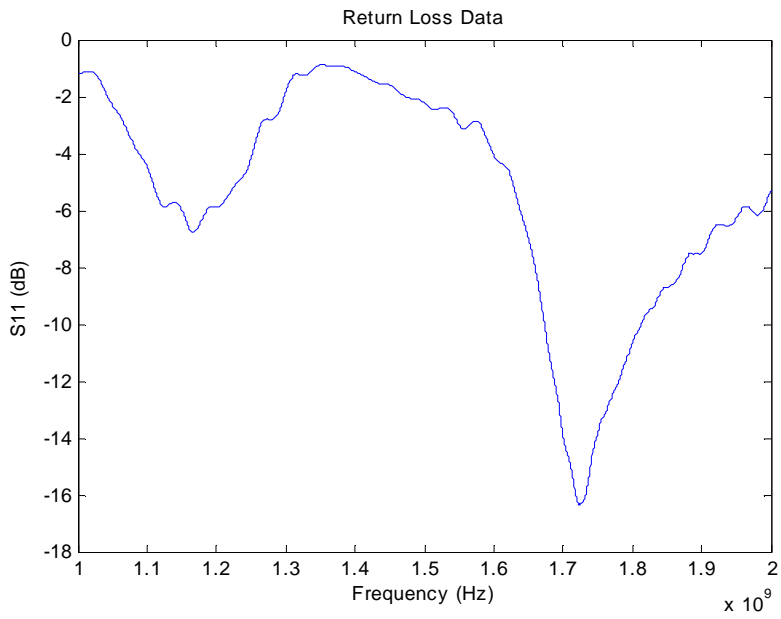
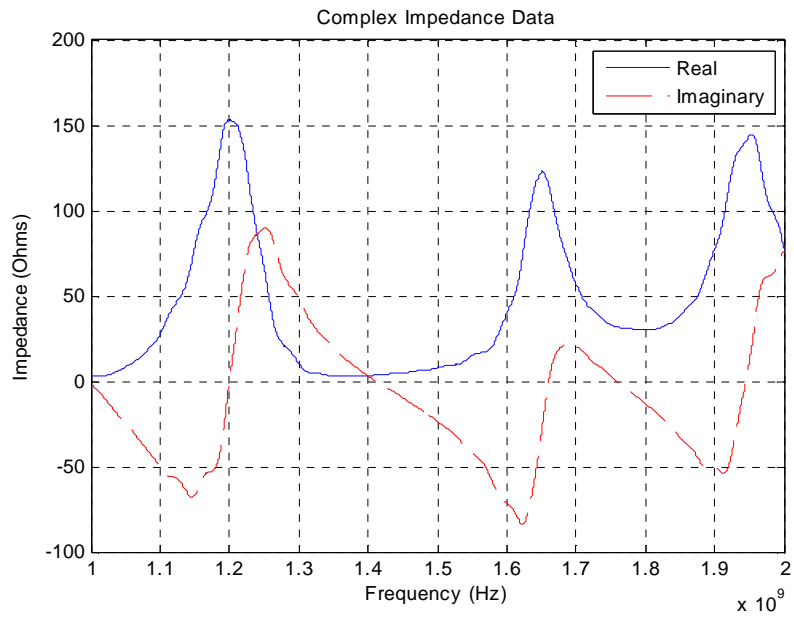
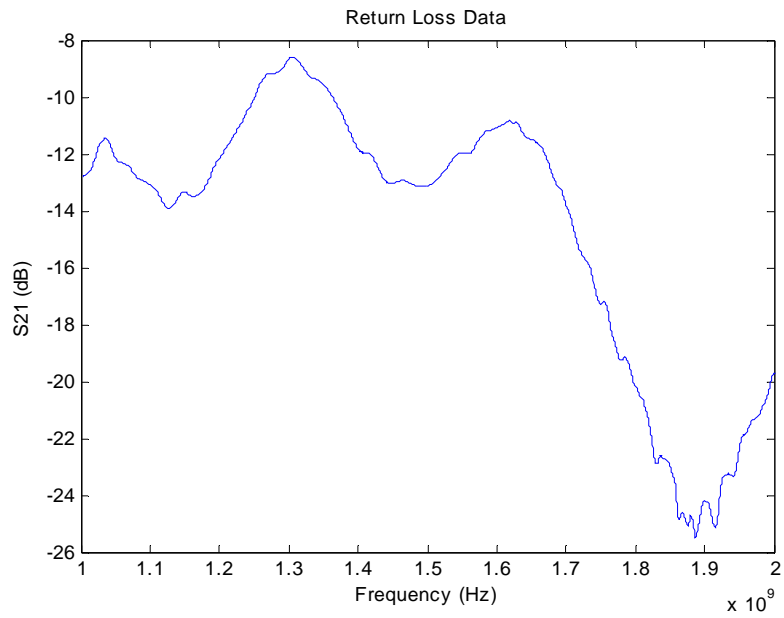


Figure 63: Antenna 3  $S_{11}$



**Figure 64: Antenna 3  $S_{11}$  Impedance**



**Figure 65: Antenna 3  $S_{21}$**

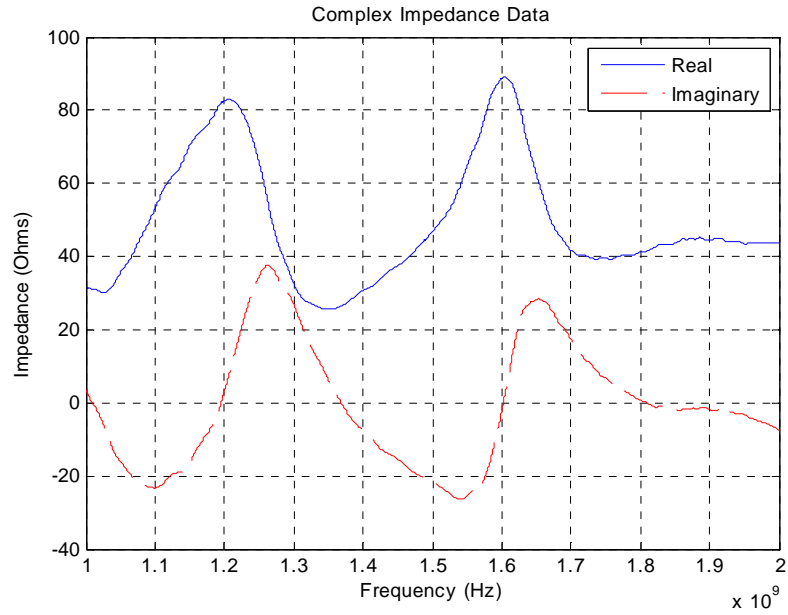


**Figure 66: Antenna 3  $S_{21}$  Impedance**

## ***Results of Testing without Ground plane***

### **Antenna 1**

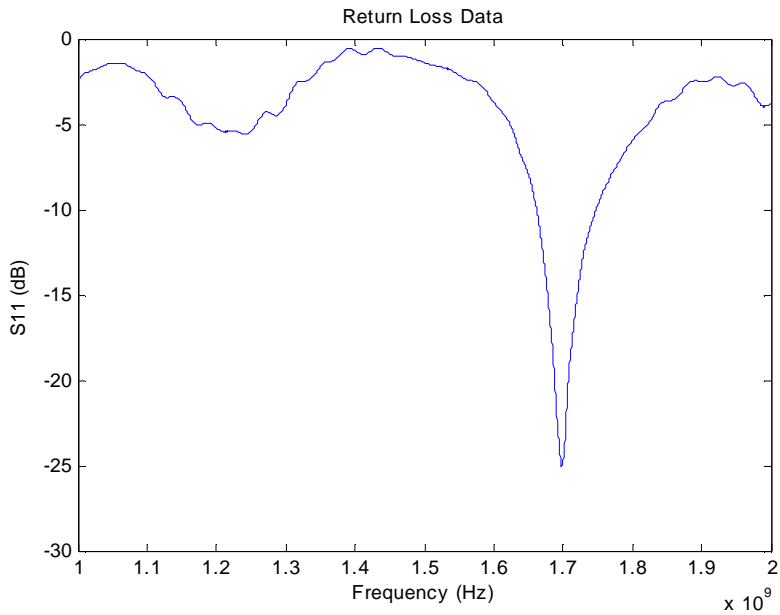


**Figure 67: Antenna 1  $S_{11}$  without Ground plane**

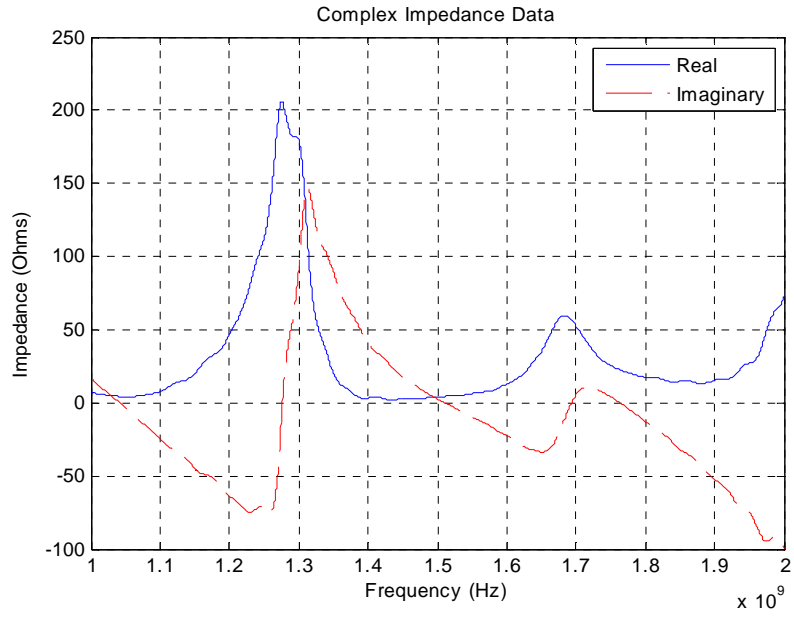


**Figure 68: Antenna 1  $S_{11}$  Impedance without Ground plane**

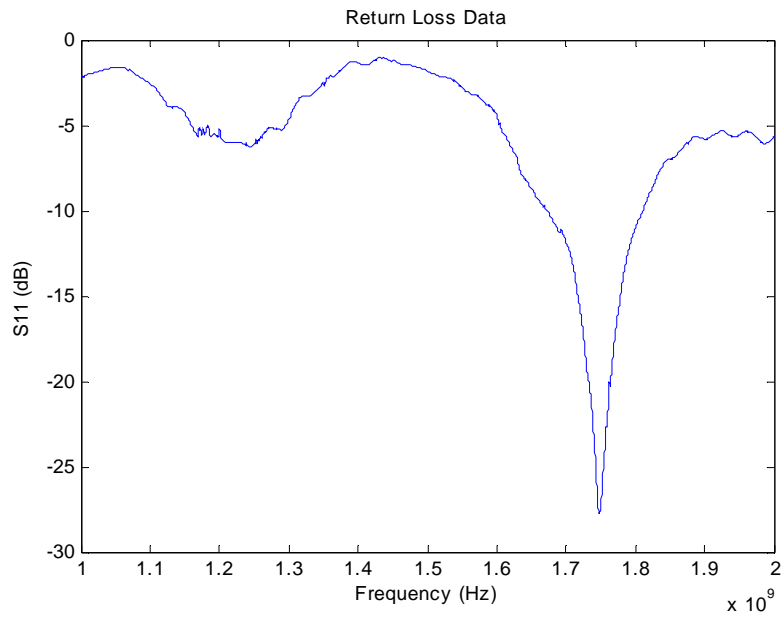


**Figure 69: Antenna 1  $S_{22}$  without Ground plane**

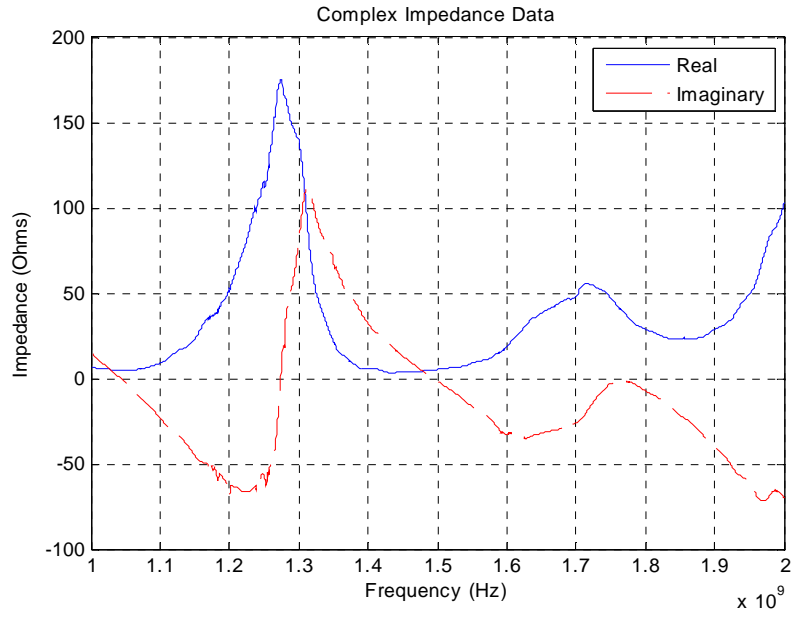


**Figure 70: Antenna 1 S<sub>22</sub> Impedance without Ground plane**

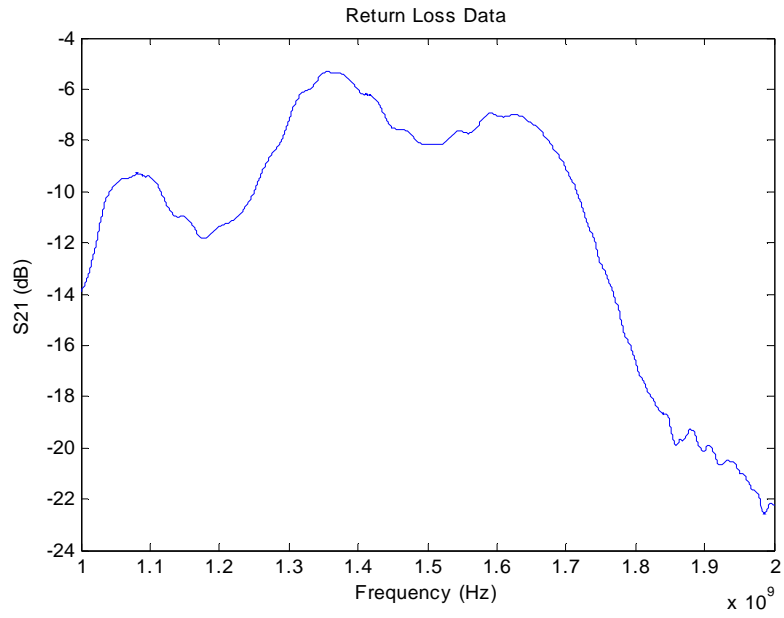


**Figure 71: Antenna 1 S<sub>21</sub> without Ground plane**

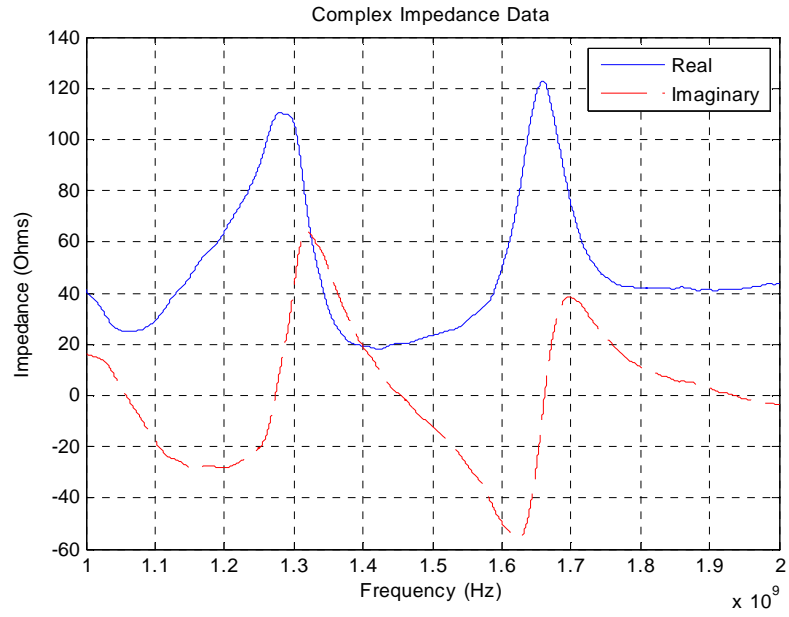


**Figure 72: Antenna 1  $S_{21}$  Impedance without Ground plane**

## Antenna 2

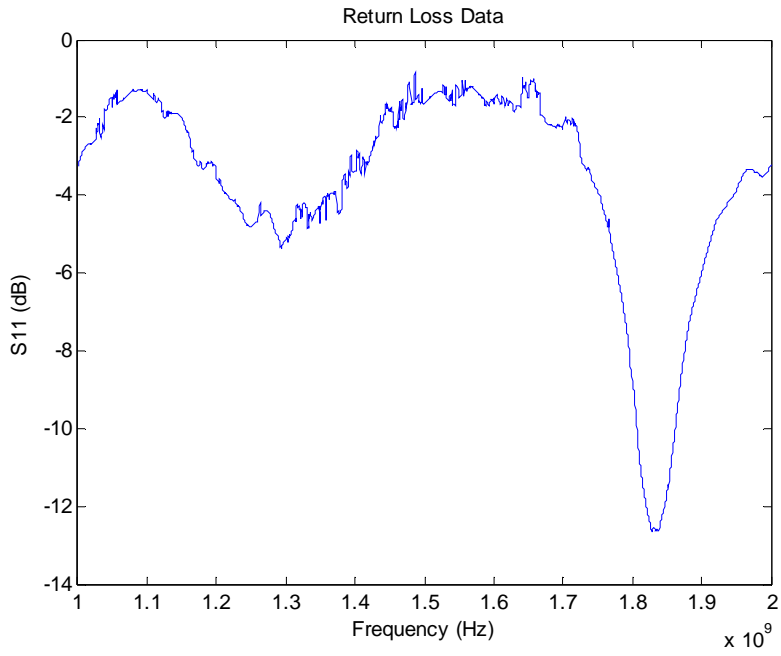


**Figure 73: Antenna 2  $S_{11}$  without Ground plane**

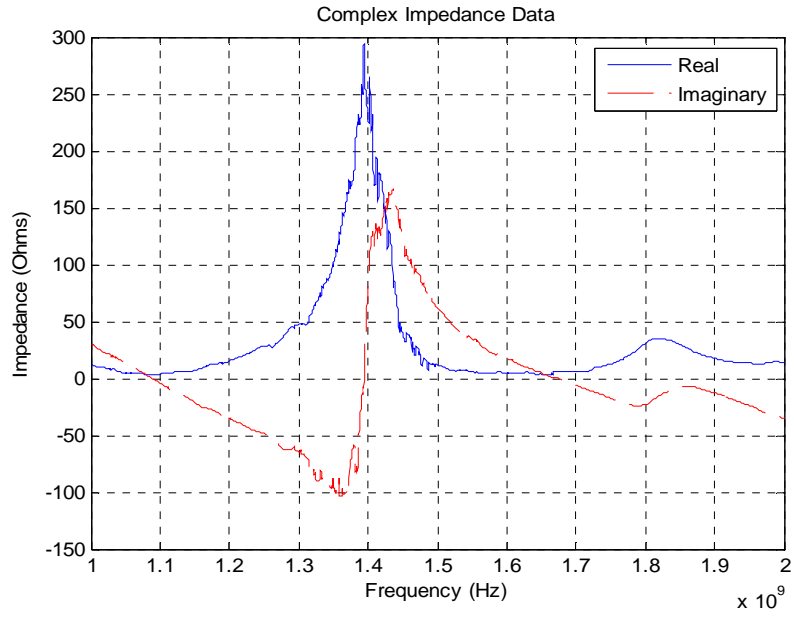


**Figure 74: Antenna 2  $S_{11}$  Impedance**

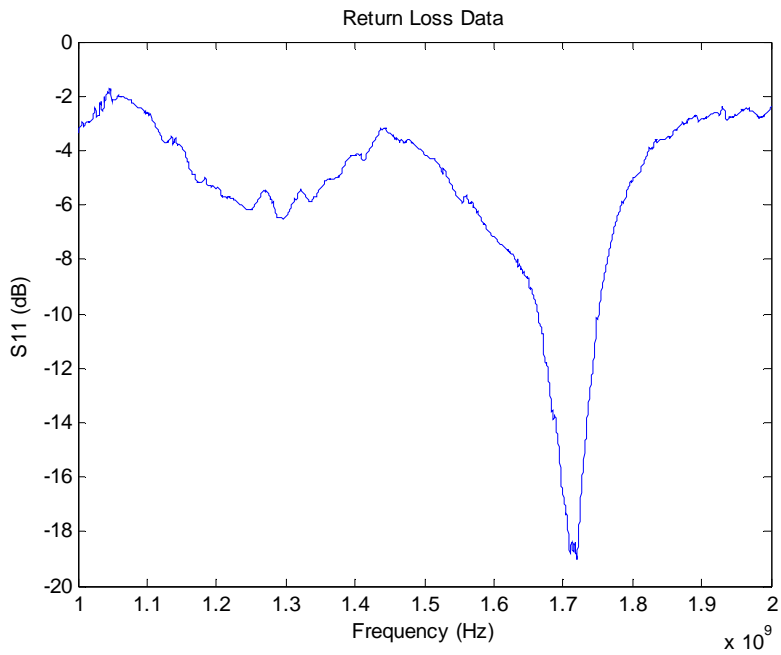


**Figure 75: Antenna 2  $S_{22}$  without Ground plane**

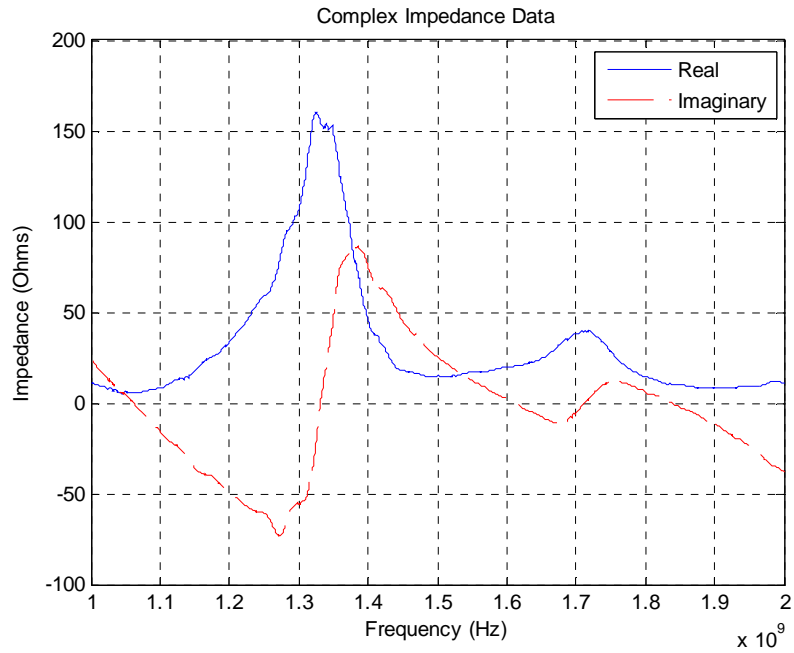


**Figure 76: Antenna 2  $S_{22}$  Impedance without Ground plane**

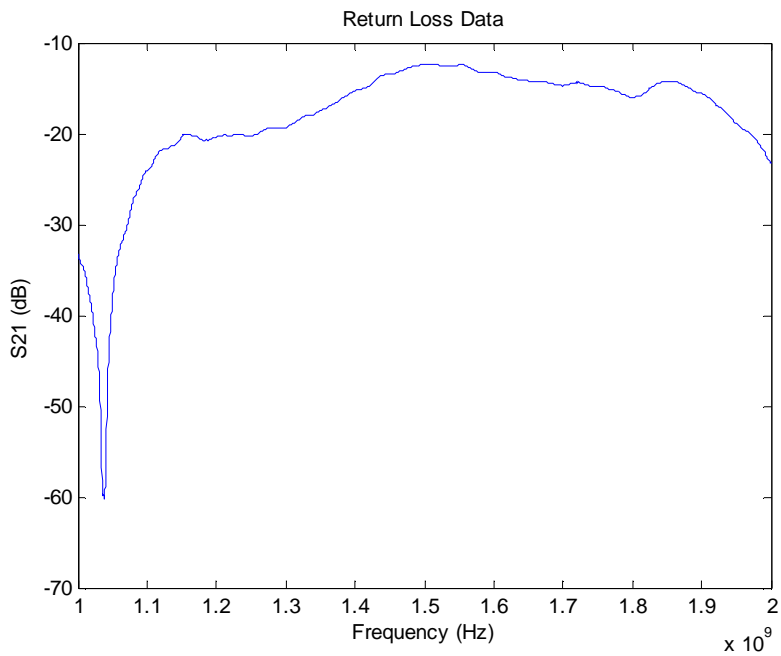


**Figure 77: Antenna 2  $S_{21}$  without Ground plane**

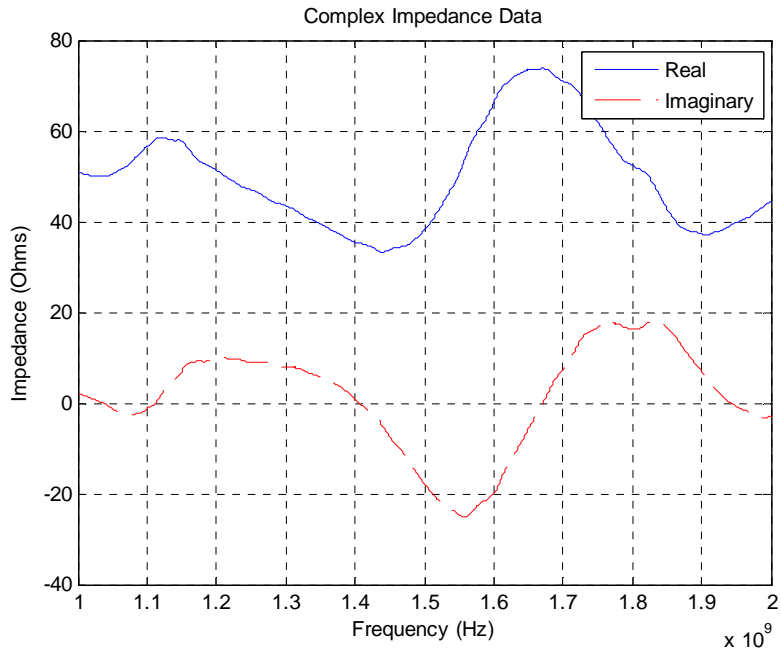


**Figure 78: Antenna 2  $S_{21}$  Impedance without Ground plane**

### Antenna 3

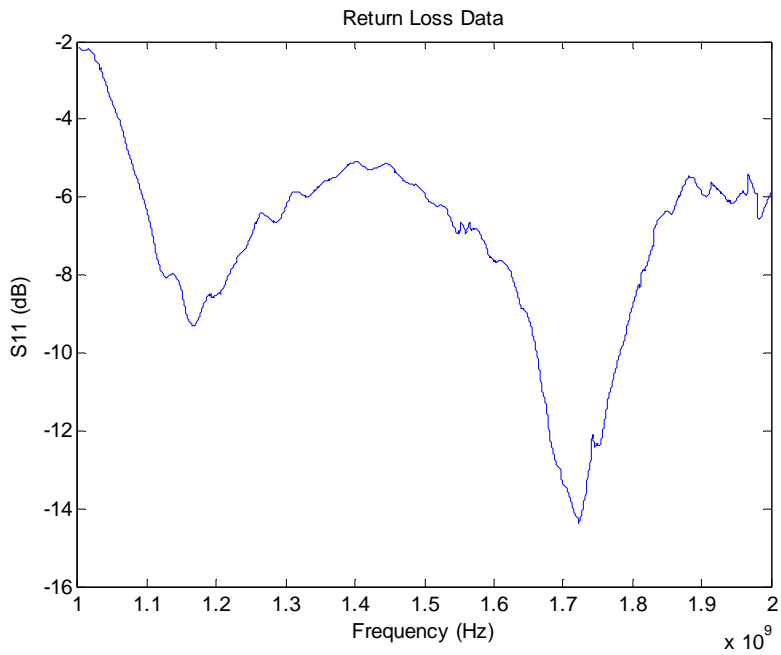


**Figure 79: Antenna 3  $S_{11}$  without Ground plane**

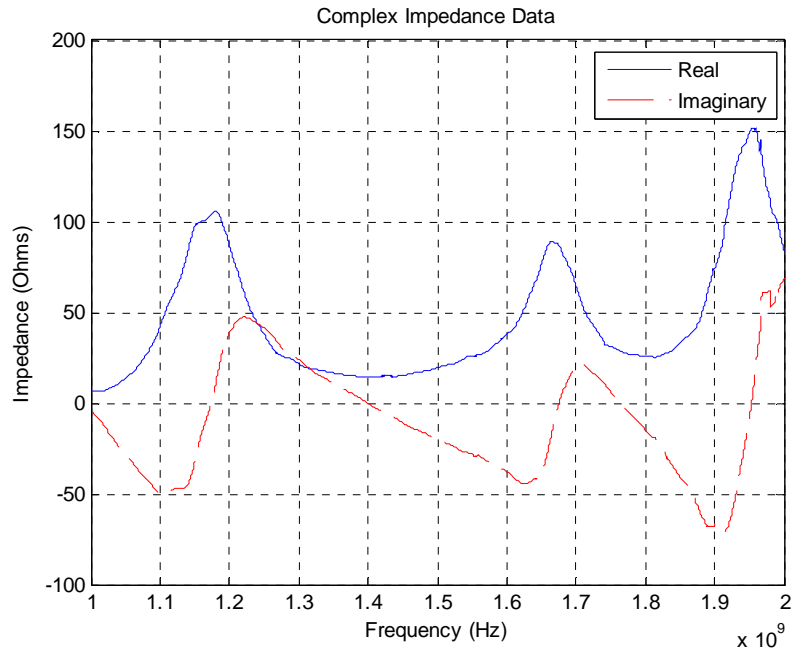


**Figure 80: Antenna 3  $S_{11}$  Impedance without Ground plane**

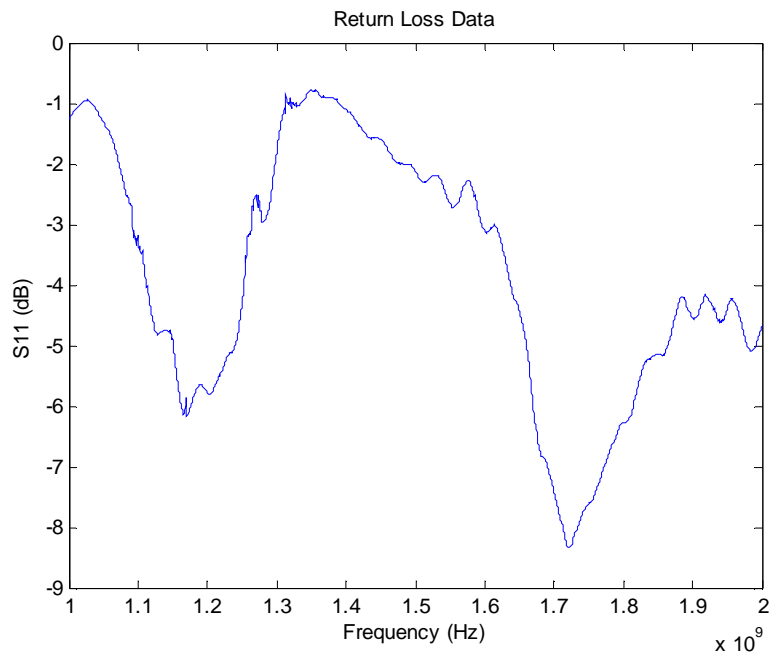


**Figure 81: Antenna 3  $S_{22}$  without Ground plane**

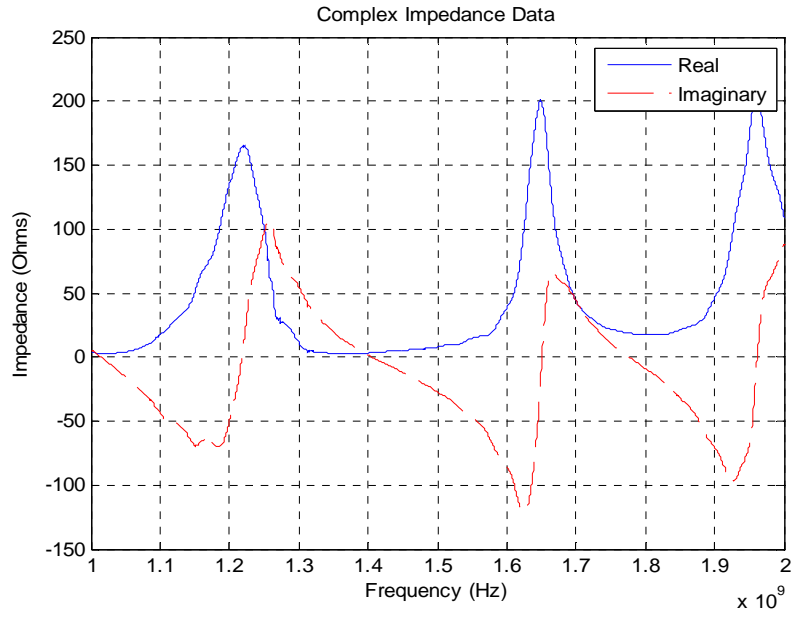


**Figure 82: Antenna 3  $S_{22}$  Impedance without Ground plane**

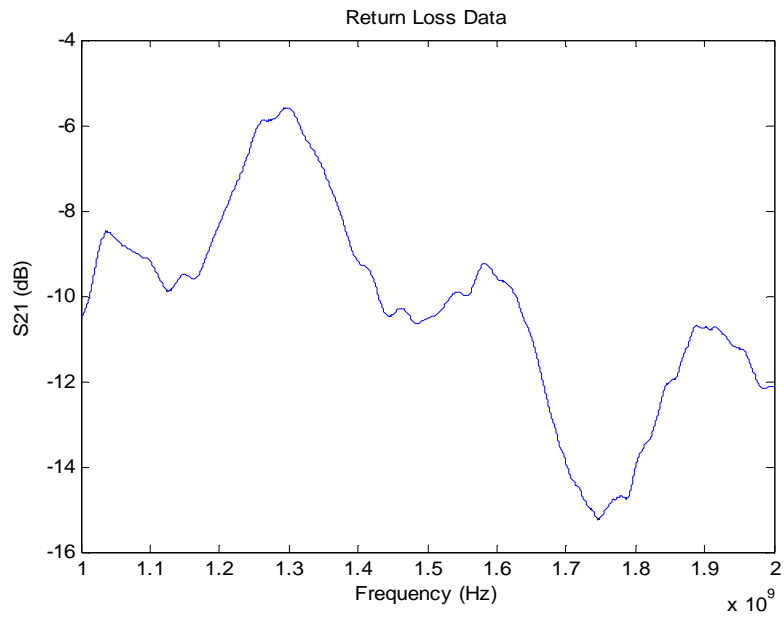


**Figure 83: Antenna 3  $S_{21}$  without Ground plane**

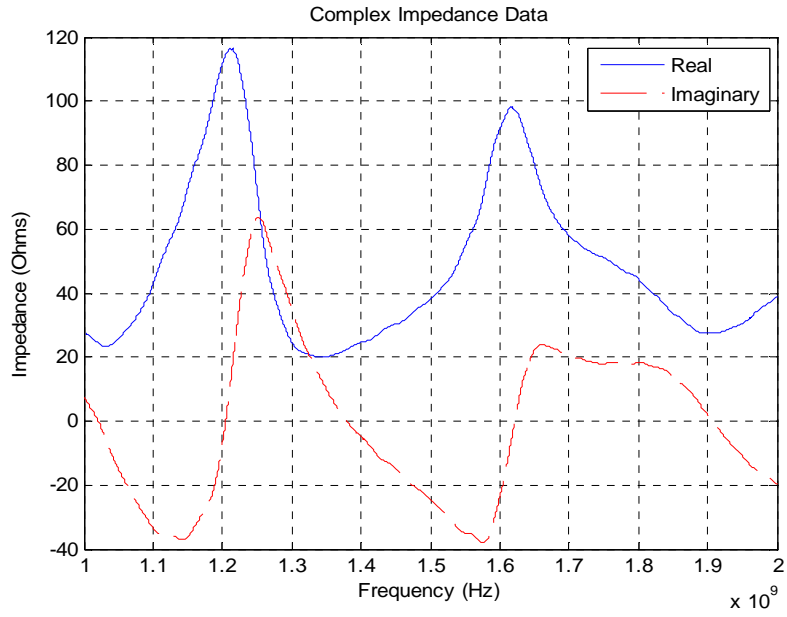


**Figure 84: Antenna 3  $S_{21}$  Impedance without Ground plane**

## ***Impedance Testing***

### **Antenna 1**

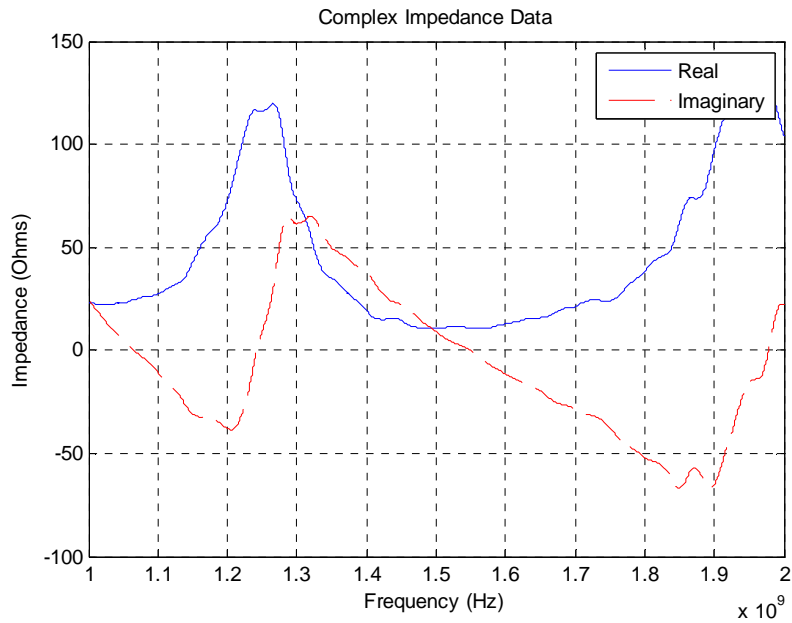


**Figure 85: Antenna 1 Port 1 Impedance**

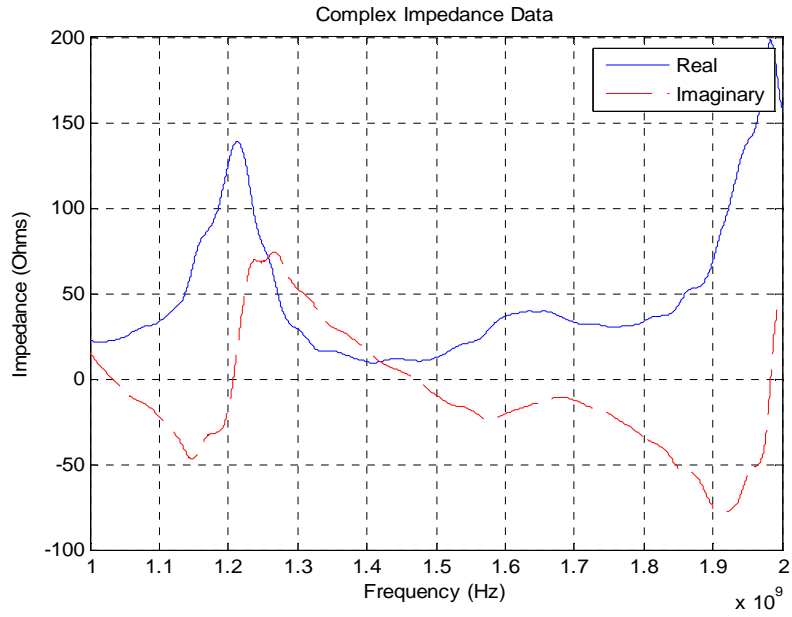


**Figure 86: Antenna 1 Port 2 Impedance**

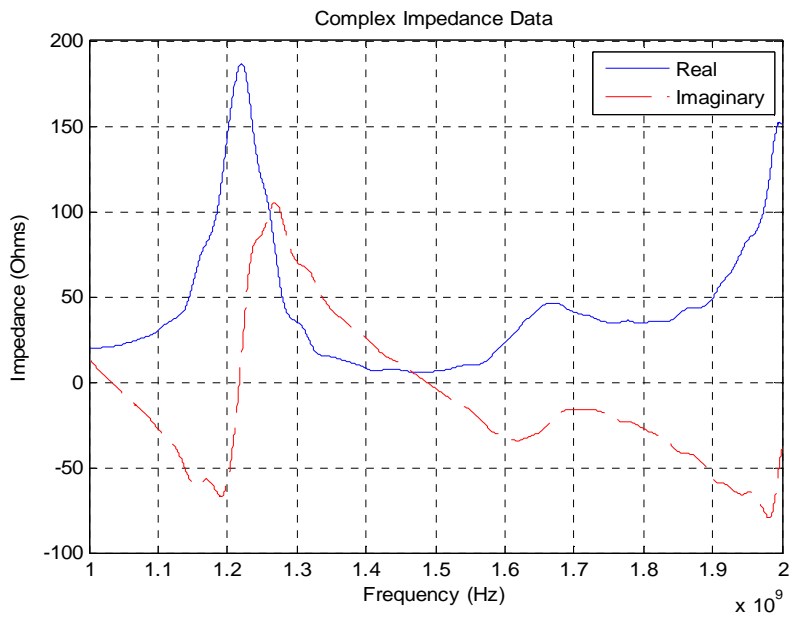


**Figure 87: Antenna 1 Port 3 Impedance**

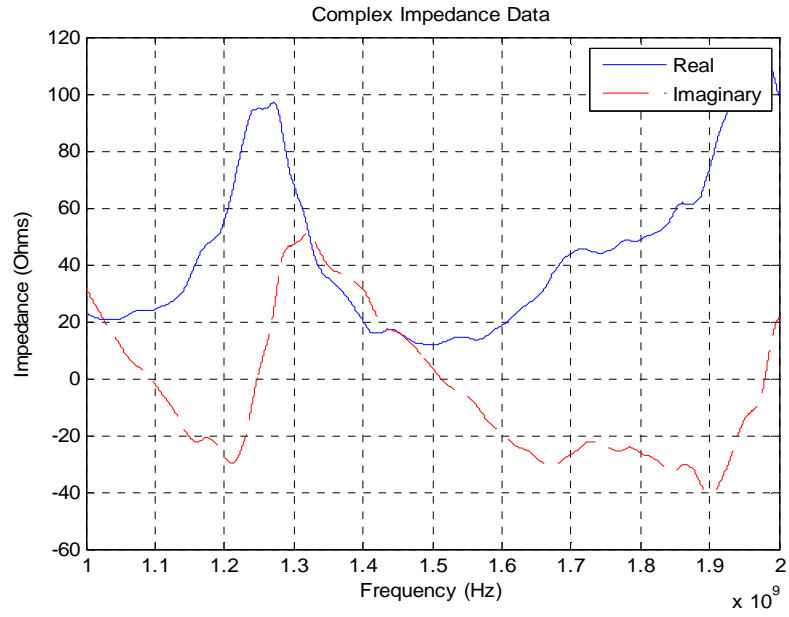


**Figure 88: Antenna 1 Port 4 Impedance**

## Antenna 2

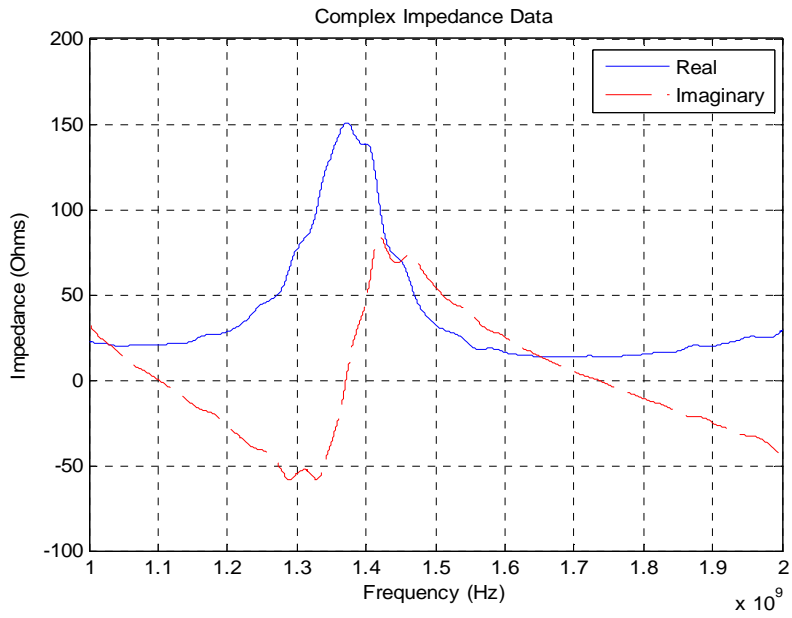


**Figure 89: Antenna 2 Port 1 Impedance**

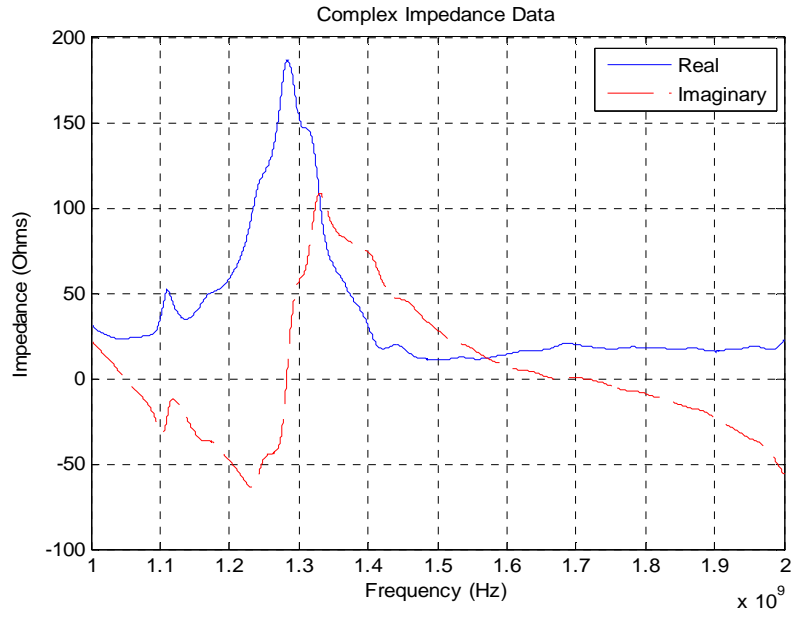


**Figure 90: Antenna 2 Port 2 Impedance**

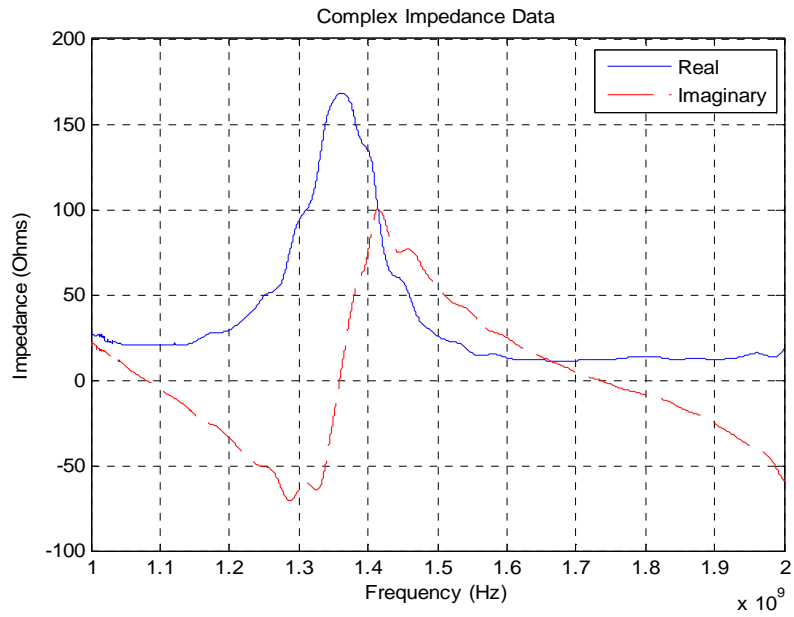


**Figure 91: Antenna 2 Port 3 Impedance**

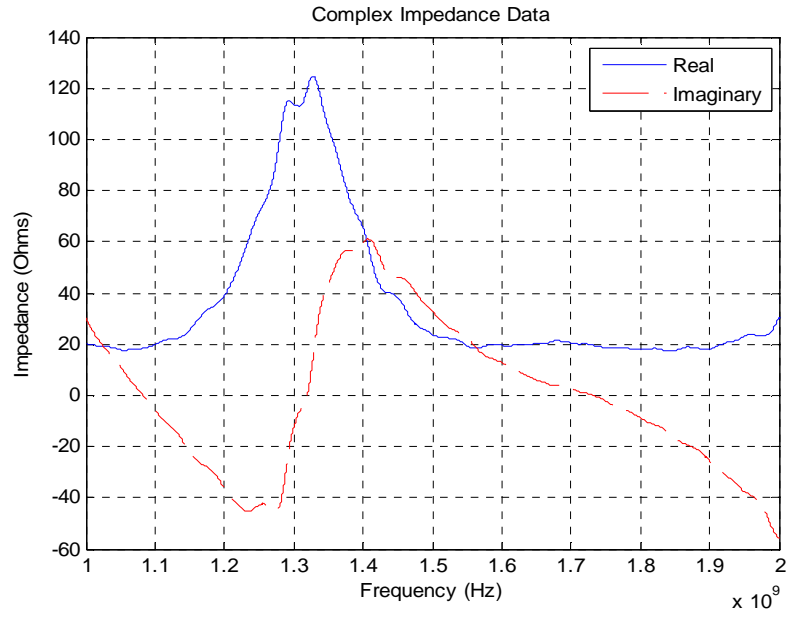


**Figure 92: Antenna 2 Port 4 Impedance**

### Antenna 3

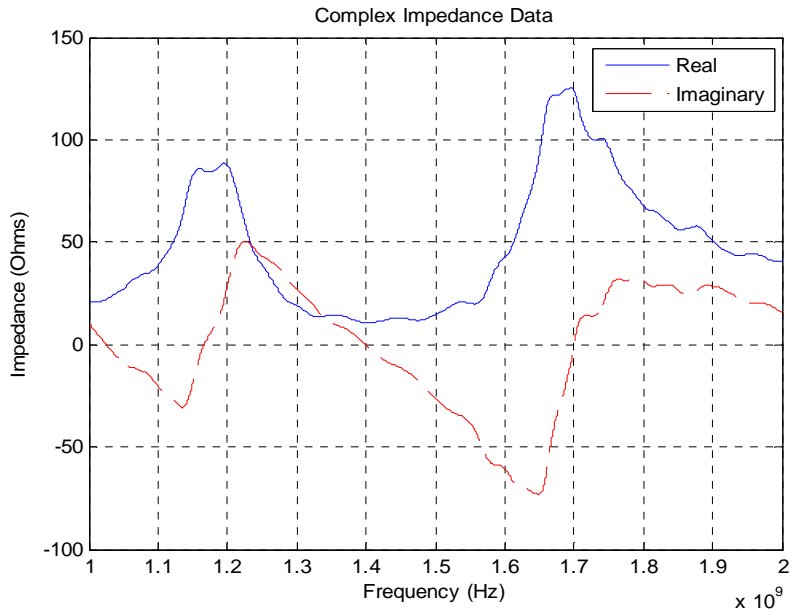


**Figure 93: Antenna 3 Port 1 Impedance**

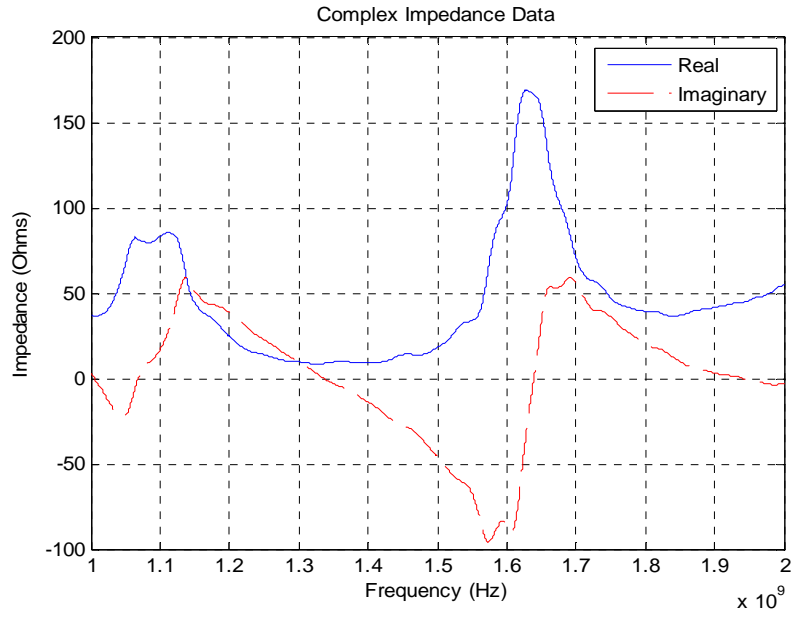


**Figure 94: Antenna 3 Port 2 Impedance**

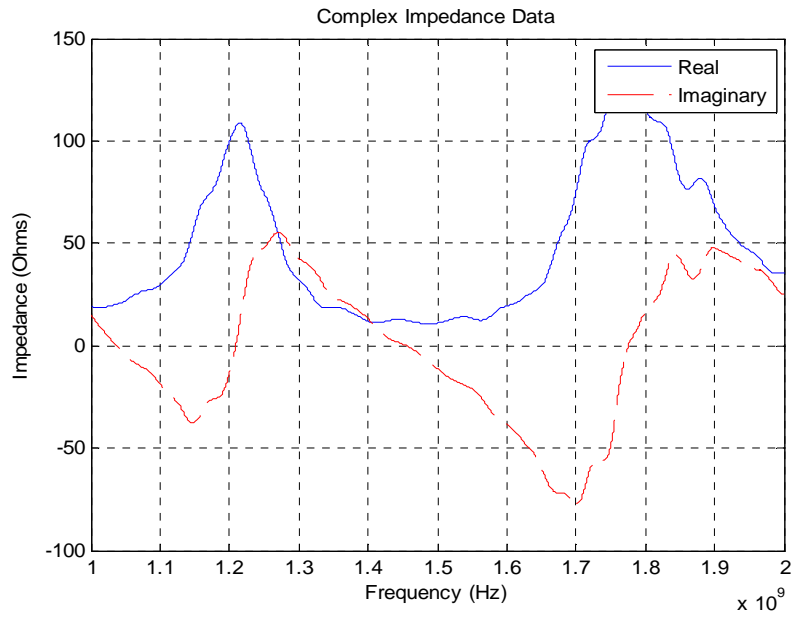


**Figure 95: Antenna 3 Port 3 Impedance**

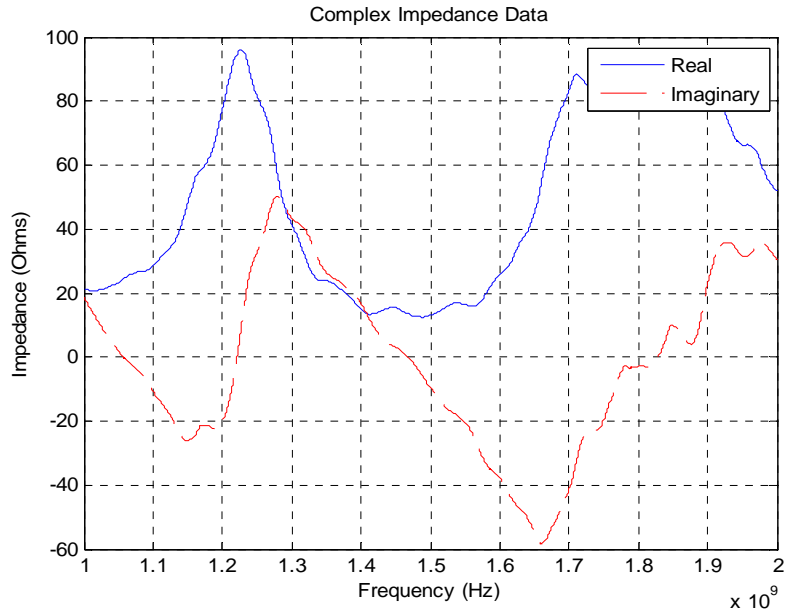


**Figure 96: Antenna 3 Port 4 Impedance**

## ***Hybrids Taped to Ground Plane***

### **Antenna 1**

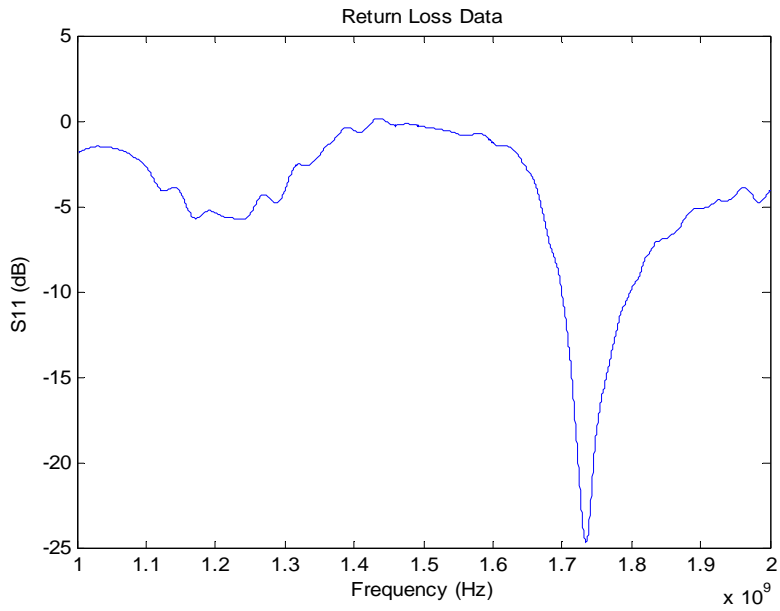


**Figure 97: Antenna 1 S<sub>11</sub> with Hybrids Taped to Ground plane**

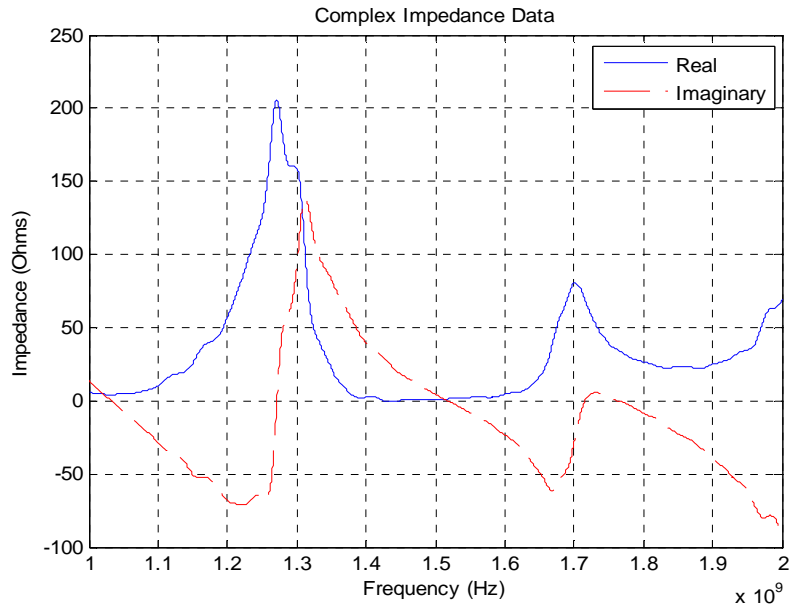


**Figure 98: Antenna 1  $S_{11}$  Impedance with Hybrids Taped to Ground plane**

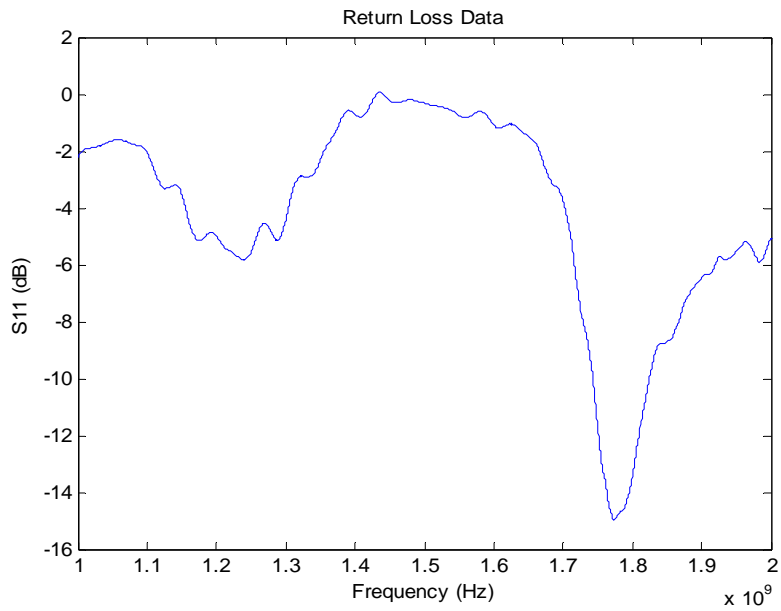


**Figure 99: Antenna 1  $S_{22}$  with Hybrids Taped to Ground plane**

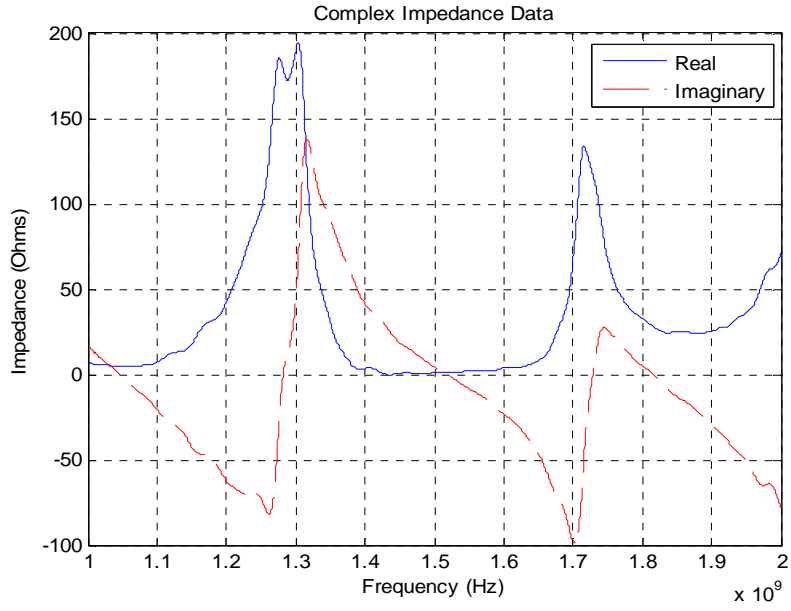


Figure 100: Antenna 1  $S_{22}$  Impedance with Hybrids Taped to Ground plane

## Antenna 2

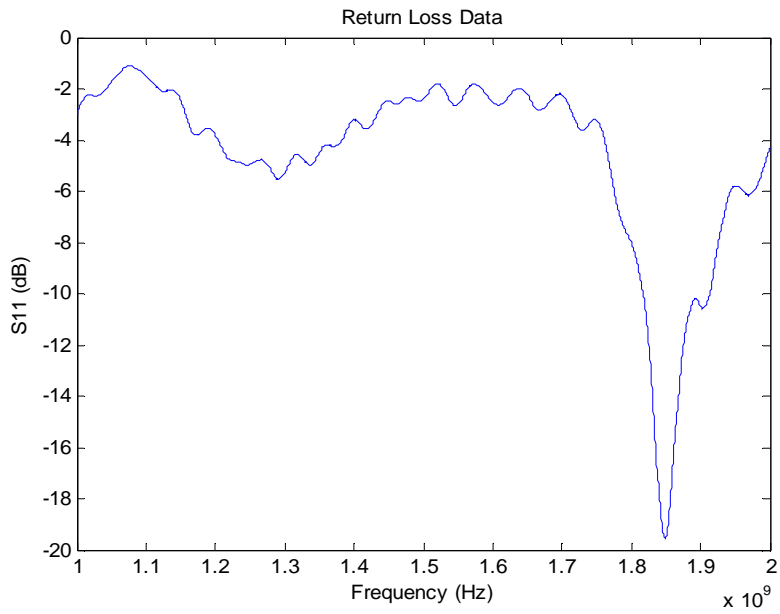
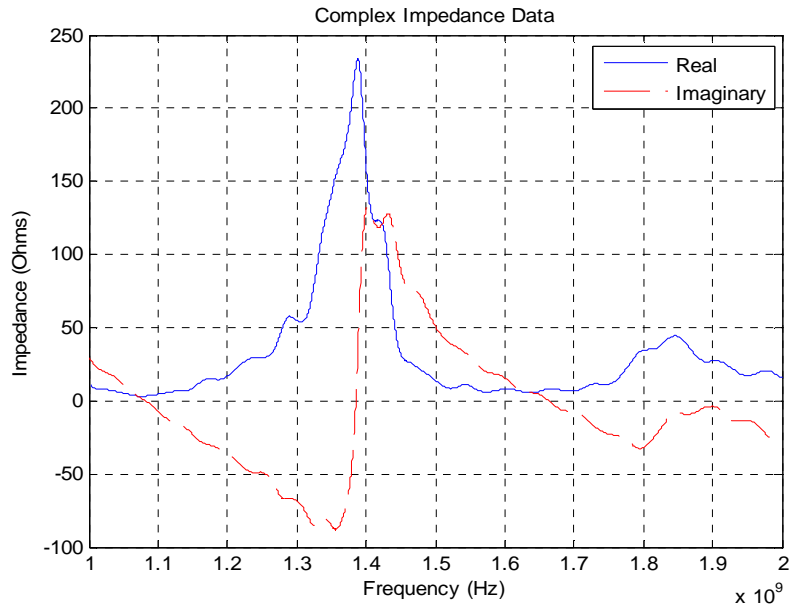
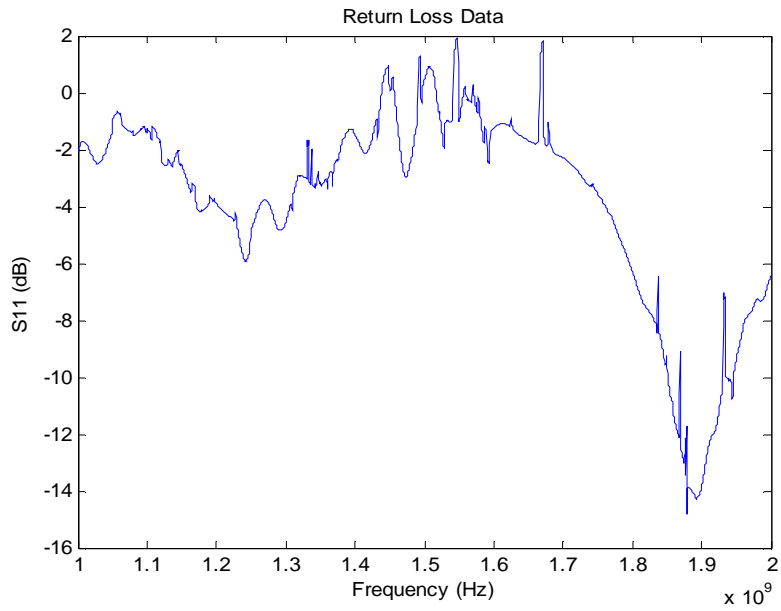


Figure 101: Antenna 2  $S_{11}$  with Hybrids Taped to Ground plane



**Figure 102: Antenna 2  $S_{11}$  Impedance with Hybrids Taped to Ground plane**



**Figure 103: Antenna 2  $S_{22}$  Impedance with Hybrids Taped to Ground plane**

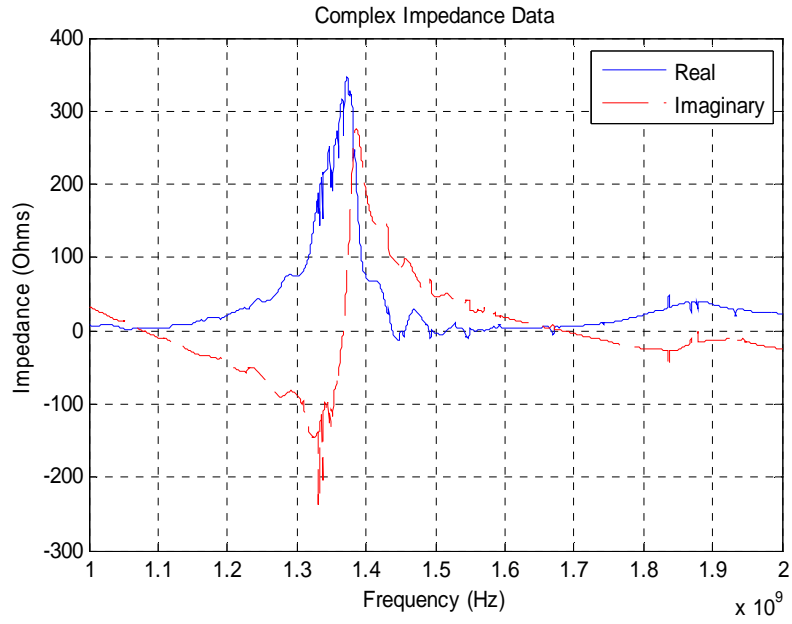


Figure 104: Antenna 2  $S_{22}$  Impedance with Hybrids Taped to Ground plane

### Antenna 3

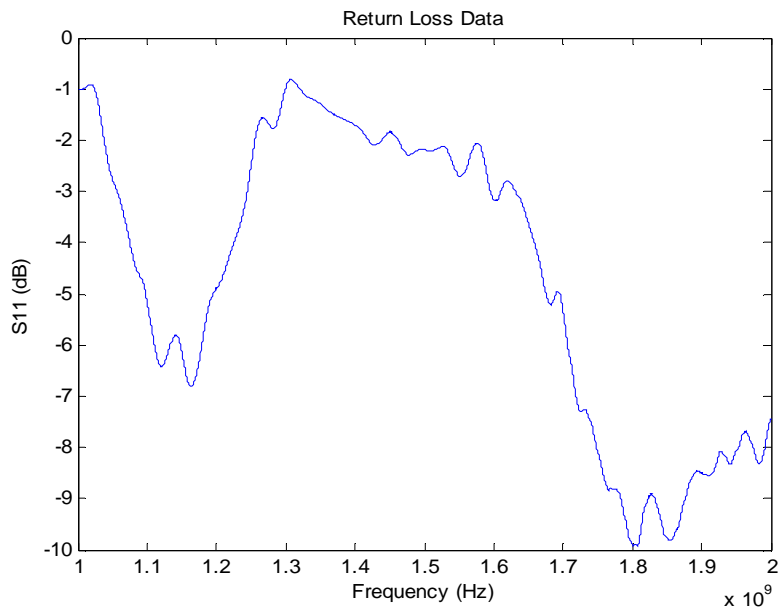
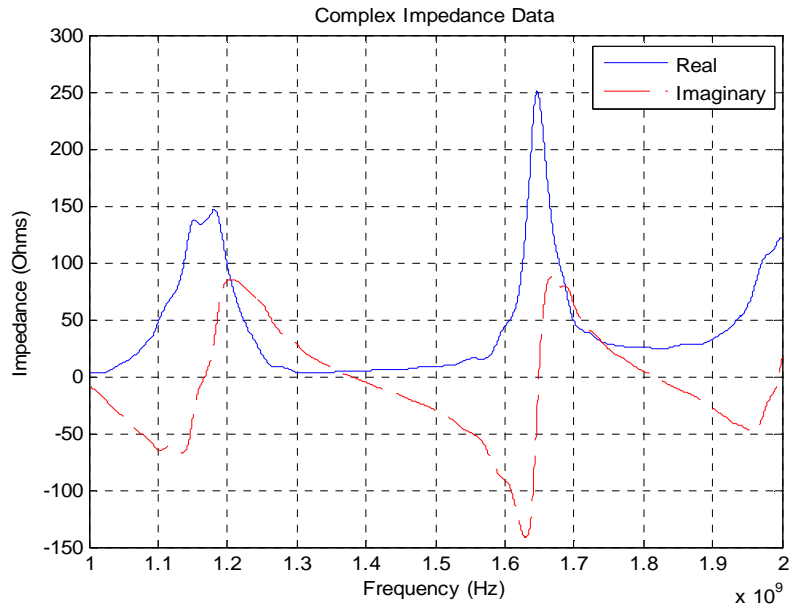
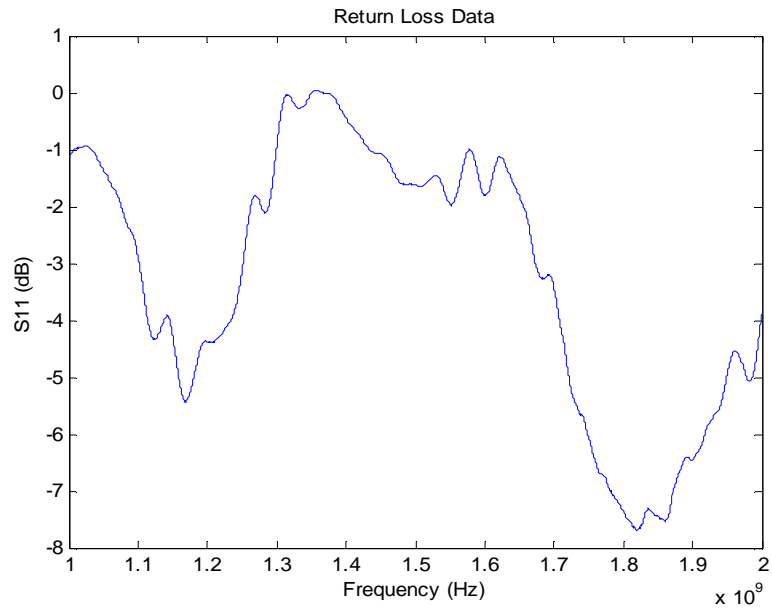


Figure 105: Antenna 3  $S_{11}$  with Hybrids Taped to Ground plane



**Figure 106: Antenna 3  $S_{11}$  Impedance with Hybrids Taped to Ground plane**



**Figure 107: Antenna 3  $S_{22}$  with Hybrids Taped to Ground plane**

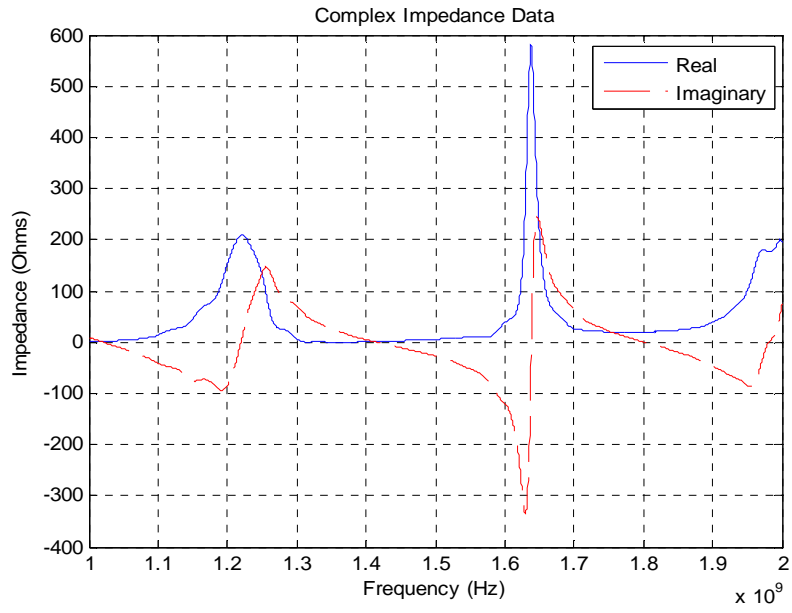


**Figure 108: Antenna 3  $S_{22}$  Impedance with Hybrids Taped to Ground plane**

# Appendix D: Testing Results of the Second Design

## 1.2 mm Center Conductor Antennas

### Antenna 1

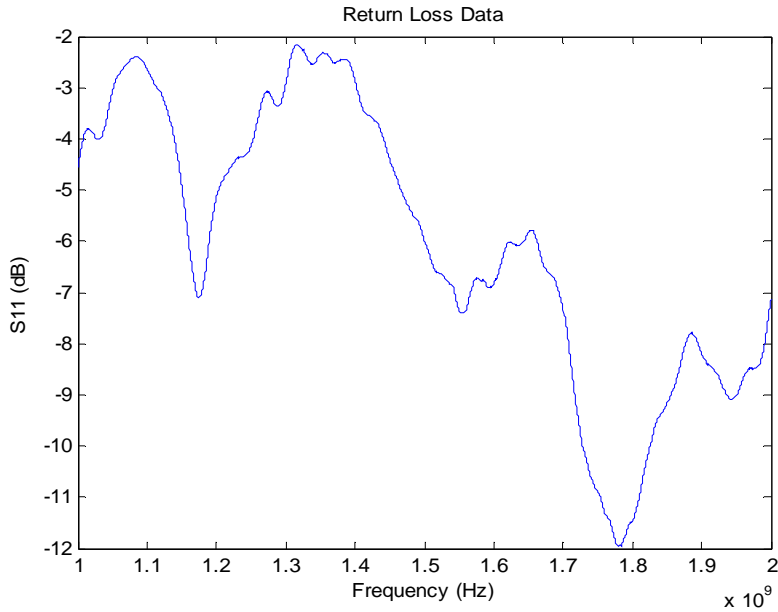


Figure 109: 1.2mm Center Conductor Antenna 1 S<sub>11</sub>

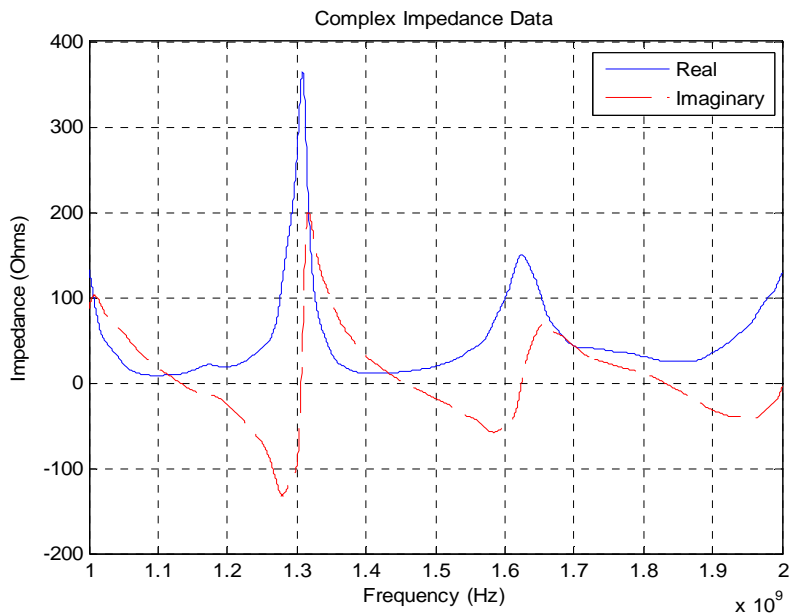
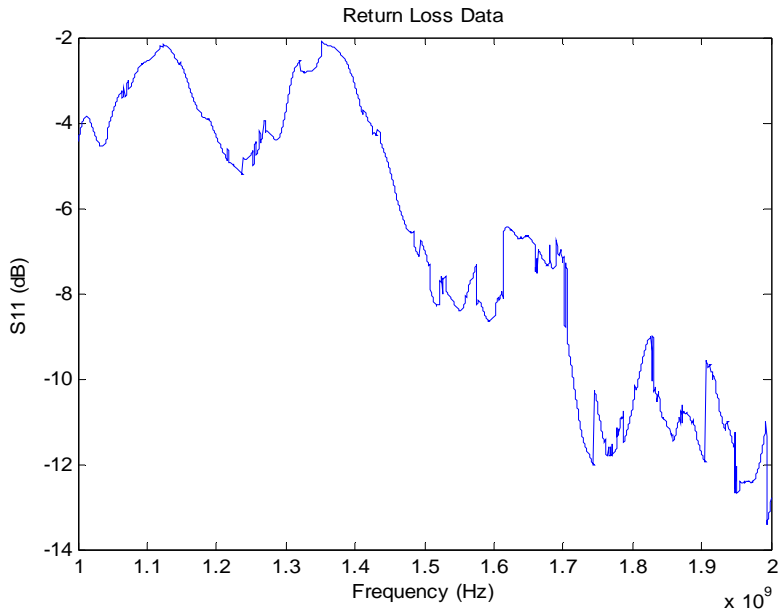
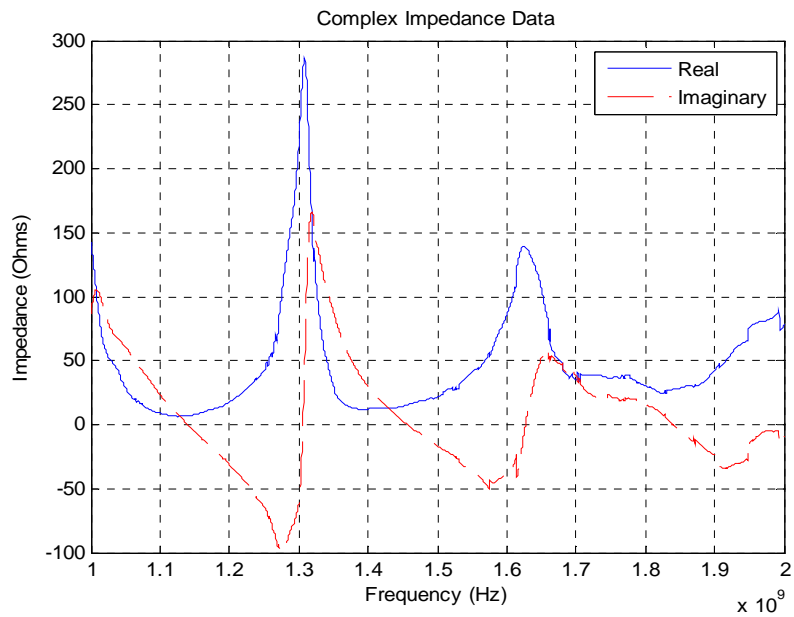


Figure 110: 1.2mm Center Conductor Antenna 1 S<sub>11</sub> Impedance



**Figure 111: 1.2mm Center Conductor Antenna 1  $S_{22}$**



**Figure 112: 1.2mm Center Conductor Antenna 1  $S_{22}$  Impedance**

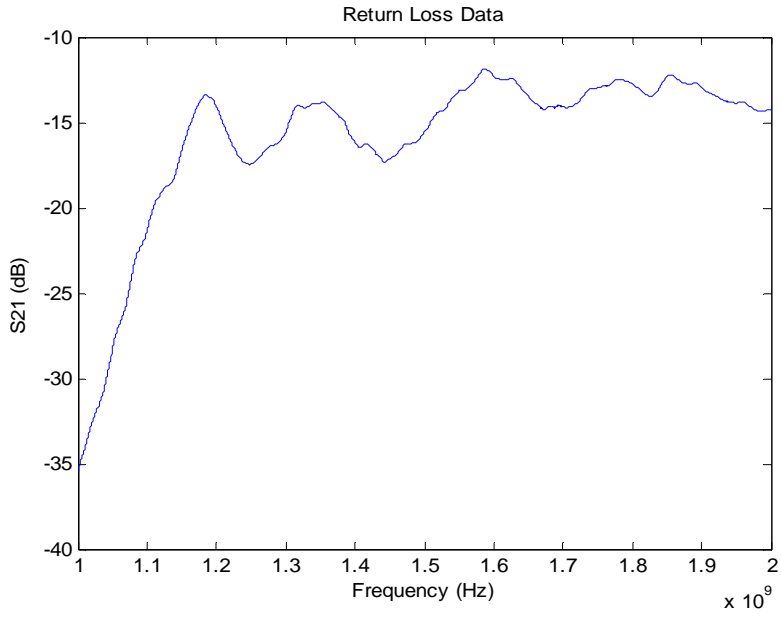


**Figure 113: 1.2mm Center Conductor Antenna 1  $S_{21}$**

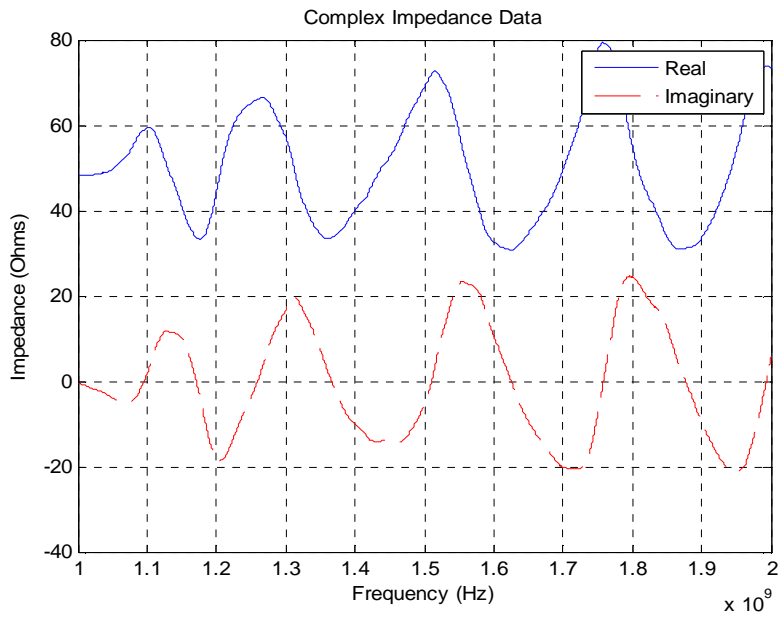


**Figure 114: 1.2mm Center Conductor Antenna 1  $S_{21}$  Impedance**

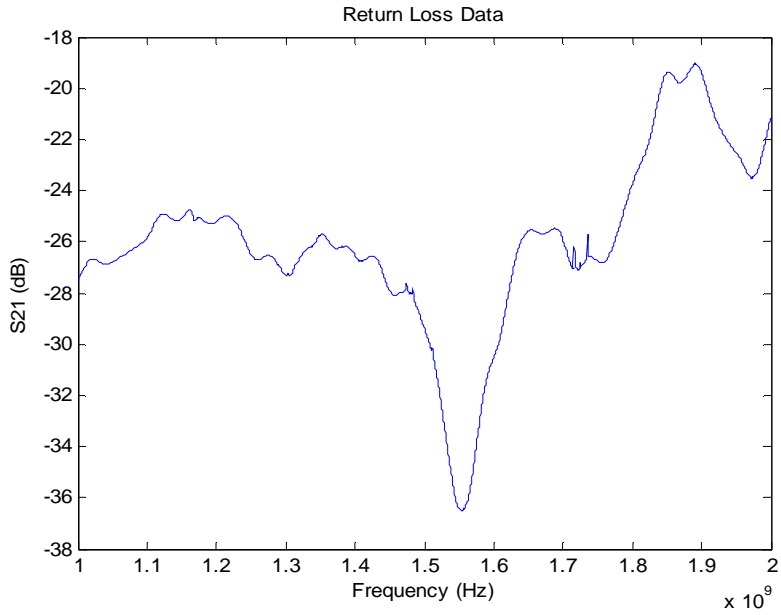


**Figure 115: Antenna 1  $S_{21}$  Measured without Teflon or Wings**

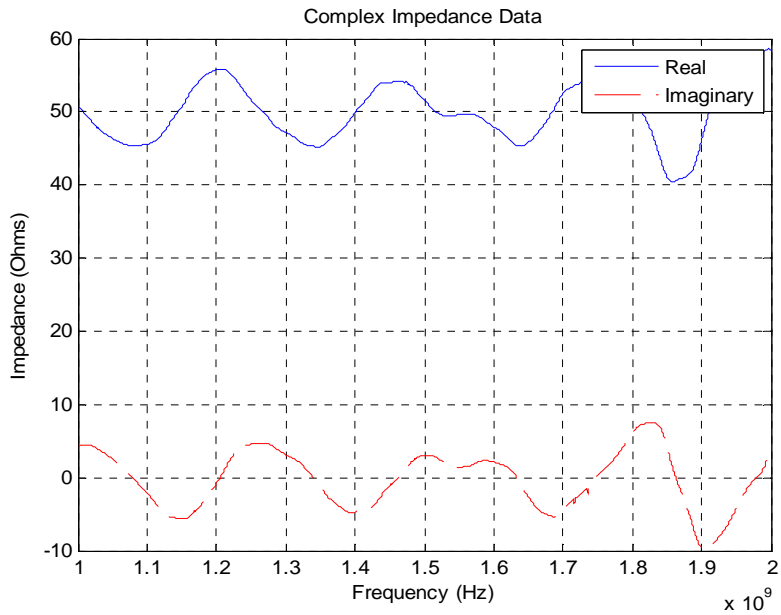


**Figure 116: Antenna 1  $S_{21}$  Impedance Measured without Teflon or Wings**

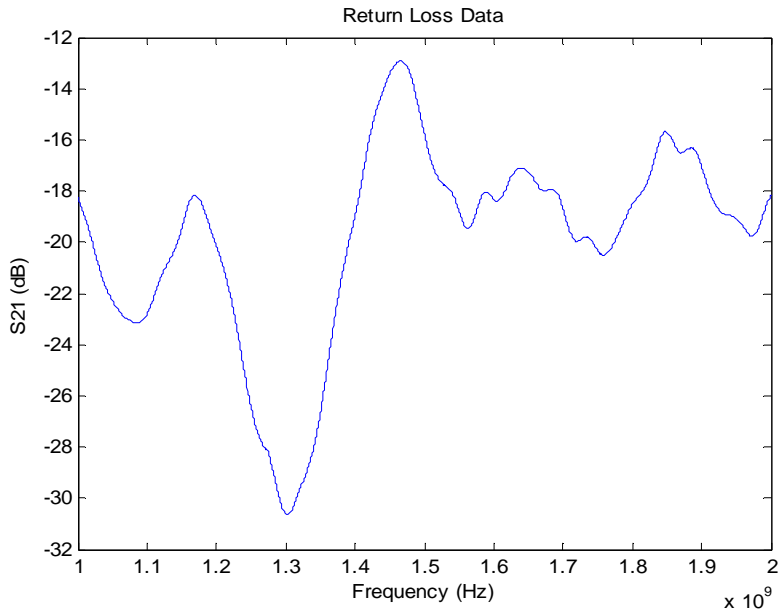


Figure 117: Antenna 1  $S_{21}$  Measured with Teflon, without Wings

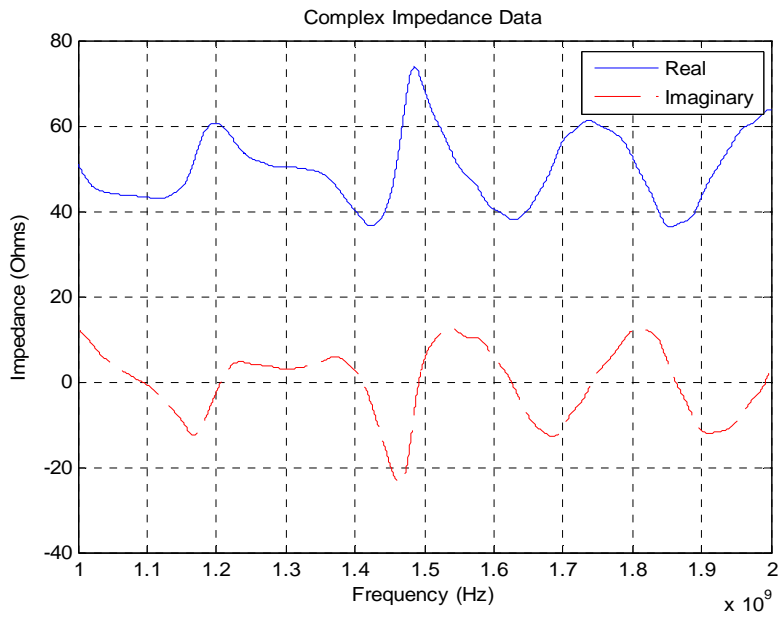
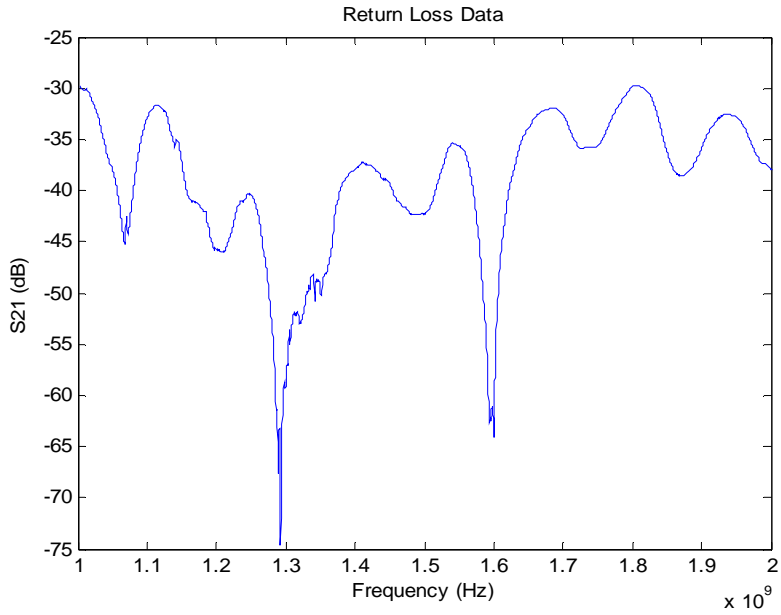
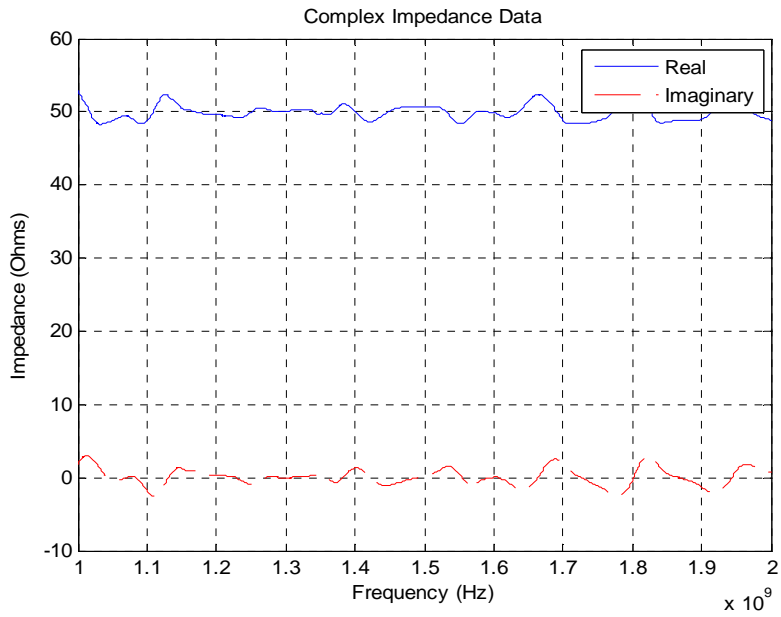


Figure 118: Antenna 1  $S_{21}$  Impedance Measured with Teflon, without Wings

## Antenna 2



**Figure 119: Antenna 2  $S_{21}$  Measured without Teflon or Wings**



**Figure 120: Antenna 2  $S_{21}$  Impedance Measured without Teflon or Wings**

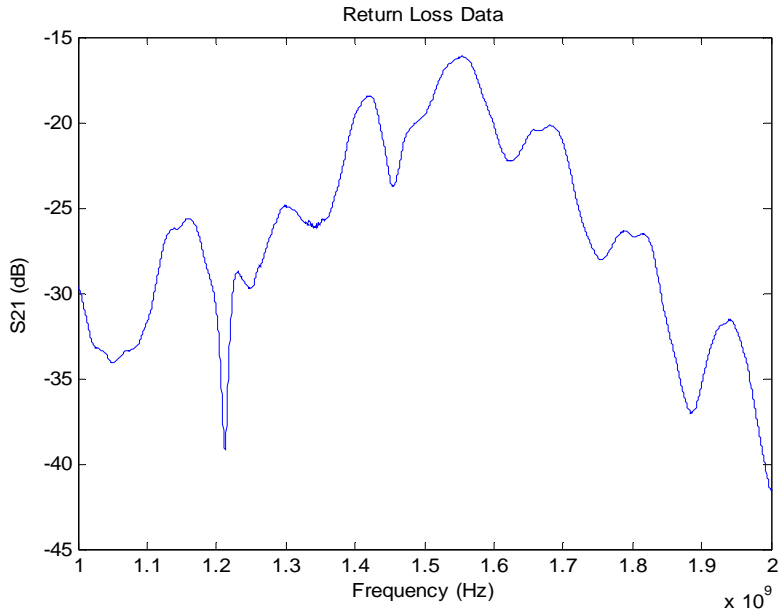


Figure 121: First Trial Antenna 2  $S_{21}$  Measured with Teflon, without Wings

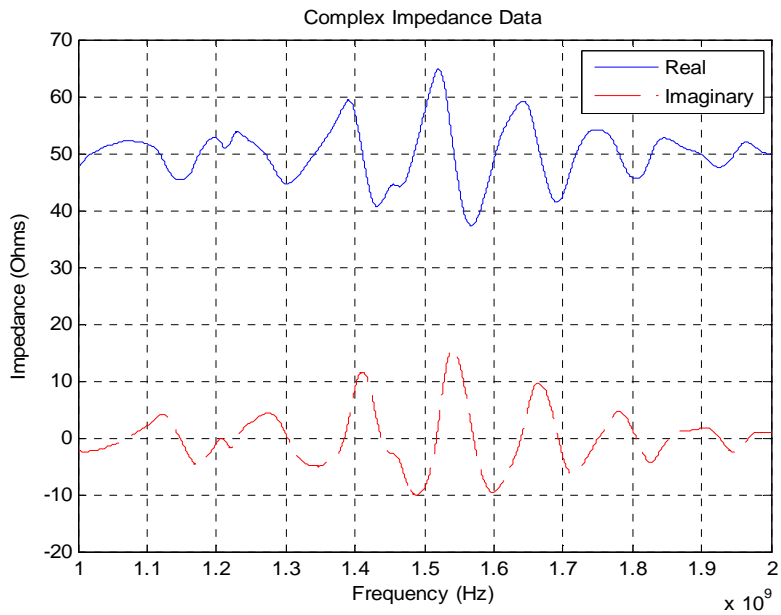
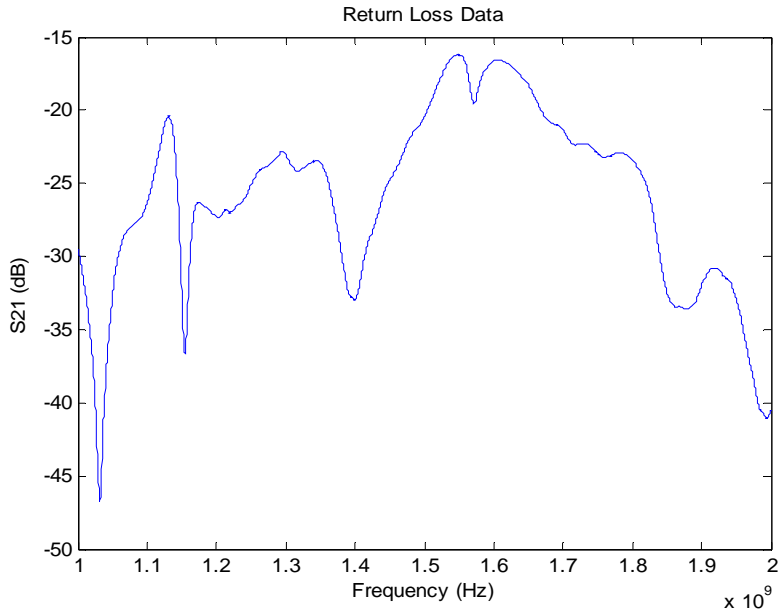
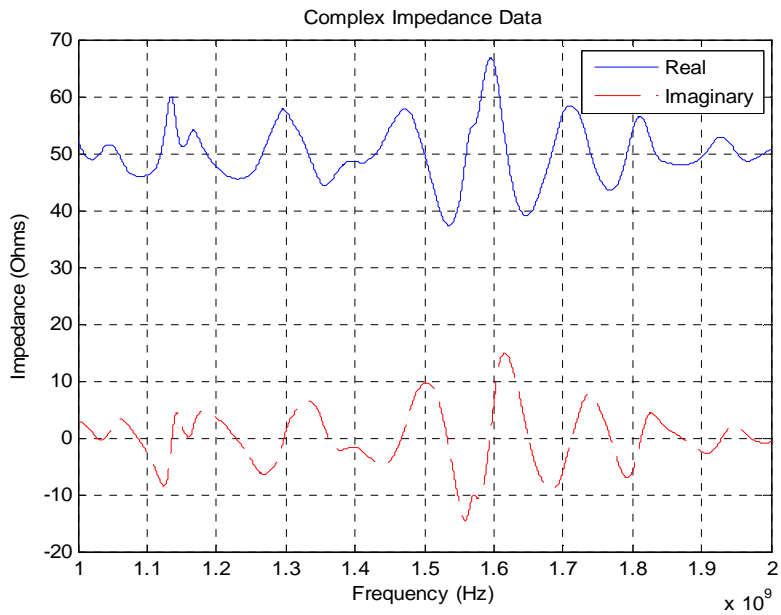


Figure 122: First Trial Antenna 2  $S_{21}$  Impedance Measured with Teflon, without Wings



**Figure 123: Second Trial Antenna 2  $S_{21}$  Measured with Teflon, without Wings**



**Figure 124: Second Trial Antenna 2  $S_{21}$  Impedance Measured with Teflon, without Wings**

## 2 mm Center Conductor Antenna

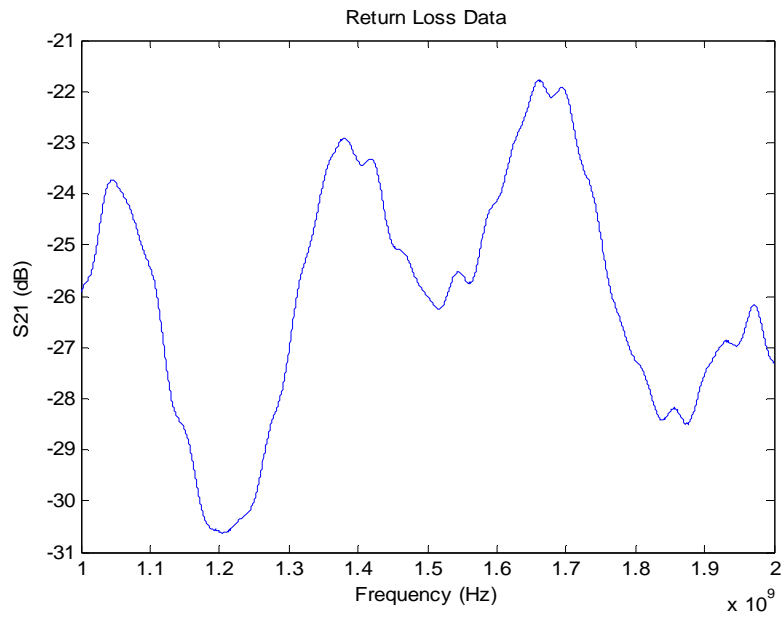


Figure 125: 2 mm Center Conductor Antenna S<sub>21</sub> Measured with no Teflon or Wings

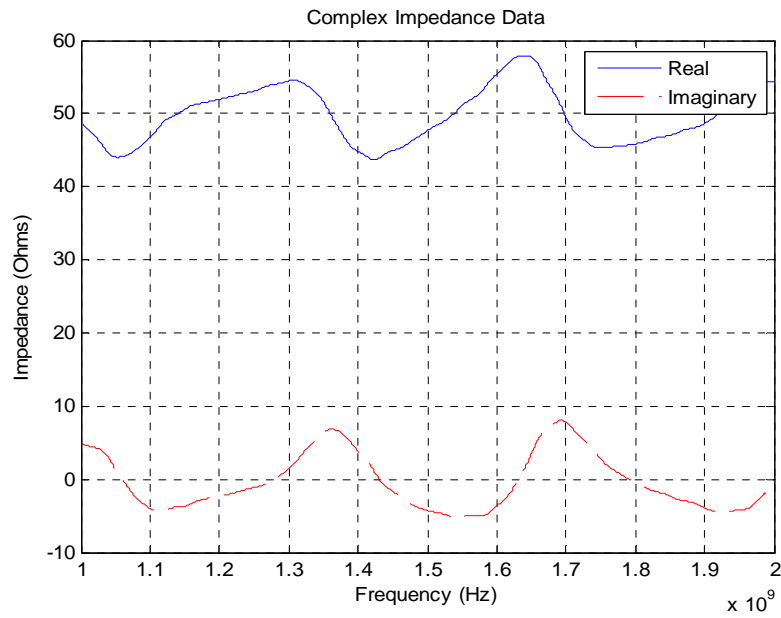
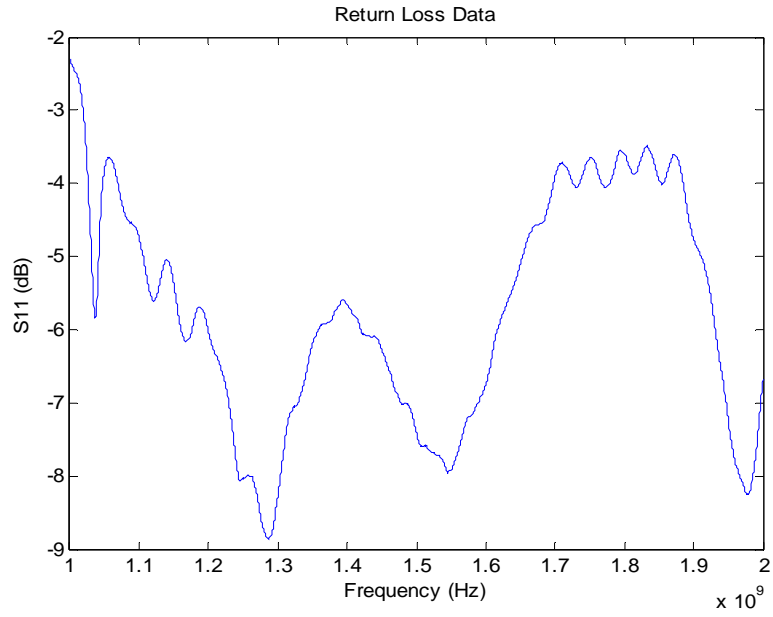
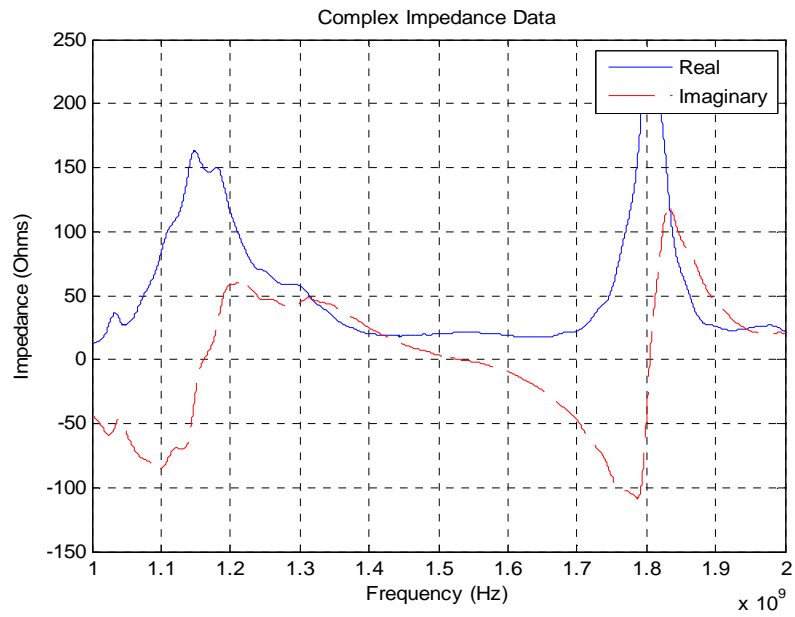


Figure 126: 2 mm Center Conductor Antenna S<sub>21</sub> Impedance Measured with no Teflon or Wings



**Figure 127: 2 mm Center Conductor Antenna S<sub>11</sub>**



**Figure 128: 2 mm Center Conductor Antenna S<sub>11</sub> Impedance**

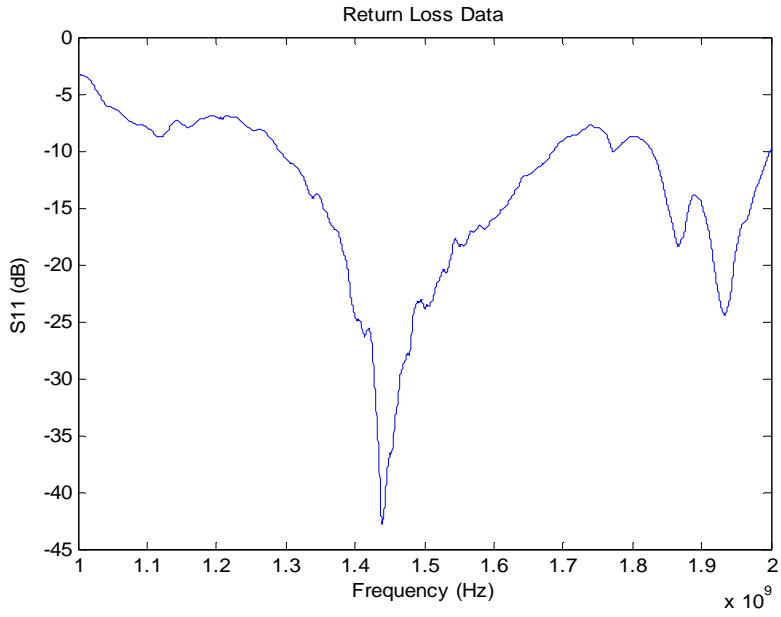


Figure 129: 2 mm Center Conductor Antenna  $S_{22}$

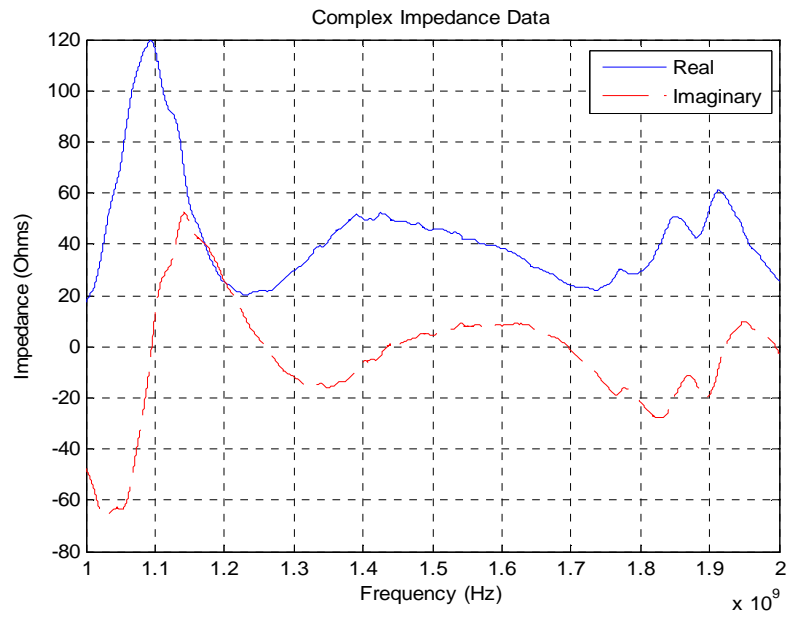


Figure 130: 2 mm Center Conductor Antenna  $S_{22}$  Impedance

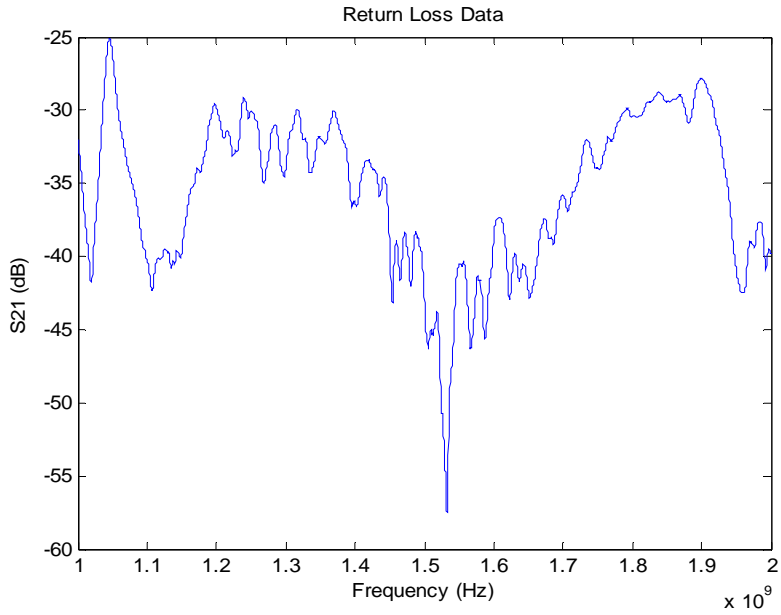


Figure 131: 2 mm Center Conductor Antenna S<sub>21</sub>

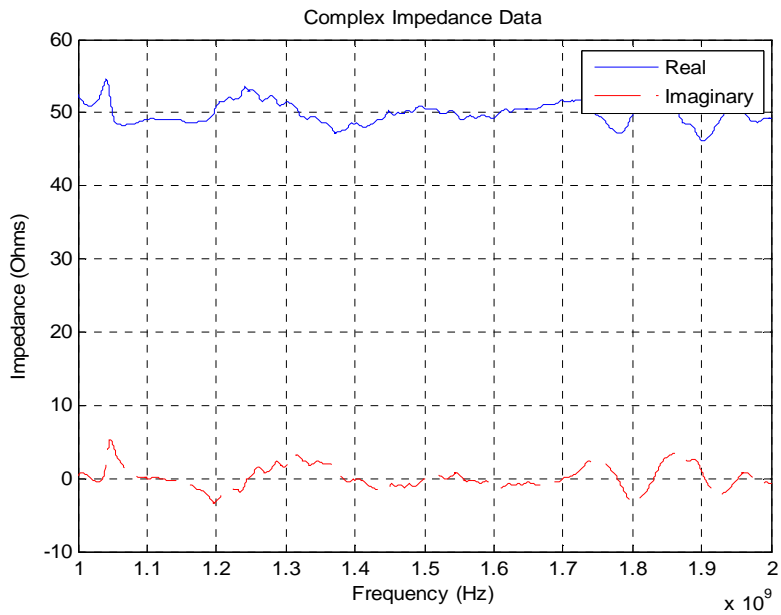


Figure 132: 2 mm Center Conductor Antenna S<sub>21</sub> Impedance

### 3 mm Center Conductor Antenna

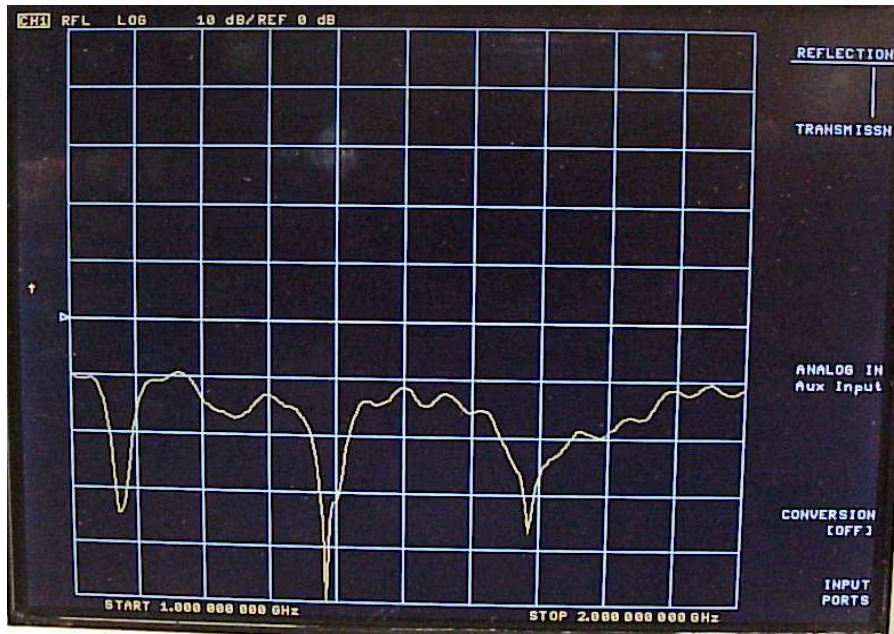


Figure 133: 3 mm Center Conductor Antenna S<sub>11</sub>

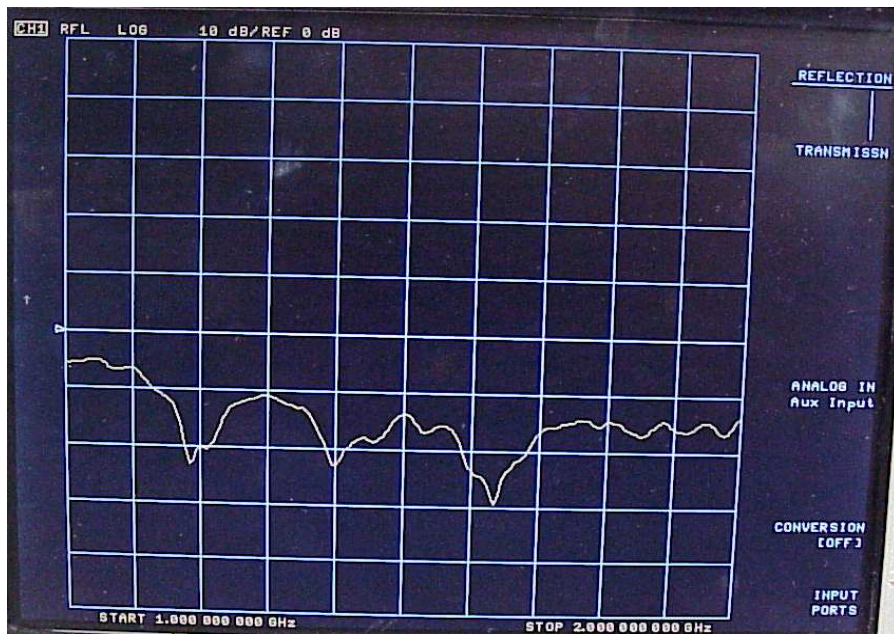


Figure 134: 3 mm Center Conductor Antenna S<sub>22</sub>

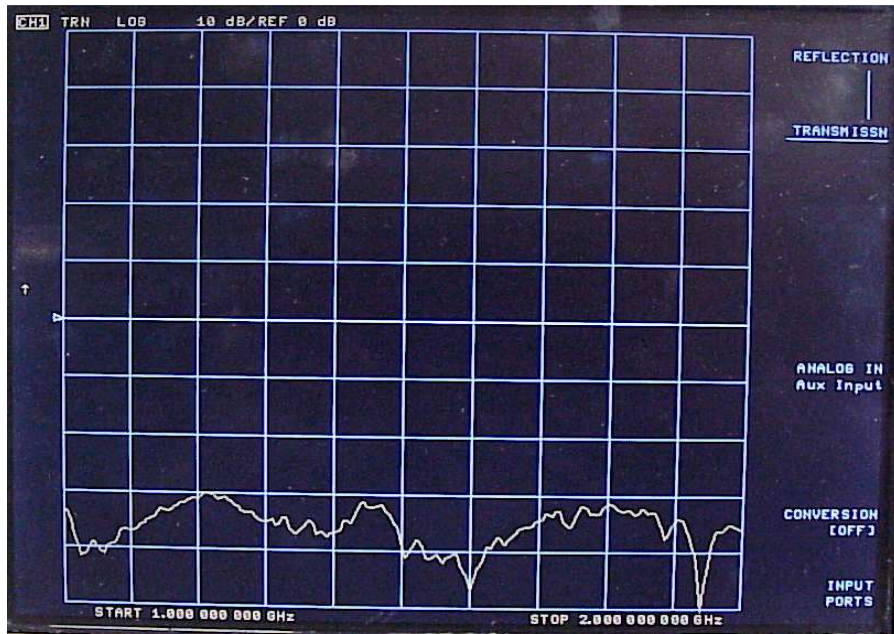


Figure 135: 3 mm Center Conductor Antenna S<sub>21</sub>

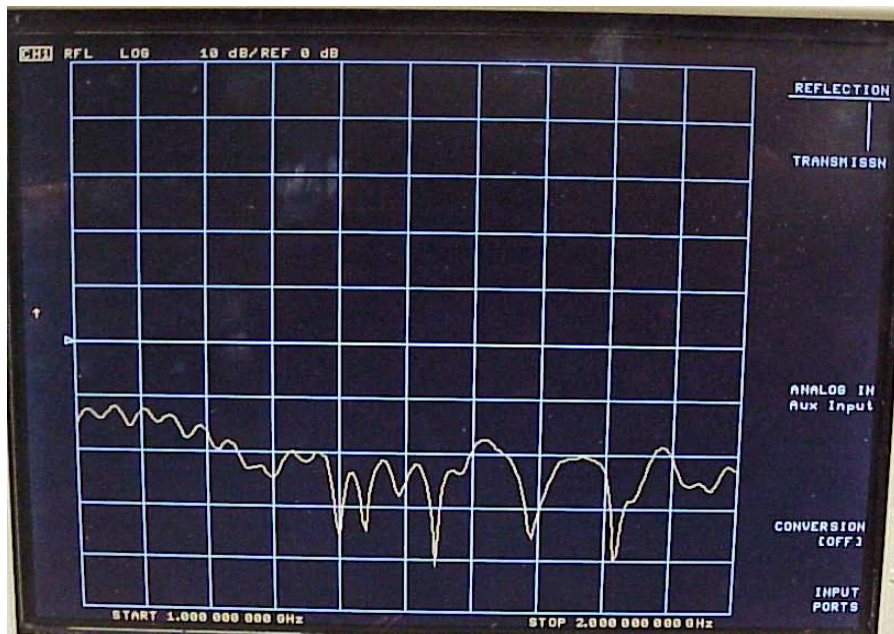


Figure 136: 3 mm Center Conductor Antenna S<sub>11</sub> with 90° Hybrid

## References

- [1] "GPS Tutorial". Trimble. 14 April, 2008  
<<http://www.trimble.com/gps/whygps.shtml>>.
- [2] Kaswarra, Bernard, and Quddus, Wasim. "'Iris" - A Broadband Base Station GPS Antenna with a Single Balun". March 2007:
- [3] McIntyre, Melville D.. "Inertially augmented GPS landing system". European Patent Office - Boeing Company. 12 April 2008 <<https://publications.european-patent-office.org/PublicationServer/documentpdf.jsp?iDocId=5201693&iebug=.pdf>>.
- [4] " Polar Services - Summit Camp GPS System - Base Station". UNAVCO. 15 April 2008 <[http://facility.unavco.org/project\\_support/polar/summit/base.html](http://facility.unavco.org/project_support/polar/summit/base.html)>.
- [5] "Circular polarization". Wikipedia. 13 April 2008  
<[http://en.wikipedia.org/wiki/Circular\\_polarization](http://en.wikipedia.org/wiki/Circular_polarization)>.
- [6] "Choke Ring Theory". Javad Navigation Systems. 15 April 2008  
<<http://www.javad.com/jns/index.html?jns/technology/Choke%20Ring%20Theory.html>>.
- [7] Ansoft HFSS, User's Guide - High Frequency Structure Simulator. Pittsburg: Ansoft Corporation, 2003.
- [8] Ludwig, Reinhold, and Pavel Bretchko. RF Circuit Design. Upper Saddle River, NJ: Prentice Hall, 2000.
- [9] Kraus, John D., Ronald J. Marhefka, and Ahmad S. Khan. Antennas for all Applications. New Delhi: McGraw-Hill, 2006.
- [10] "Permanent GPS Stations - Choke Ring Antenna Calibrations". UNAVCO. 14 April, 2008  
<[http://facility.unavco.org/project\\_support/permanent/equipment/antennas/ant\\_cal.html](http://facility.unavco.org/project_support/permanent/equipment/antennas/ant_cal.html)>.
- [11] Puzella, Angelo, Li, Tao, and Makarov, Sergey N. "A Quad-Line Vertical Balun Column for the Use with a Dyson Balun and a Turnstile Radiator ". 2008:
- [12] Pozar, David M. Microwave Engineering, 3rd ed. New York: Wiley, 2005.